NPL
National Physical Laboratory

Report

NPL REPORT MAT 9

PAMRIC: Properties of Alloys and Moulds Relevant to Investment Casting

L A Chapman, R Morrell,
P N Quested, R F Brooks,
Li-Hung Chen, D Ford

January 2008

National Physical Laboratory | Hampton Road | Teddington | Middlesex | United Kingdom | TW11 0LW
Switchboard 020 8977 3222 | **NPL Helpline** 020 8943 6880 | **Fax** 020 8614 0446 | **www.npl.co.uk**

Department for **Innovation, Universities** & **Skills**

PAMRIC:
Properties of Alloys and Moulds Relevant to Investment Casting

L A Chapman, R Morrell, P N Quested, and R F Brooks

Industry and Innovation Division
National Physical Laboratory
Teddington, Middlesex TW11 0LW, UK.
and
Li-Hung Chen, formerly Doncasters plc., and D Ford, DAF Associates

National Physical Laboratory
Teddington, Middlesex TW11 0LW, UK

ISSN 1754-2979

NOTE:
This version of the final report PAMRIC Studio Project at NPL is the public version of NPL report MATC (D) 141 issued in 2003 to the project partnership, and in accordance with the terms of the DTI contract, is placed into the public domain after a due period.

Approved on behalf of Managing Director, NPL,
by Dr M G Cain, NPL Industry and Innovation Division

ABSTRACT

PAMRIC was a collaborative project established between NPL and industry in the field of metal casting. The objective of this project was to measure the thermophysical properties (enthalpy; heat capacity; density and thermal diffusivity) of four metal alloys and eight ceramic mould systems relevant to the investment casting industry.

The alloys chosen by the partners were the nickel alloys IN738LC; CM186LC; CMSX10 and Rene 80. The following physical properties for both the solid and liquid states of these alloys were measured between 700°C and 1500 ^{o}C.

(i) Heat capacity, enthalpy, enthalpy of fusion, fraction solid.
(ii) Thermal diffusivity and derived thermal conductivity.
(iii) Density, thermal expansion coefficient.
(iv) Solidus and liquidus temperatures.

The heat capacity measurements revealed that there were two major transitions (i) the γ/γ' transformation which occurred between ca 1000-1100 ^{o}C and 1200-1300 ^{o}C and (ii) the fusion process.

The industrial partners supplied eight proprietary ceramic moulds, and for four of them fairly detailed descriptions were given of their construction, whereas little detail was given about the other four. The shrinkage on firing was measured by a simple test on the dimensions and the following other properties were measured:

(i) Heat capacity and enthalpy,
(ii) Thermal diffusivity and derived thermal conductivity.
(iii) Density, thermal expansion coefficient.

The results for the moulds carry a higher uncertainty of measurement for thermal diffusivity and heat capacity compared with the alloy results. This is attributed to the greater structural inhomogenity of the moulds. For the thermal diffusivities experimental difficulties in measuring the very small values were experienced, whereas thermal contact was perceived as a problem for the heat capacity measurements.

It is concluded that for the moulds it is probably sufficient to estimate the heat capacity from the weighted values of the main constituents of the mould rather than direct measurement. For the density (thermal expansion) the results at high temperatures are particularly affected by the time at temperature and the industrial processing conditions need to be assessed when estimating the change in dimensions of the mould. It is postulated that creep will also play some part in the change in dimensions.

Sensitivity analysis for changes in the values of the shell conductivity and heat capacity; effect of dimensional changes and interfacial conductivity for the solidification of a model casting with varying dimensions (Small; medium and large.) were performed by the industrial partners. For all parts the total solidification time was strongly effected by the thermal conductivity of the mould; changes in the heat capacity did effect initial solidification time whereas the interfacial conductivity generally had a small effect although a greater effect for thick sections.

One of the industrial partners modelled the differential scanning calorimeter (DSC) and investigated the effects of poor thermal contact between specimen and sample.

CONTENTS

SYMBOLS, ABBREVIATIONS, UNITS

a	thermal diffusivity	$m^2 s^{-1}$
Cp	heat capacity	$J g^{-1} K^{-1}$
f_s	fraction solid	
h	heat transfer coefficient	$W m^{-2} K^{-1}$
H	enthalpy	$J g^{-1}$
H_T-H_{25}	enthalpy relative to that at 25 ^oC	$J g^{-1}$
ΔH^{fus}	enthalpy of fusion	$J g^{-1}$
ΔH^{trans}	enthalpy of transition	$J g^{-1}$
T	temperature	^oC or K
T_{liq}	liquidus temperature	^oC or K
T_{sol}	solidus temperature	^oC or K
α	linear thermal expansion coefficient	K^{-1}
λ	thermal conductivity	$W m^{-1} K^{-1}$
ρ	density	$kg m^{-3}$

DSC	differential scanning calorimeter
DTA	differential thermal analysis
DTSC	differential temperature scanning calorimeter

1. INTRODUCTION

The principal objective of this project was to provide reliable physical property data for the following properties of nickel-based superalloys, heat capacity, enthalpy, enthalpy of fusion, fraction solid, thermal diffusivity and conductivity, and density. Similar measurements viz. the heat capacity; thermal diffusivity; density and thermal expansion coefficient were made for typical industrial mould materials, together with shrinkage on firing.

These properties are needed to improve the accuracy of predictions of defects in castings. Thus the above properties have been measured over a wide temperature range in the solid and the liquid phases of four nickel-based superalloys, IN738LC (NPL metal store code PGA), CM186LC (PGK), CMSX4 (PGZ) and Rene 80 (PHC) and eight commercial investment moulds in the solid. (PCB; PGC; PGD; PGF; PGM; PGL; PGN; PHG).

It should also be noted that, ideally, the physical property values should be those obtained for a cooling rate similar to that for the casting and not those for equilibrium or steady state conditions. Although some of the techniques used are dynamic in nature such as thermal analysis methods *(e.g.* DTSC, thermal expansion) others rely on achieving steady temperature at the point of measurement (*e.g.* laser pulse method for thermal diffusivity). Thus in some cases it has been necessary to combine '*equilibrium*' values for a property with those obtained for other properties derived when using a certain cooling rate.

The γ/γ' transition in the nickel alloys is sluggish, and during the cooling cycle the ordering process is dependent upon various factors such as the cooling rate, the size of the sample, the thermal contact of the sample in the cell etc. These factors also influence the solidification process and the question is which conditions (*e.g.* sample size) reflect the closest match to the solidification of the casting. One of the industrial partners also attempted to investigate the effect of poor thermal contact between the sample and thermocouple in the DSC.

The results for the moulds carry a higher uncertainty of measurement compared with the alloy results. This is thought to be due to the greater structural inhomogenity of the moulds. For the thermal diffusivities experimental difficulties in measuring the very small values were also experienced.

One of the industrial partners performed sensitivity analysis for changes in values of the shell conductivity and the interfacial conductivity between the mould and the metal casting for different sized castings.

2. EXPERIMENTAL

2.1 MATERIALS

The alloys IN738LC (PGA), CM186LC (PGK), CMSX10 (PGZ) and Rene 80 (PHC) were supplied as machined samples from three of the industrial partners: Howmet; Cannon-Muskegon and Chromalloy. The *nominal* compositions of these alloys are given in Table 2.1. A brief description of the moulds is given in Table 2.2 together with their identification.

Table 2.1 Nominal compositions of the alloys

Alloy	Sample	Ni	Cr	Co	Mo	W	Ta	Al	Ti	C	B	Others
IN 738LC	PGA	bal	16	8.5	1.7	2.6	1.7	3.4	3.4	0.11	10	0.9 Nb
CM186LC	PGK	bal	6	9	0.5	8	3	5.7	0.7	0.007	0.015	1.4 Hf 3.0 Re
CMSX10	PGZ	bal	2.3	3.4	0.41	5.6	8.3	5.78	0.32	0.10	<25ppm	0.03Hf 6.4 Re
Rene 80	PHC	bal	14	9.5	4	4	-	3	5	0.17	0.015	Zr 0.03

Table 2.2. Various mould types supplied by the Industrial Partners.

NPL Code	Mould type
PGB	Zircon water base slurry; molochite stucco
PGC	Fused silica water based slurry; Cerametal 05-1 stucco
PGD	Dual system slurry, Cerametal 05-1 stucco
PGF	Non-disclosable
PGM	Alumina based
PGL	Alumina based
PGN	Zircon/silica slurry with molochite stucco.
PHG	Non-disclosable

Samples to the various dimensions needed were manufactured at NPL from blanks supplied by the industrial partners.

2.2 METHODS, PROCEDURES

2.2.1 Heat Capacity and enthalpy measurements

In thermal analysis there are two pans and the temperature differences between these are continuously monitored by a differential thermocouple. If one crucible (pan) contains a sample, and the whole assembly is heated at a known heating rate when the specimen undergoes, for instance, an endothermic transition (such as melting) the temperature of the sample pan will lag behind that of the reference pan. This results in a departure from the base line. This is the principle of differential thermal analysis. Quantitative DTA is often referred to as differential scanning calorimetry (DSC) and this type of DSC where the temperature difference is monitored is referred to as differential temperature scanning calorimetry (DTSC).

Heat capacity measurements of the alloys for temperatures between 700 and 1500 °C were obtained using a Stanton Redcroft DSC 1500, (Figure 1) which is based on the differential temperature scanning calorimetry (DTSC) principle. The sample is in the form of a disc (3.5 mm diameter x 0.5 to 1 mm). The calorimeter is run with an empty reference pan against (i) a matched empty sample pan, then (ii) the sample pan containing a sapphire reference material and (iii) the sample pan containing the sample [1]. The Cp and $(H_{T_2} - H_{T_1})$ values were obtained as described by Richardson [1] using a spreadsheet constructed at NPL. The heat capacities and enthalpies obtained with this method for reference materials were within ± 4% of the certified reference values. (NPL Procedure QPCMMT/B/149 “Measurement of Heat capacity and Enthalpy by Differential Scanning Calorimetry”).

The enthalpy of fusion was determined by measuring (i) the area under the Cp-T relation (for the fusion peak) and (ii) extrapolation of enthalpy curves.

The fraction solid (f_s) was determined for any specific temperature (T) in the fusion range by measuring the enthalpy given out between T_{liq} and T and comparing it with the enthalpy given out between T_{liq} and T_{sol} :

$$f_s = \left(\frac{H_T - H_{T\,liq}}{H_{T\,sol} - H_{T\,liq}} \right) \qquad (1)$$

For the moulds, their heat capacity was measured with the specimens in the form of powder using a similar method.

2.2.2 Linear thermal expansion

The specimens were tested in a Linseis alumina dilatometer. The instrument operates in the horizontal mode with specially constructed alumina apparatus comprising a recrystallised alumina tube with a cut-away section near the end into which is inserted a rod with a flat end which acts as a contact for one end of the test-piece. An alumina push-rod contacts the other end of the test-piece and transmits the changes in length to a linear displacement transducer as the specimen is heated and cooled. The temperature of the specimen is measured using a type R thermocouple, and the outputs of the thermocouple and the transducer are recorded at two-minute intervals by a data logger for later analysis.

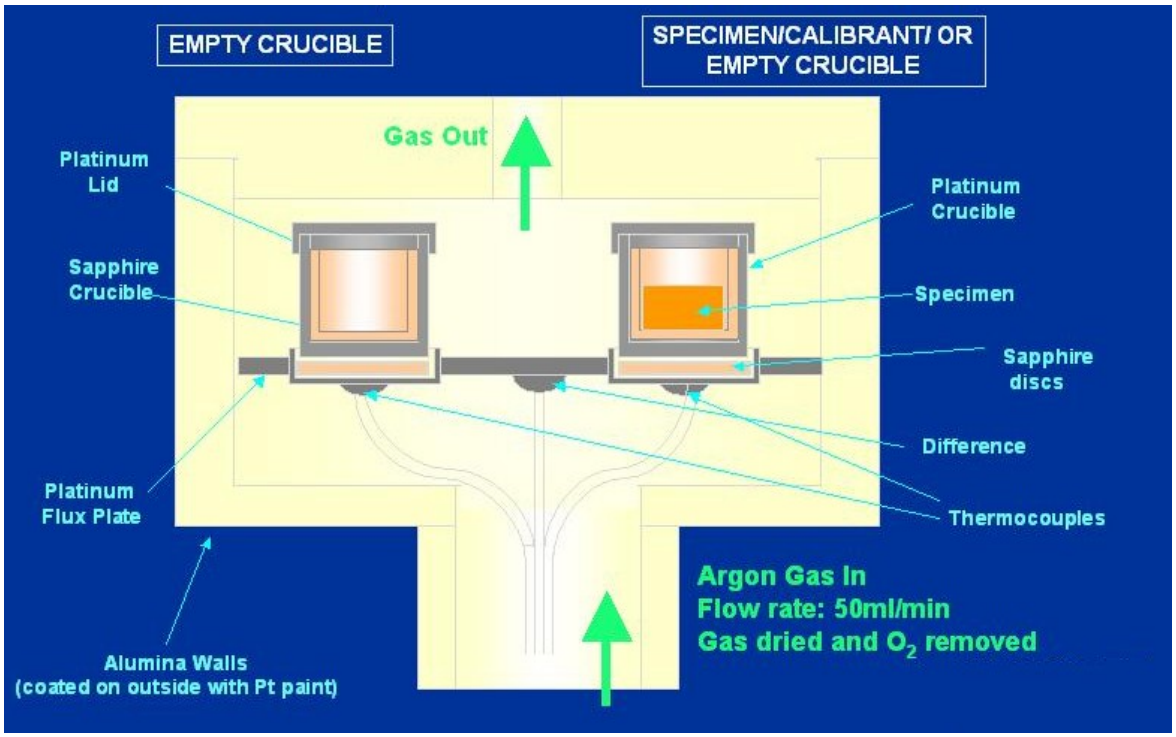

Figure 1: Schematic drawing of the high temperature DSC (DTSC) used to measure the enthalpy and heat capacity.

The instrument is calibrated in the following manner. The alumina specimen holder is removed, and replaced by a drum micrometer that is used to move the push-rod prescribed amounts. In this way the absolute sensitivity of the transducer may be determined. The apparatus is reassembled and run over the required temperature range with the push-rod contacting the far end of the apparatus, and any shift of the baseline output, corresponding to differential temperature distributions in the specimen support and push-rod, is determined. This is used to correct the output from testing an unknown. The correction for the expansion coefficient of the apparatus itself is determined by inserting a certified reference specimen, normally SRM 739, Fused Silica from the National Institute for Standards and Technology, USA up to 700 ^{o}C, and a platinum standard for higher temperatures. The procedure is documented in NPL DMMQP/B/120, which is in line with EN 821-1.

The overall accuracy of the measurement is controlled by the mechanical stability of the specimen in the apparatus. Assuming complete stability, the measurement accuracy is considered to be approximately $\pm$ 0.1 x 10^{-6} K^{-1} over a 1000 K temperature range.

The mode of operation employed for the present tests involved resting the test-piece on a thin layer of ceramic fibre insulation lining the test-piece support tube, and heating it in an Ar-flushed atmosphere initially to about 1200 ^{o}C at a heating rate of 2 K min^{-1}, followed by cooling at the same rate to room temperature. The selection of upper temperature was made according to expectations of the melting temperature, increasing the maximum temperature a little for second and subsequent cycles. At least three thermal cycles were made on each test-piece, except that in some cases the melting temperature was just exceeded. When this occurred, the test-piece collapses, and cooling data could be obtained.

Logger data were transferred to a computer program containing the calibration data, and thermal expansion data calculated. Mean thermal expansion coefficients over the reported

temperature ranges were calculated by linear interpolation between logged points and averaged for heating and cooling.

2.2.3 Bulk solid density measurements

The density of the alloys at room temperature was measured by immersing the samples in water and using the Archimedean method.

In the case of shell moulds, the samples were baked at 120 °C for 2 h to constant mass. They were weighed dry, then immersed in water for at least 60 minutes, weighed immersed in water, then weighed again after removal and superficial drying of the surface with a damp cloth. In this way, the bulk density and apparent porosity can be determined in accordance with EN623-2.

Density measurements at elevated temperatures were calculated from the room temperature bulk density and the thermal expansion behaviour, assuming isotropic behaviour, using the equation:

$$\rho(T) = \rho(25)/(1+\overline{\alpha}(T-25))^3 \qquad (2)$$

where $\overline{\alpha}$ is the mean linear expansion coefficient over the temperature range 25 °C to T °C.

2.2.4 Liquid and mush densities for alloys [2]

Attempts were also made to measure the alloy melting curves using piston dilatometry and a schematic diagram is shown in Figure 2. The procedure for this was as follows. Cells and pistons both 50 mm in length were specially made from high-purity Frialit-Degussit AL23 alumina supplied via Degussa (UK) Ltd. The fit of the piston in the 4 mm diameter cell was lapped to a smooth easily sliding fit. The cylinders and pistons were then cut to form a double-acting unit about 22 mm in cylinder length with two 12 mm pistons. The cell internal diameter was measured at both ends to the nearest 0.01 mm using a travelling microscope, and the piston lengths and diameters were measured to the nearest 0.001 mm using a vernier micrometer. A cylindrical test-piece of the test alloy was made to a diameter approximately 1% less than that of an alumina double piston cell, i.e. 3.96 mm diameter x typically 8 mm in length. The test sample was placed inside the cell, the pistons inserted, and the unit placed in the alumina push-rod dilatometer and treated as any normal test-piece. The samples were heated to about 20 - 30 °C above the suspected liquidus temperature at a heating rate of 2 °C/min, and cooled at a similar rate. On completion of the thermal cycle, the logged data were first processed as a normal solid test-piece to give apparent fractional length change as a function of temperature. Then, using a solid calibration for the expansion of the length of the alumina pushrods, the alumina calibration allows the true volume of the cell between the pistons to be determined, and assuming this is full of mush or liquid, the apparent density can be computed from the starting mass and cell volume. The solid thermal expansion of the test-piece to the apparent solidus[1] can be determined by subtracting the expansion of the two pistons. Above the 'apparent solidus' the sample collapses to fill the cavity with mush, and,

[1] The term 'apparent solidus' is used because the overall intention is that the test-piece should fill the diameter of the mould at the solidus temperature, so as liquid is produced and the alloy starts to collapse, the pistons are pushed outwards. Small amounts of liquid initially produced at the true solidus may not have a measurable effect on piston position. It may require significant amounts of liquid to be produced before it can be argued that liquid is present.

above the liquidus, with liquid. As the liquid expands, it pushes the pistons out relative to the cell. Since the cell cross-sectional area as a function of temperature is known, the volumetric expansion of the mush and liquid can be determined. On cooling, a similar sequence of events should occur down to the point at which the mush freezes to a solid skeleton, and liquid feeding occurs. At this point the method no longer gives the true metal volume. In practice, reactions between the metal, the cell wall and any residual atmosphere can limit the ability of the measurement to behave correctly. Some leakage of the cell can occur, due to low surface tension of the molten metal, and a thin oxide skin is thought to be desirable to retain liquid within the cell. Leakage generally leads to cell jamming and invalid measurements. Prior to the present work, the method had been shown to work well and consistently with aluminium alloys and cast iron, but had not been attempted with nickel-based alloys.

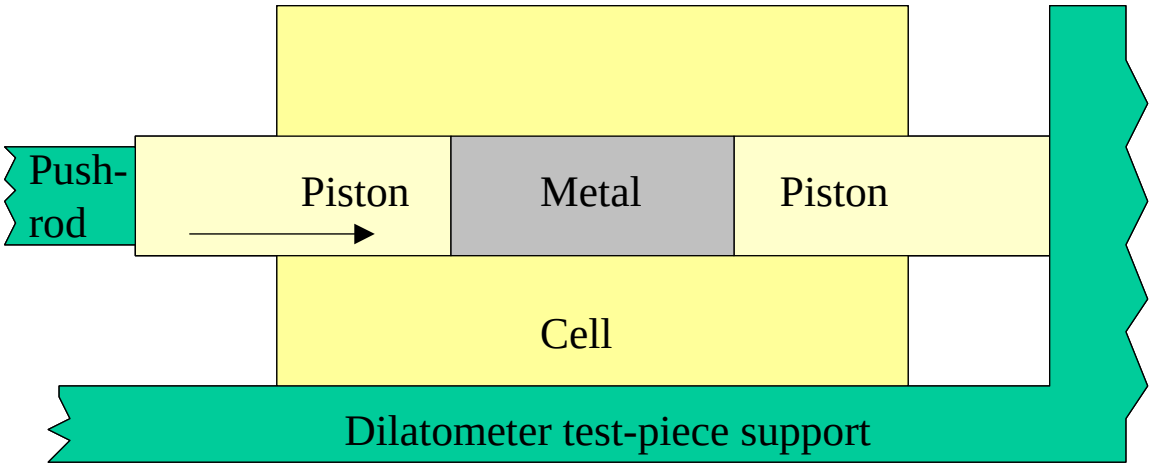

Figure 2: Schematic drawing of the piston technique for measuring the density of the alloy in the mush and liquid.

2.2.5 Bulk shrinkage of moulds

Squares or rectangles of the supplied mould materials were cut using a diamond saw, and the edges flattened and squared off by hand using a flat diamond-grinding lap. If a coloured hot-face coating had been employed, to avoid contamination most of this was gently removed using a flat abrasive lap. After drying the lateral dimensions of the test-pieces were measured to the nearest 0.01 mm using a 0 - 25 mm or a 25 - 50 mm micrometer. The test-pieces were then laid flat on an insulating firebrick with the metal contact side face down, and fired to a maximum temperature of 1320 or 1420 °C with a two-hour hold before cooling to room temperature. The dimensions were re-measured, and the shrinkages calculated.

2.2.6 Thermal diffusivity measurements

Thermal diffusivity measurements between 100 and 1200 ^{o}C in the solid were obtained at selected fixed temperatures using the laser pulse method with a Netzsch 427 laser flash apparatus (LFA). A schematic of the LFA is given in the Figure 3.

The technique was originated by Parker et al [3], and more details about the technique may be found by reference to Maglic et al. [4]. The method followed for solids at NPL is described in NPL Procedure QPCMMT/B/172 “Procedure for the measurement of Thermal Diffusivity using LFA” and the method is UKAS accredited.

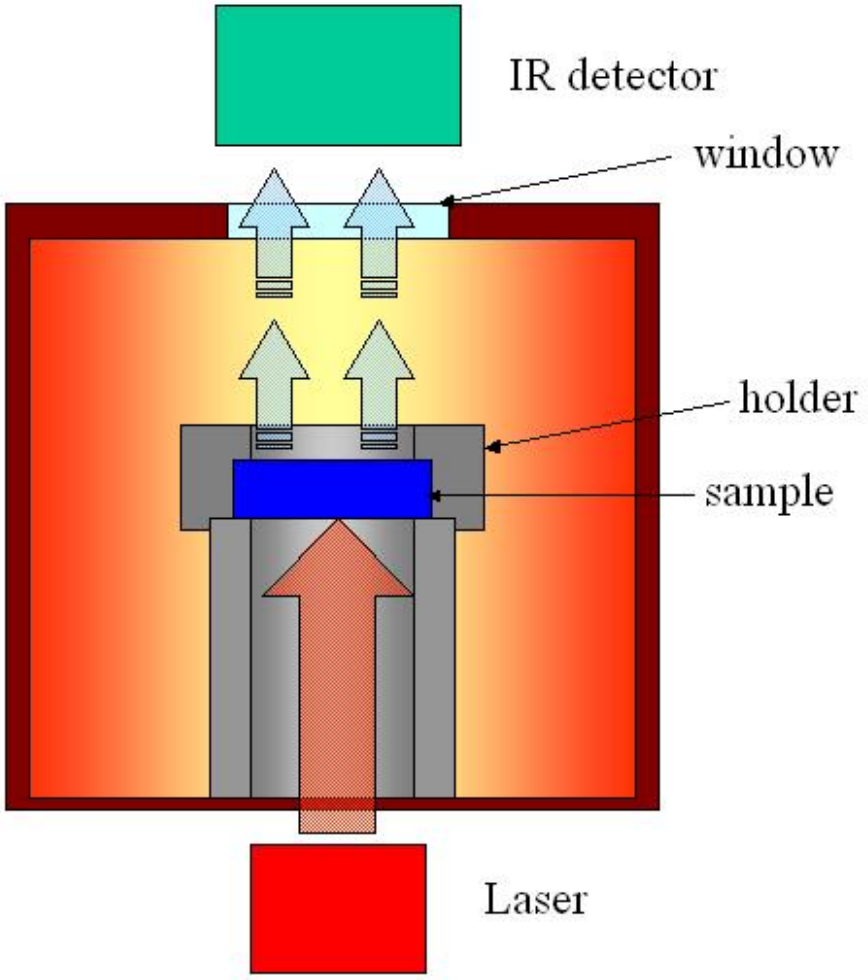

Figure 3: Schematic drawing showing the principle of the laser pulse method for determining thermal diffusivities of alloys

Briefly, the measurement consists of heating the bottom face of a disc shaped sample (typically 1 - 3 mm in thickness depending on the value of thermal diffusivity) using a high intensity laser pulse and monitoring the temperature rise on the top face using an InSb infra red detector. From the temperature rise, the thermal diffusivity (a) can be calculated by:

$$a = 1.37 l^2 / t_{0.5} \qquad (3)$$

where l is the thickness of the specimen and $t_{0.5}$ is the time taken for the temperature to reach the half the value of the maximum temperature rise. Equation 3 assumes ideal adiabatic conditions for an idealised instantaneous energy pulse. Corrections [5] provided by Netzsch in software are applied for heat loss effects and the finite width of the laser pulse. The specimen was sprayed with a thin coat of graphite on the surface exposed to the laser pulse to improve the signal to noise. Measurements were made in a flowing atmosphere of argon.

Uncertainty of measurement for the metal measurements is calculated to be ±4% with a coverage factor of 2. This value is somewhat greater for the mould materials and is caused by their lower diffusivity and the inhomogeneity of the samples compared to the metals.

The thermal diffusivity of the liquid alloys was attempted. The sample is contained within a sapphire crucible, which is transparent at the wavelength of the laser radiation. The sample is designed to fill the crucible at the melting point and the required thickness is calculated from the expansion coefficient of the metal.

Thermal conductivity values can be calculated from the thermal diffusivity results using Equation 4 and the measured *Cp* and density values.

$$\lambda = a.\, Cp.\rho \qquad (4)$$

2.3 ACCURACY OF MEASUREMENTS

Uncertainties of measurement for the different techniques are estimated in Tables 2.3 and 2.4.

Table 2.3 Estimated uncertainties associated with the various experimental methods for alloys.

Heat capacity	Density		Thermal diffusivity	
DTS	Solid	Liquid	Solid	Liquid
< ± 4%	±1%	± 2%	± 5%	±10%

Table 2.4 Experimental uncertainties associated with the various experimental methods for moulds.

Heat capacity	Density	Thermal diffusivity
< ± 6%	±1%	±15%

2.4 Sensitivity analysis

To gain some understanding of the sensitivity of a casting model to changes in thermophysical data, an analysis was performed by Lu Hung Chen at Doncasters. The component chosen was an idealised blade section, and the model employed was ProCAST[2]. The parameters analysed were:

- Effects of shell conductivity
- Effects of dimension changes using three sizes, with the overall lengths chosen to be 75, 300 and 1050 mm, approximately 30, 120 and 420 mm width and 1.5, 6 and 21 mm at the ‘trailing edge’. Full dimensions are given in Annex B.
- Effects of interfacial conductivity

[2] ESI group finite element analysis casting program, see: www.esi-group.com/newsite/products/casting/

3. RESULTS

At the behest of the industrial partners the results for the alloys are grouped under alloy type for the alloys, but under properties for the moulds. Appendix A lists all data acquired.

4. DISCUSSION

4.1. ALLOY RESULTS

4.1.1 Heat capacity and fraction solid

DTSC is a dynamic method and can therefore provide property values for different cooling (or heating) rates. However, when a specimen undergoes a phase change during cooling, the kinetics of the transformation will be dependent upon (a) the nature of the transition itself, (b) other instrumental effects such as the cooling (or heating) rate, specimen size, the thermal resistances of the specimen/pan and pan/cell interfaces and other instrumental effects. Obviously a smaller sample will tend to respond quicker to a transition and for this reason is preferred for transition range measurements. However, small samples produce smaller signals and thus larger samples provide more accurate *Cp* values when the specimen is not undergoing transformation. For these studies a compromise was adopted.

There are two types of transformation: first order transitions and second order transitions.

In first order transformations such as melting, enthalpy is absorbed as the temperature increases. For systems with more than one component this transformation may occur over a range of temperatures and this absorption of enthalpy appears as a peak in the curve representing the variation of heat capacity with temperature. The area under this curve, after allowing for the intrinsic heat capacity of the individual phases, represents the enthalpy associated with the transformation.

In second order transformations, which will generally be associated with an internal ordering within a given phase, there will be no such discontinuous change in these properties. Such transformations will occur over a range of temperatures. Examples of order-disorder transformations might be magnetic ordering (eg ferromagnetic to paramagnetic) or chemical ordering (B2 to A2) and could be either first order or second order.

The melting of the alloy is a first order transition. In order to derive enthalpies of transition or fusion it is necessary to extrapolate intrinsic *Cp* values of the individual phases to provide a baseline. This is frequently difficult, *e.g.*:

(i) It is difficult to draw a baseline for the γ/γ' transition, because the phase boundaries representing the equilibrium between the phases vary with temperature.

(ii) There is only a small plateau in *Cp-T* curve between the γ/γ' and the fusion transitions and it is difficult to establish an accurate value for *Cp* (solid); this is particularly true for values for CMSX10 where *Cp* (solid) = 1.4 J g^{-1} K^{-1} was recorded (much higher than ca. 0.8 J g^{-1} K^{-1} recorded for the other alloys), this has the effect of raising the base line and consequently the *Cp* and the thermal conductivity for the 'mush'. For IN738LC and

Rene 80 the γ' transition is more separated from the fusion and the heat capacity depends on whether sample is heated or cooled.

The γ/γ' transition is a sluggish solid/solid transformation. As a result the actual *Cp* values and peak temperatures will be dependent upon specimen size.

It has been assumed here that γ/γ' (gamma prime) transition is *First order*.

The fraction solid at temperature *T* within the mushy range of temperature is calculated from the enthalpy values. Hunt [6] has mathematically modelled the heat transfer in DTSC and states that the fraction solid values may be in error when calculated in this manner. This is a consequence of the fact that the sample and reference pans are at different temperatures when the sample is undergoing a thermal event such as solidification/fusion. Further work will be needed to confirm these findings and was the reason for modelling the DSC. Thus it may be necessary to review the f_s values cited in this report when further information becomes available.

The measured T_L is affected by undercooling whereas T_S is affected by time constant of DSC on cooling. Therefore the results at 10°C min^{-1} need to be interpreted with care [7].

In Appendix 1 the measured enthalpies are compared with the calculations using the data base supplied with the solidification program, PROCAST, and it can be seen that the enthalpy of fusion measured are a little greater than those calculated. That said they probably provide a reasonable estimate for models involving mould filling and macrosolidification used by industry.

4.1.2 Density measurements

Solid measurements shows changes due to γ' changes and the temperature where there is significant change in the density in the mush region is different from the indicated T_S from the DTSC measurements. It is postulated that the mush remains strong enough to withstand the pressure of the piston for small liquid fractions and one is measuring a softening point of a solid/liquid mixture.
The piston method worked well for three of the alloys indicating the change in density through the mush and a density at T_L. Although we determined the variation of density with temperature of the liquid the results were variable. From Iida and Guthrie [8], it is clear that there is a large variation in this coefficient for the elements measured by different workers so it is difficult to establish if this variation is real or indicates jamming of the piston.

We were unable to obtain sensible measurements through the mush for the alloy CM186LC, in spite of several efforts, due to either leakage or jamming of the piston. After discussions with the partners it was decided to use the other results to indicate the expansion on melting.

4.1.3 Thermal diffusivity measurements

The laser pulse method entails heating a specimen to a specified temperature and then leaving it time to equilibrate before measuring the thermal diffusivity. Thus it is a *steady state technique* and not a *dynamic technique* like DTSC. Consequently, it is possible that recorded thermal diffusivity values for the γ/γ' transition range may refer to a structure with a greater degree of

transformation than that recorded by DTSC. Furthermore, the energy pulse supplied by the laser may be used to create an increased γ fraction.

For a similar reason thermal diffusivity values recorded in the (solid + liquid) region are erroneous since the energy pulse is partially used to produce further melting of the sample.

All the alloys appear to have similar values of the thermal diffusivities. In the solid the temperature dependence can be divided into two with a division at about 800°C. It is conjectured this is related again to the γ/γ' transition.
We experienced some difficulties in measuring the thermal diffusivity of all the alloys in the liquid state. We have therefore estimated them based on these limited values and previous work, which indicates that the thermal diffusivity is comparable to the solid at the solidus temperature.

4.2 MOULD RESULTS

4.2.1 Heat capacity

These measurements were characterized by relatively small signals especially at the higher temperatures. In order to obtain good thermal contact between the sample and the pan powder was used after attempting measurements with solid samples where the outputs appeared small, possible due to poor thermal contact between the sample and the pan wall.

The values of the heat capacity were similar to those expected from literature values of alumina, zirconia and silica and their relative proportions. It is suggested that the calculation of the heat capacity from the literature values for heat capacity of the constituents and their relative masses would be sufficient for many applications.

4.2.2 Mould density/expansion/shrinkage

Results from these tests were not always repeatable from sample to sample. It raises the problem of how homogeneous the moulds are and thus how representative the samples cut from them are likely to be. There is also a question about variations in local mechanical contact, which may lead to variations in apparent shrinkage.

Shrinkage of the mould increases with hold time and increasing temperature whereas the expansion and contraction are reasonably consistent. At the highest temperatures it is postulated that there is an expansion/contraction effect as well as creep of the mould contributing to changes in the dimensions. This last point is very important technically since the dimensional control of castings is paramount for many applications and the dimensional tolerances that can be achieved are critically dependent on the thermal cycle the mould experiences.

4.2.3 Thermal diffusivity

The measured values are low for the moulds and considerably reduced from the values for the consolidated oxides by typically a factor of 5 - 10. The temperature dependence of the thermal diffusivity is very similar to constituent oxides.

It is thought that although the values of thermal diffusivity of the moulds are useful and representative of UK practice, the higher uncertainty of measurement may need to be

addressed since the sensitivity analysis suggests the cooling rates are dominated by the thermal conductivity of the moulds.

4.2.4 Sensitivity analysis

Detailed curves showing the effects of altering the parameters are shown in Appendix C. The major findings are summarised as follows:

Parameter	Small	Medium	Large
Specific heat, C_p	Affects initial solidification time	Affects initial solidification time	Little effect
Thermal conductivity, λ	Strongly affects solidification time	Strongly affects solidification time	Dominates cooling
Heat transfer coefficient, h	Small effect	Small effect (more important where thick)	Small effect (more important where thick)

5. POTENTIAL FUTURE WORK

This study has shown that useful measurements of the major properties needed for modelling the solidification of investment castings can be achieved, and the industrial partners are already utilizing some of the results. However, there is still room for improvement of the application of the techniques:

1) The DTSC method used to measure the enthalpy and heat capacity works well provided that there are no enthalpy changes associated with phase changes. This is associated with the sluggish response of the thermocouples placed outside the sample and is particularly difficult in determining the melting range [7]. This was recognized at the outset of the project and was the reason for a preliminary study by one of the industrial partners to model the DSC. Also independent work [9] measuring the transition temperatures with different cooling rates and extrapolating these values to zero cooling rate is an improvement but time consuming. The problem has been largely solved at lower temperatures by the introduction of the single pan calorimeter where the thermocouple is placed directly in the sample [10, 6].

   Further work to model the DSC to correct for these failings and also the development of a single pan calorimeter to achieve higher temperatures is a possibility.

2) For the measurement of the density of the mush and liquid the piston dilatometer shows great promise, but further work is required to establish its limitations and to investigate possible solutions to problems of leakage and jamming.

3) The thermal diffusivity values for the moulds are low and we need to introduce new methods for analysing the data to achieve lower uncertainties of measurement. This would appear to be important since the results of the models appear to be sensitive to these values.

4) The dimensional control of castings is industrially important and the changes in dimensions with varying thermal cycles observed in this work highlight the difficulties. The dimensional control of moulds especially at high temperatures requires further investigation.

6. CONCLUSIONS

1) Heat capacity, enthalpy, enthalpy of fusion, fraction solid; thermal diffusivity and derived thermal conductivity; density and thermal expansion coefficient and solidus and liquidus temperatures for the four nickel base alloys CMSX10; Rene 80; IN738LC; CM186LC and Rene 80 were measured in the temperature range 700-1500°C.

2) Heat capacity, enthalpy; thermal diffusivity and derived thermal conductivity, density and thermal expansion coefficient; and shrinkage on firing were measured for eight industrially proprietary moulds.

3) The results for the moulds carry a higher uncertainty of measurement for thermal diffusivity and heat capacity compared with the alloy results. This is thought due to the greater structural inhomogenity of the moulds. For the thermal diffusivities experimental difficulties in measuring the very small values were experienced, whereas thermal contact was perceived as a problem for the heat capacity measurements.

4) For the moulds it is probably sufficient to estimate the heat capacity from the weighted values of the main constituents of the mould rather than direct measurement.

5) For the density (thermal expansion) of the moulds the results at high temperatures are particularly affected by the time at temperature. This indicates that the industrial processing conditions should be considered when estimating the change in dimensions of the mould. It is postulated that creep will also play some part in the change in dimensions.

6) Sensitivity analysis showed the total solidification time was strongly effected by the thermal conductivity of the mould; changes in the heat capacity did effect initial solidification time whereas the interfacial conductivity generally had a small effect although a greater effect for thick sections.

7) One of the industrial partners modelled the DSC and investigated the effects of poor thermal contact between specimen and sample.

7 REFERENCES

1. M.J. Richardson: *Compendium of Thermophysical Property Measurement Techniques, Vol. 2: Recommended Measurement Techniques and Practices,* edited K. Maglic *et al.*, publ. Plenum, New York, (1992), p 519.

2. R. Morrell and P N Quested, “Dilatometric Measurement of Melting Behaviour of Metal Alloys.” NPL Report CMMT (A) 106, March 1998.

3. W.J. Parker, R.J. Jenkins, C.P. Butler and G.L. Abbott, *J. of Appl. Phys.*, 1961, **32**, 1679

4. K.D. Maglic and R.E. Taylor, "An apparatus for thermal diffusivity measurement by the laser pulse method" in *Compendium of Thermophysical Property Measurement Methods Vol. 2, Recommended Measurement Techniques and Practices,* edited by K.D. Maglic, A. Cezairliyan and V.E. Peletsky, Plenum Press, New York, 1992. ISBN 0-306-433854-2.

5. L. Dusza, *High Temperatures-High Pressures*, 1995, **27**, 467.

6. H. Dong and J.D. Hunt, "Comparison of a novel single-pan calorimeter with a conventional heat-flux differential scanning calorimeter", *High Temperatures - High Pressures*, 2000, **32**(3), 311-319.

7. G. Höhne. W. Hemminger and H.J. Flammersheim, *Differential scanning calorimetry*, Springer Verlag, Berlin 1996.

8. T. Iida and R.I.L. Guthrie, *The Physical Properties of Liquid Metals*, Clarendon Press, Oxford, 1988, ISBN 0-19-856331-0.

9. L. Chapman, Unpublished results with the alloy CMSX4, October 2002.

10. L.A. Chapman and J.A.L. Robinson, "Improved Thermal Analysis by Single Pan Calorimetry", NPL Report MATC (D) 110, November 2002.

APPENDIX A - TEST RESULTS

A.1 SUMMARY OF MATERIALS INVESTIGATED

A.1.1 Alloys

NPL code	Alloy	Samples received	Chemical analysis	Enthalpy measurement	Density	TCE	Thermal diffusivity
PGA	**IN738LC**	Howmet End July 01	Yes	Complete	Solid & liquid complete	Complete	Solid complete Liquid values estimated
PGK	**CM186LC**	Cannon-Muskegon 09/10/01	Yes	Complete	Solid complete Liquid attempted - unsuccessful	Complete	Solid complete Liquid values estimated
PGZ	**CMSX10**	Cannon Muskegon 22/01/02	Yes	Complete	Solid & liquid complete	Complete	Solid Liquid attempted
PHC	**Rene 80**	Chromalloy End Jan 02	Yes	Complete	Solid & liquid complete	Complete	Solid Liquid values measured

A.1.2 Mould Materials

NPL code	Mould Type	Heat capacity	Density	Thermal diffusivity	Thermal Expansion	Firing Shrinkage	Micro-structure
PGB	Zircon water based slurry, molochite stucco	Y	Y	Y	Y	Y	Y
PGC	Fused silica water-based slurry, Cerametal 05-1 stucco	Y	Y	Y	Y	Y	Y
PGD	Dual System slurry, Cerametal 05-1 stucco	Y	Y	Y	Y	Y	Y
PGF	Non-disclosable	Y	Y	N	Y	Y	Y
PGM	Alumina –based	Y	Y	Y	Y	Y	Y
PGL	Alumina –based	Y	Y	Y	Y	Y	Y
PGN	Zircon/silica slurry with molochite stucco	Y	Y	Y	Y	Y	Y
PHG	Zircon Flour, silica Binder, stucco of alumina & molochite (aluminosilicate)	N	Y	Y	Y	Y	Y

A.2 ALLOY MATERIALS

A.2.1 IN738LC – code PGA

A.2.1.1 Chemical analysis

Element (%)	Cast Sample IN738LC	Typical IN738LC
C	0.1	0.11
Si	0.03	-
Mn	0.01	-
P	<0.005	-
S	0.001	-
Al	3.53	3.4
B	0.1	0.001
Co	8.26	8.5
Cr	15.85	16
Cu	<0.01	-
Fe	0.04	-
Mo	1.73	1.7
Nb	0.82	0.9
Ni	bal	Bal
Ta	1.73	1.7
Ti	3.49	3.4
W	2.57	2.6
Zr	0.03	0.005

Chemical Analysis by Howmet

A.2.1.2 Thermal diffusivity data

From room temperature until 750°C the equation can be used. Above 750°C the measurements are more variable with much flatter temperature dependence. These results have been corrected for expansion using data from the dilatometer.

Average measured values for solid thermal diffusivity of PGA (from minimum of three measurements)

T (°C)	PGA, heating a, 10^{-4} m^2 s^{-1}	T (°C)	PGA Cooling a, 10^{-4}m^2 s^{-1}
20	0.0266	750	0.0471
101	0.0285	719	0.0472
196	0.0314	707	0.0460
307	0.0348	425	0.0383
515	0.0401	209	0.0321
609	0.0432	110	0.0293
655	0.0449	-	-
705	0.0466	-	-
770	0.0468	-	-
808	0.0461	-	-
857	0.0472	-	-
912	0.0469	-	-
1005	0.0487	-	-
1080	0.0487	-	-

Fitted curve: Thermal diffusivity, $a = 2.86 \times 10^{-5} T + 0.0260$ [20°C >T< 750°C]

Values for Thermal Diffusivity of PGA from fitted curve

T °C	PGA a, 10^{-4} m^2 s^{-1}
20	0.0265
50	0.0274
100	0.0288
150	0.0303
200	0.0317
250	0.0331
300	0.0346
350	0.0360
400	0.0374
450	0.0388
500	0.0403
550	0.0417
600	0.0431
650	0.0446
700	0.0460
750	0.0474

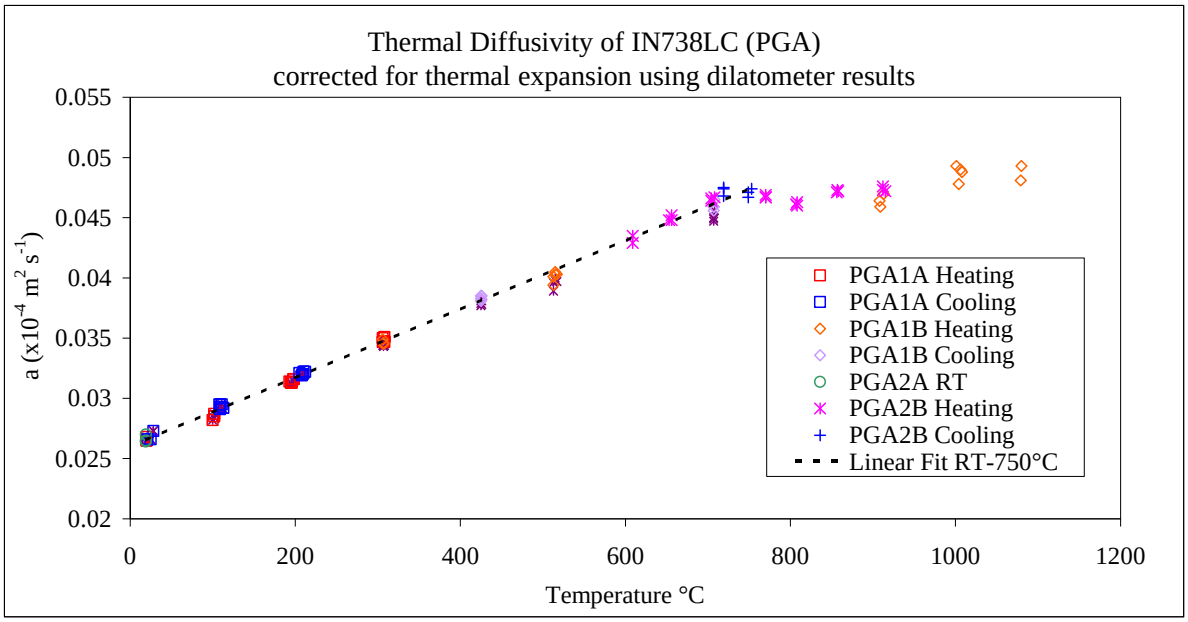

From previous work the value of thermal diffusivity in the liquid is estimated at 0.05×0^{-4} $m^2 s^{-1}$.

A.2.1.3 Heat Capacity and Enthalpy Data

Cp in J/g/K

PGA	860°C	900°C	950°C	1000°C	1050°C	1100°C	1150°C	1190°C	1250°C	1300°C	1350°C	1400°C
heat 1	0.65	0.67	0.71	0.79	0.87	0.98	1.02	0.74	0.69	4.45	0.67	0.70
heat 2	0.63	0.65	0.67	0.72	0.77	0.85	0.91	0.61	0.88	3.79	0.72	0.70
heat 3	0.64	0.67	0.70	0.76	0.81	0.88	0.93	0.62	0.91	3.63	0.72	0.68
ave	**0.64**	**0.66**	**0.69**	**0.76**	**0.82**	**0.90**	**0.95**	**0.66**	**0.83**	**3.95**	**0.70**	**0.69**
PGA	**860°C**	**900°C**	**950°C**	**1000°C**	**1050°C**	**1100°C**	**1150°C**	**1190°C**	**1250°C**	**1300°C**	**1350°C**	**1400°C**
cool 1	0.64	0.69	0.78	0.89	1.01	1.18	0.73	0.71	2.09	1.05	0.99	-
cool 2	0.64	0.87	0.78	0.88	1.01	1.18	0.72	0.72	2.03	2.75	0.96	-
cool 3	0.65	0.70	0.79	0.91	1.05	1.20	0.75	0.73	2.03	4.45	0.96	-
ave	**0.64**	**0.75**	**0.79**	**0.90**	**1.02**	**1.19**	**0.73**	**0.72**	**2.05**	**2.75**	**0.97**	**-**

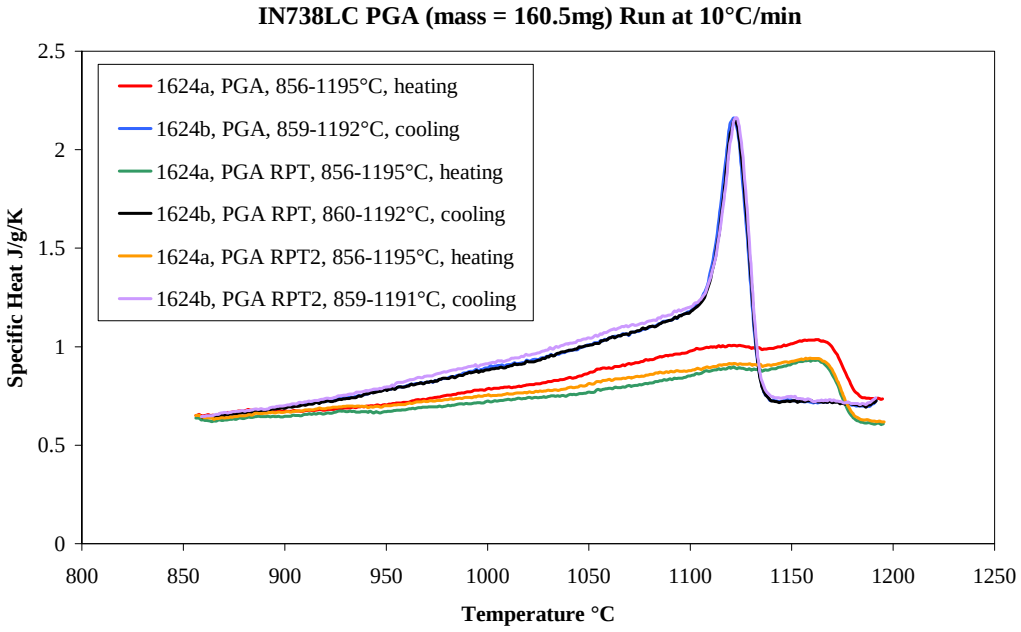

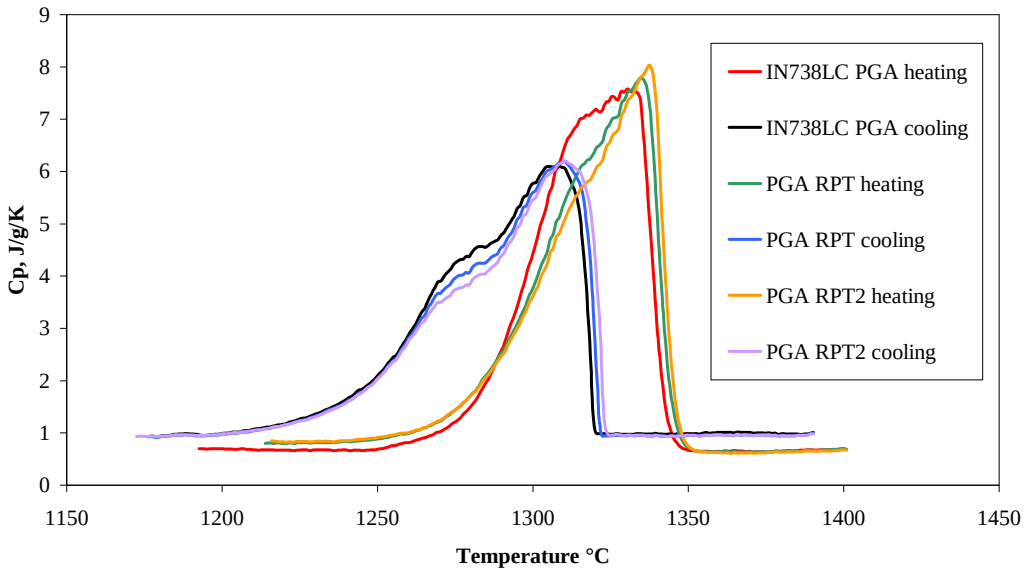

PGA	Solidus, °C	Liquidus, °C	Enthalpy, J/g
heat 1	1246	1352	289.5
heat 2	1235	1356	278.6
heat 3	1237	1357	277.3
ave	**1239**	**1355**	**281.8**
PGA	**Solidus**	**Liquidus**	**Enthalpy, J/g**
cool 1	1178	1323	259.3
cool 2	1178	1332	251.1
cool 3	1178	1324	258.8
ave	**1178**	**1326**	**256.4**

IN738LC PGA Run at 10°C/min

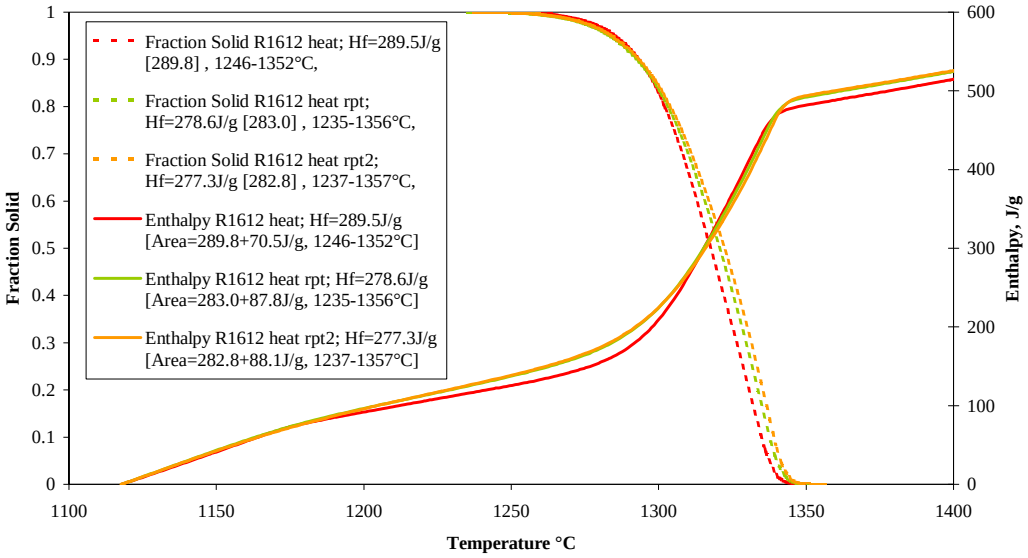

IN738LC PGA Run at 10°C/min

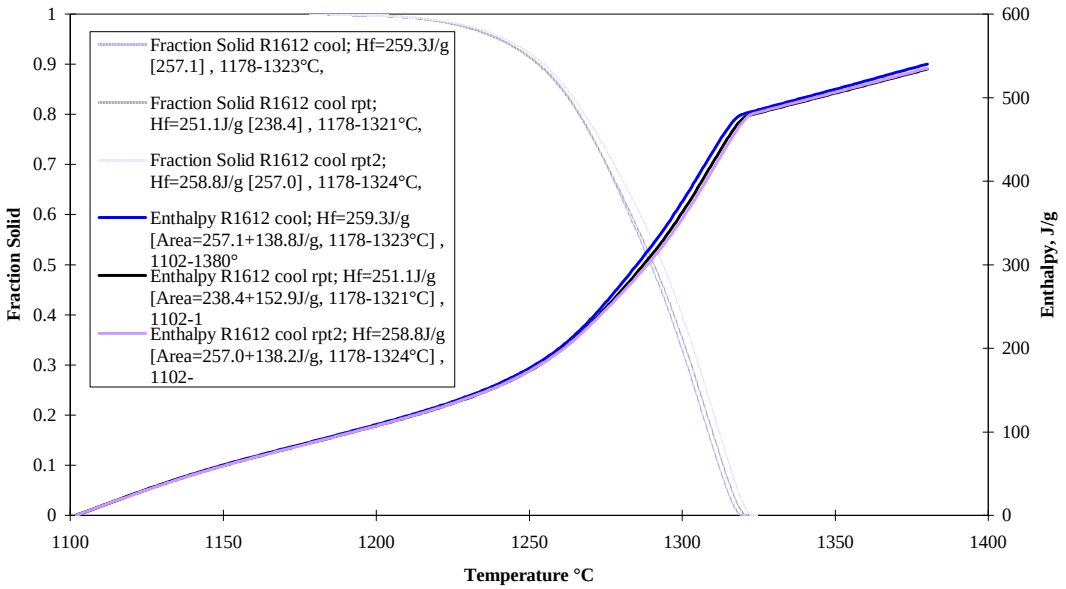

A.2.1.4 Thermal expansion and melting behaviour data on IN738LC

1. Solid thermal expansion

Temperature, °C	Fractional length change, ppm	Mean coefficient from 25 °C to temp, 10^{-6} K^{-1}	Expansivity at temperature, 10^{-6} K^{-1}	Density, Mg m^{-3}
25	0		13.6	8.177
50	230	9.2	13.5	8.171
100	860	11.5	13.4	8.156
150	1510	12.1	13.4	8.140
200	2170	12.4	13.4	8.124
250	2860	12.7	13.5	8.107
300	3560	12.9	13.6	8.091
350	4280	13.2	13.8	8.073
400	5010	13.4	14.1	8.056
450	5750	13.5	14.5	8.038
500	6490	13.7	15.0	8.021
550	7260	13.8	15.6	8.003
600	8070	14.0	16.4	7.984
650	8900	14.2	17.2	7.964
700	9780	14.5	18.2	7.944
750	10660	14.7	19.4	7.924
800	11630	15.0	20.6	7.901
850	12650	15.3	22.1	7.878
900	13730	15.7	23.7	7.854
950	14930	16.1	25.5	7.826
1000	16260	16.7	27.5	7.797
1050	17760	17.3	29.6	7.763
1100	19450	18.1	32.0	7.726
1150	21650	19.2	34.6	7.678
1200	23110	19.7	37.4	7.647
1250	24330	19.9	40.4	7.621

Solid state phase change visible at about 1150 °C, leading to reduction in expansivity above this temperature, not fully reflected in data in table above.

Temperature for onset of collapse in melting: 1300 °C
Temperature of liquidus: 1332 °C

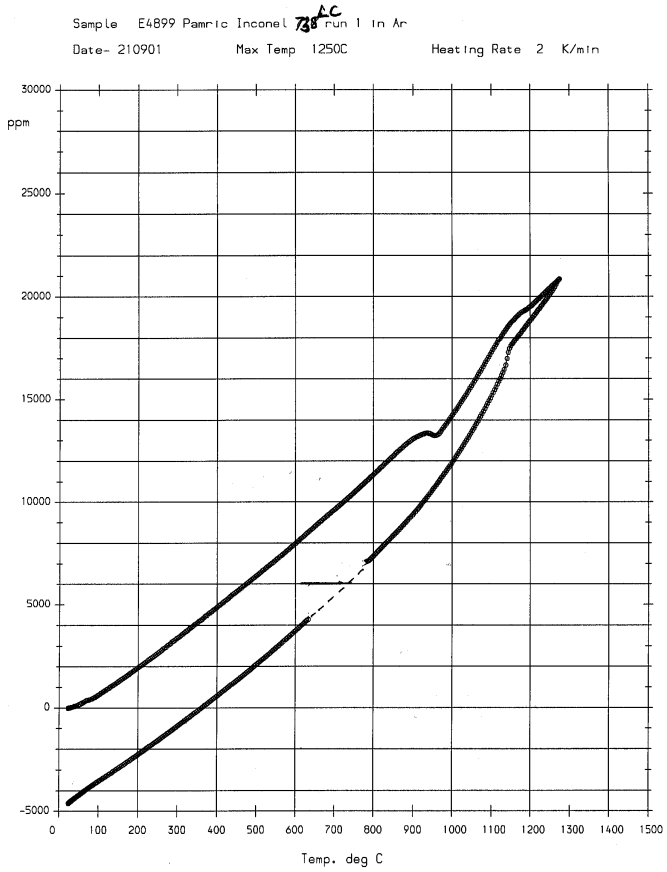
Sample E4899 Pamric Inconel 738LC run 1 in Ar
Date- 210901
Max Temp 1250C
Heating Rate 2 K/min
ppm
30000
25000
20000
15000
10000
5000
0
-5000
0 100 200 300 400 500 600 700 800 900 1000 1100 1200 1300 1400 1500
Temp. deg C

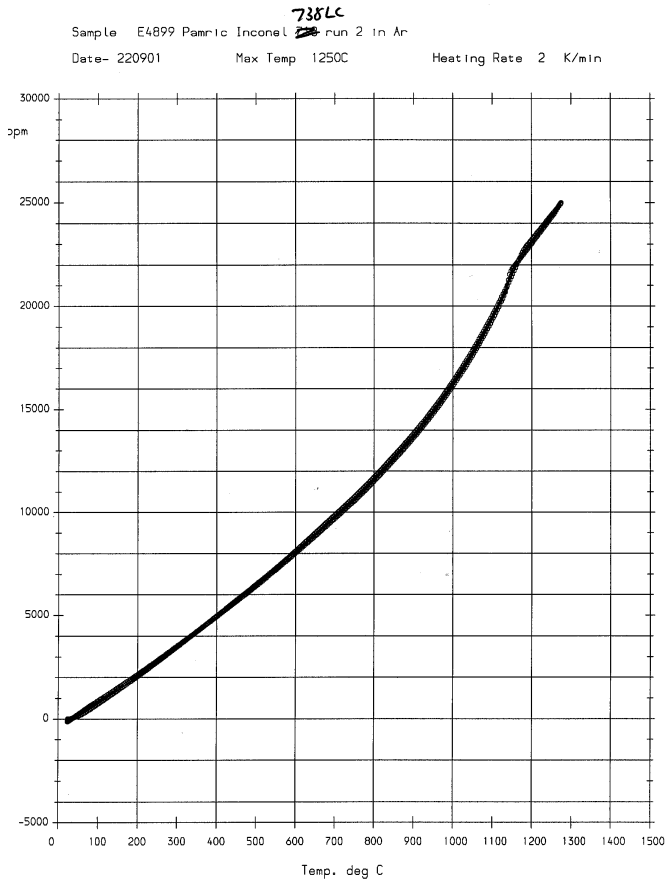
Sample E4899 Pamric Inconel 738LC run 2 in Ar
Date- 220901
Max Temp 1250C
Heating Rate 2 K/min
ppm
30000
25000
20000
15000
10000
5000
0
-5000
0 100 200 300 400 500 600 700 800 900 1000 1100 1200 1300 1400 1500
Temp. deg C

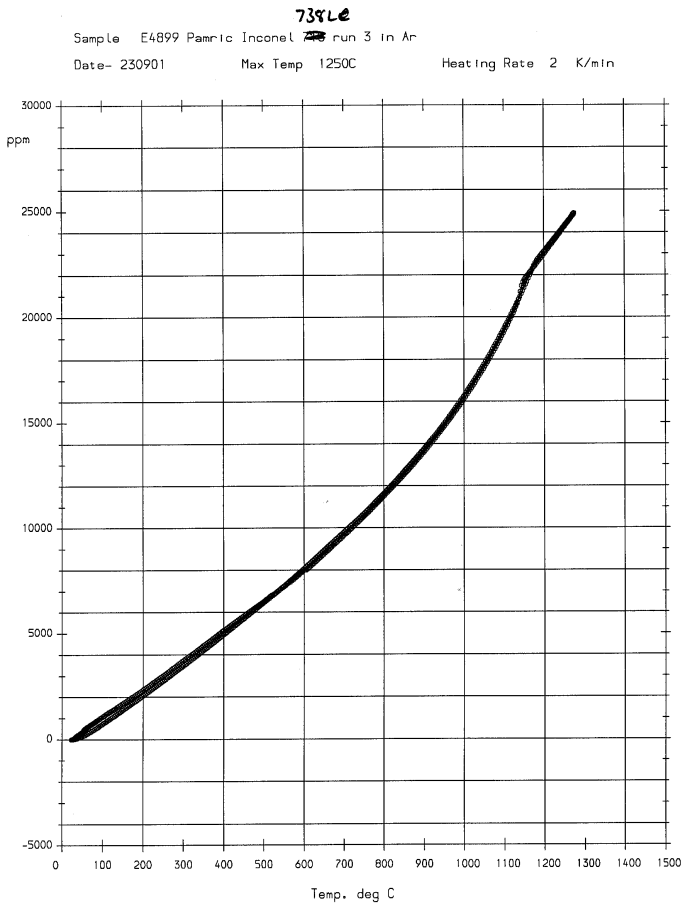
738LC
Sample E4899 Pamric Inconel run 3 in Ar
Date- 230901
Max Temp 1250C
Heating Rate 2 K/min
ppm
30000
25000
20000
15000
10000
5000
0
-5000
0
100
200
300
400
500
600
700
800
900
1000
1100
1200
1300
1400
1500
Temp. deg C

2. Melting behaviour

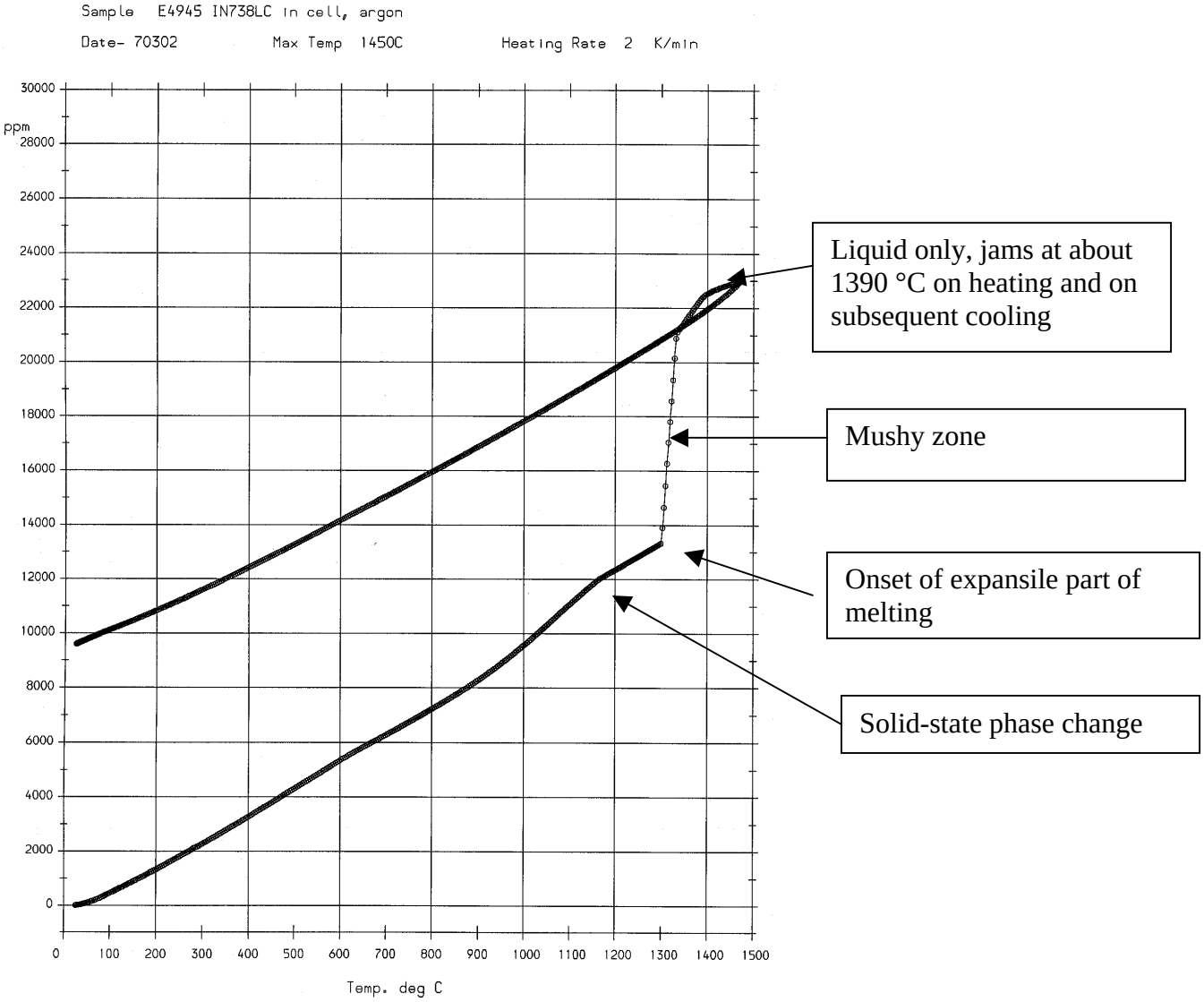

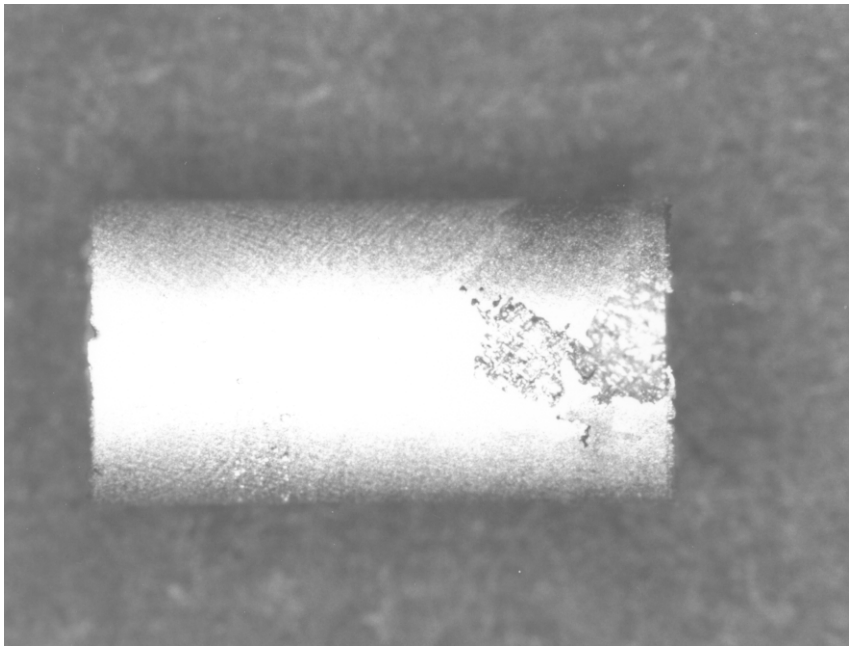

IN738LC sample after running in cell – note 'sucking in' due to lack of feeding.

2 mm

Apparent expansion of sample in cell after correction for expansion of pistons:

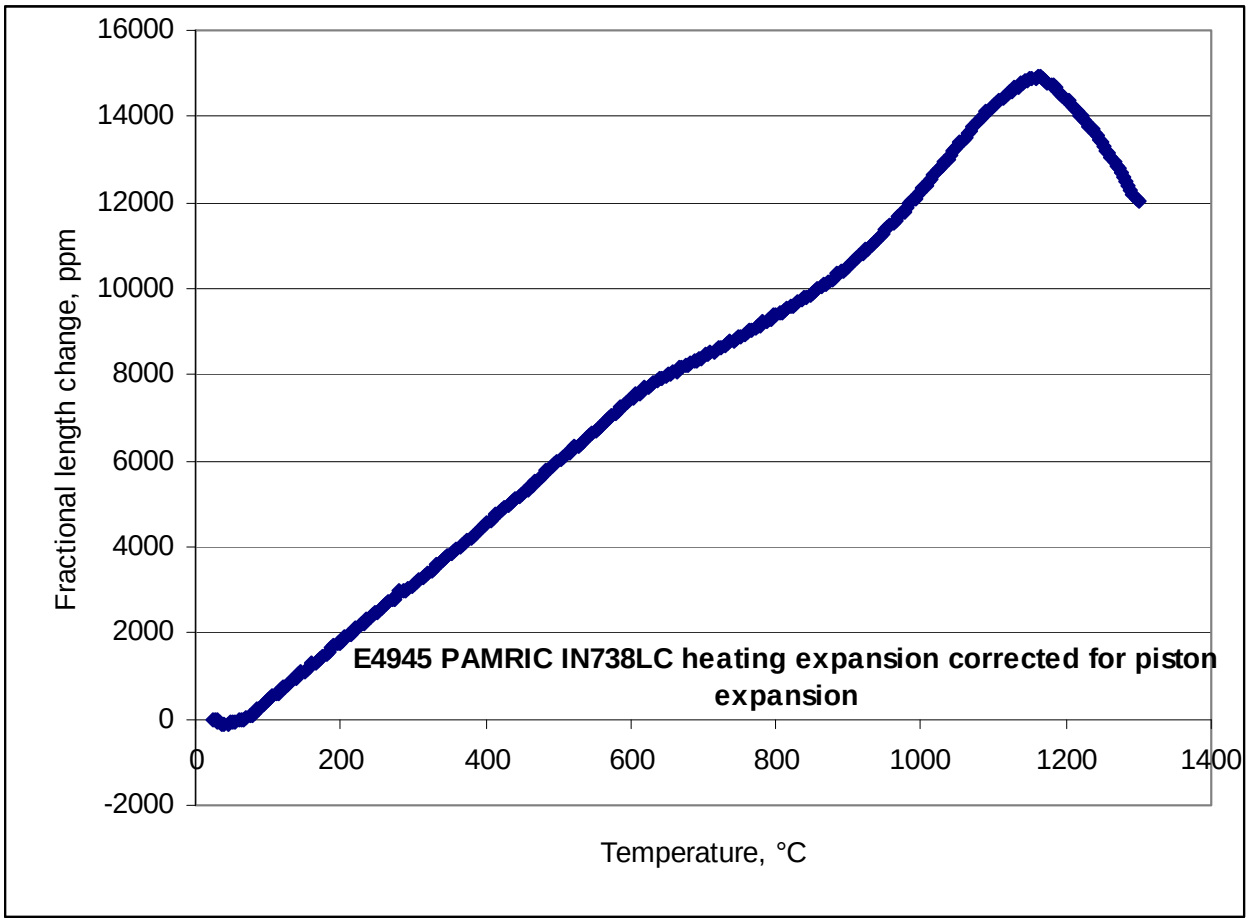

Note apparent softening above 1100 °C.

Apparent metal density in mushy zone and during melting:

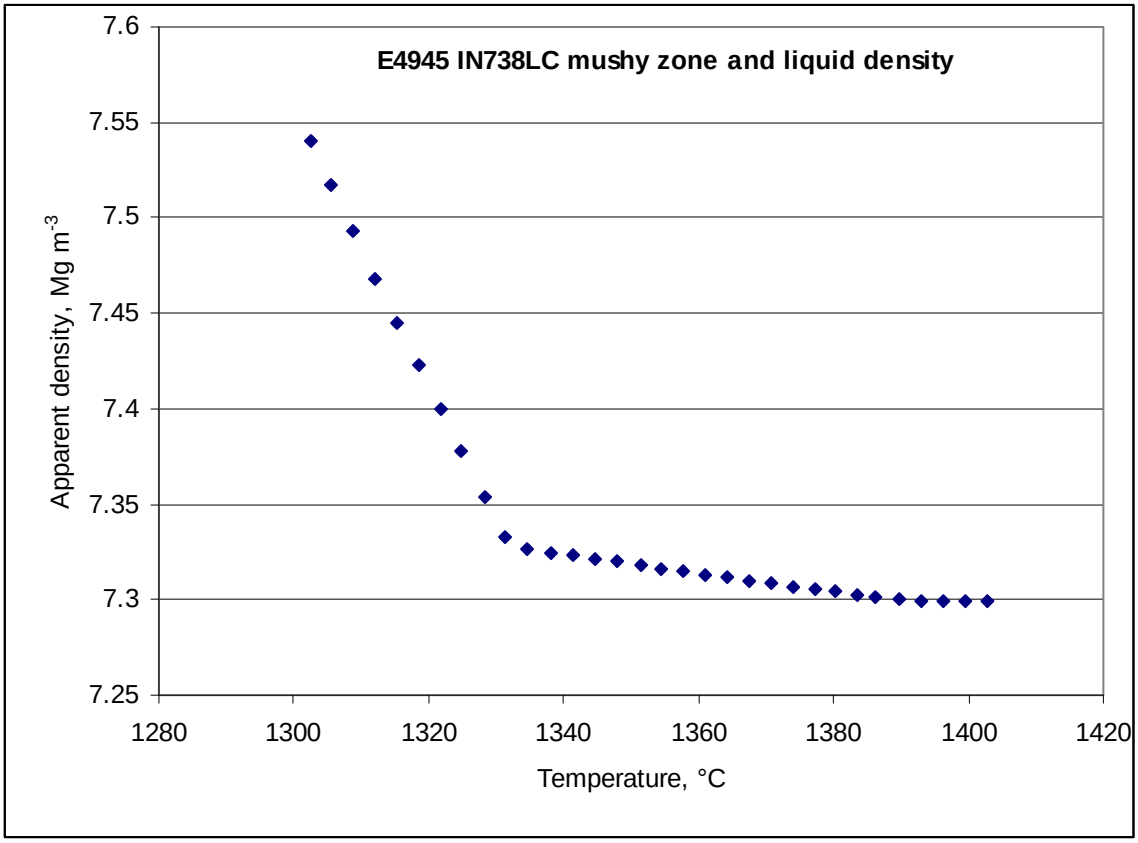

Apparent cubical expansion coefficient of liquid metal is 66 x 10^{-6} K^{-1}:

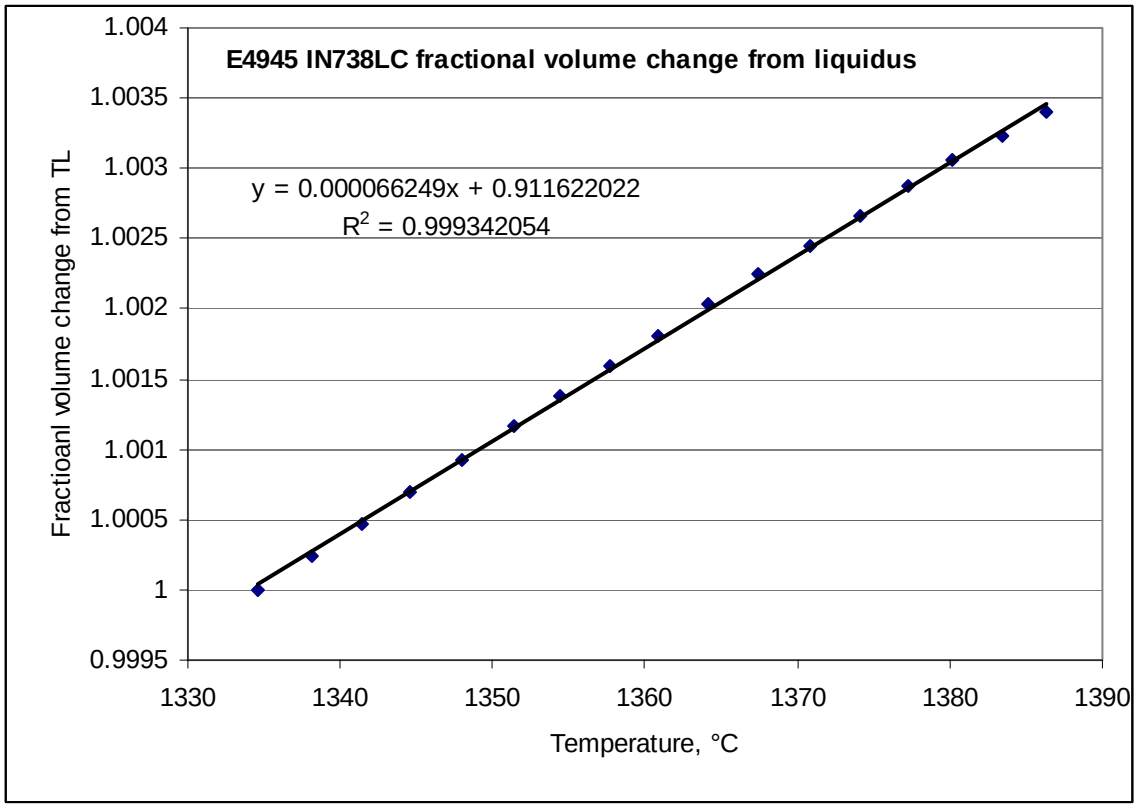

Density of IN738LC as a function of temperature from solid data and from cell melting data:

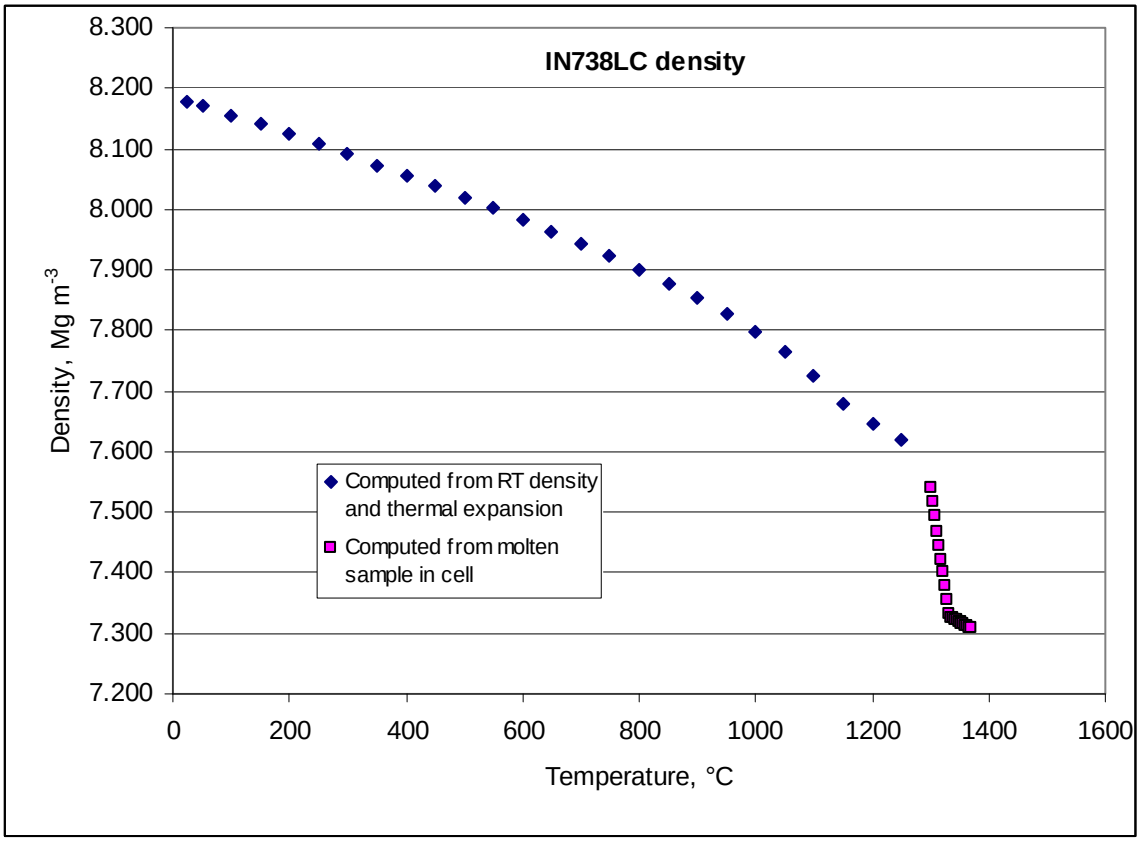

IN738LC – density in the mush and liquid from piston dilatometry

Temperature, °C	Density, Mg m^{-3}	
	Mush	Liquid
1300	7.559	-
1310	7.484	-
1320	7.411	-
1330	7.342	-
1340	-	7.324
1350	-	7.319
1360	-	7.314
1370	-	7.309

A.2.2 CM186LC – code PGK

A.2.2.1 Chemical analysis

Element (%)	PGK (CM186LC®)	Typical CM186LC
Co	9.4	9
Cr	6.0	6
W	8.5	8
Mo	.50	0.5
Ta	3.5	3
Re	2.9	3
Al	5.74	5.7
Ti	.74	0.7
Hf	1.32	1.4
C	<.05	0.007
B	.015	0.015
Zr	.004	0.005
Si	<.05	-
Mn	<.01	-
Cu	<.01	-
Fe	<.05	-
Hf	1.32	-
P	<.005	-
V	<.01	-
Ni	bal	bal

Chemical Analysis by Cannon Muskegon

A.2.2.2 Heat capacity, J/g/K and enthalpy, J/g

PGK	860°C	900°C	950°C	1000°C	1050°C	1100°C	1150°C	1200°C	1250°C	1300°C	1350°C	1400°C
heat 1	0.63	0.62	0.63	0.66	0.71	0.77	0.89	0.97	1.02	1.27	4.97	0.75
heat 2	0.62	0.62	0.64	0.67	0.71	0.76	0.94	1.02	1.05	1.38	4.31	0.72
heat 3	0.62	0.62	0.62	0.66	0.70	0.74	0.88	0.94	0.96	1.26	4.04	0.69
ave	**0.62**	**0.62**	**0.63**	**0.66**	**0.70**	**0.76**	**0.90**	**0.98**	**1.01**	**1.30**	**4.44**	**0.72**
PGK	**860°C**	**900°C**	**950°C**	**1000°C**	**1050°C**	**1100°C**	**1150°C**	**1200°C**	**1250°C**	**1300°C**	**1350°C**	**1400°C**
cool 1	0.62	0.66	0.72	0.80	0.87	0.94	0.95	1.17	1.14	2.30	5.16	-
cool 2	0.62	0.66	0.72	0.79	0.87	0.95	0.96	1.13	1.11	2.22	5.08	-
cool 3	0.61	0.65	0.71	0.79	0.86	0.93	0.97	1.13	1.10	2.13	5.04	-
ave	**0.62**	**0.65**	**0.72**	**0.79**	**0.87**	**0.94**	**0.96**	**1.14**	**1.12**	**2.22**	**5.09**	**-**

CM186LC PGK (mass = 164.20 mg) Run at 10.0°C/min,

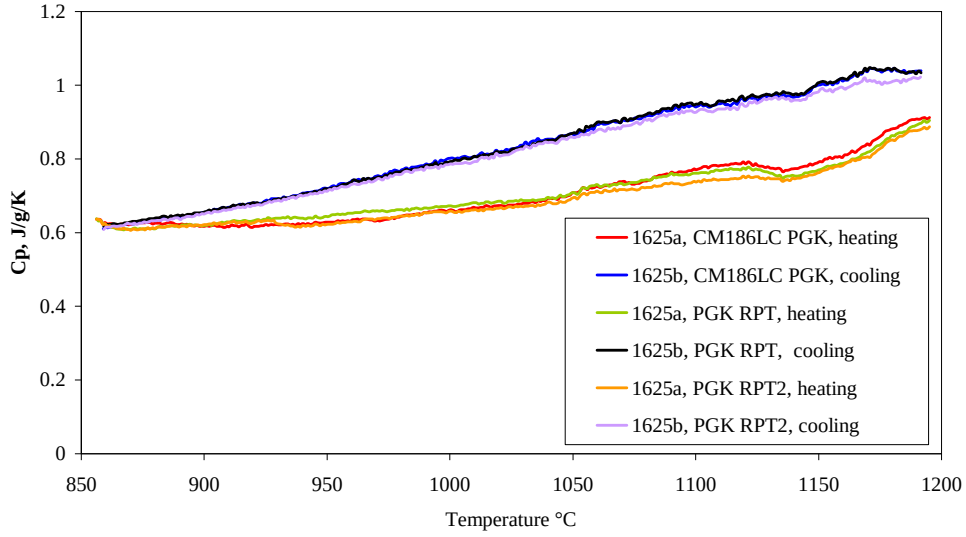

CM186LC PGK (mass = 159.40 mg) Run at 10°C/min

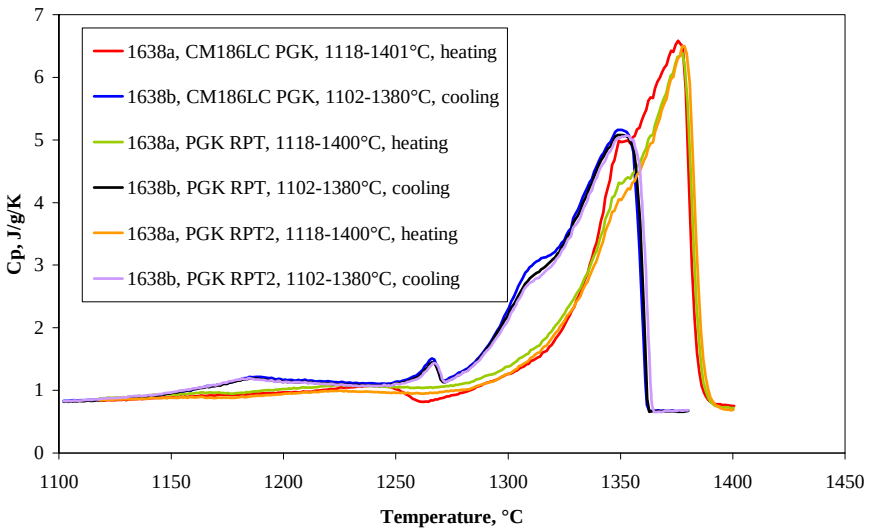

Heating	Solidus, °C	Liquidus, °C	Enthalpy J/g
Heat 1	1265	1391	245.4
Heat 2	1268	1392	221.9
Heat 3	1266	1395	225.4
Ave	1266	1393	230.9
Cooling	**Solidus, °C**	**Liquidus, °C**	**Enthalpy J/g**
Cool 1	1241	1363	189.5
Cool 2	1243	1364	188
Cool 3	1248	1366	189
Ave	1244	1364	188.8

CM186LC PGK (mass = 159.40 mg) Run at 10°C/min

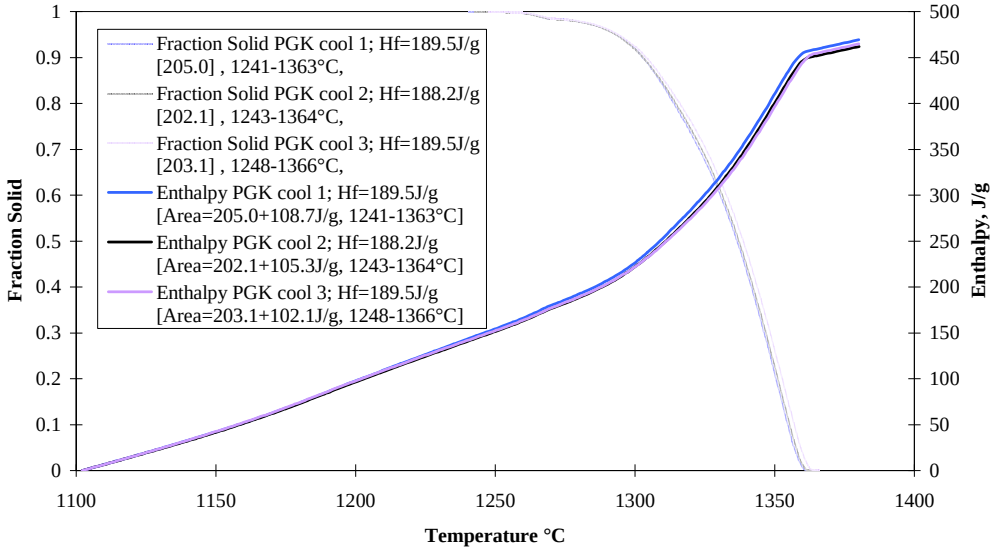

CM186LC PGK (mass = 159.40 mg) Run at 10°C/min

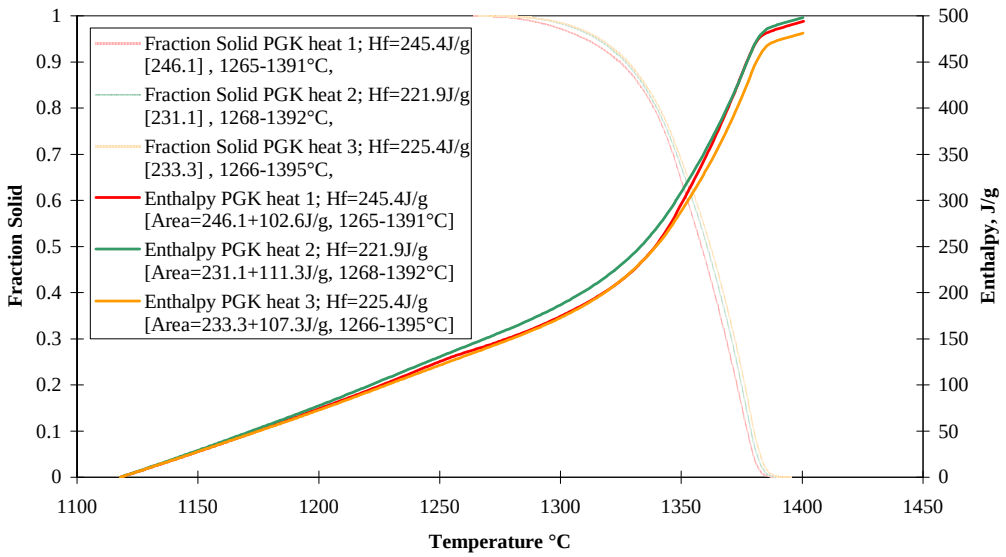

A.2.2.3 Thermal diffusivity

From room temperature until 800°C the formula can be used. These results are corrected for thermal expansion using the expansion values given on p37.

Thermal diffusivity, $a = 2.92 \times 10^{-5} T + 0.0218$ [20°C>T<800°C]

Average measured thermal diffusivity values for PGK

T, °C (T1)	PGK1 Heating	T (°C) (T1)	PGK1 Cooling
12	0.0220	920	0.0445
18	0.0227	820	0.0454
100	0.0246	631	0.0406
202	0.0278	426	0.0340
309	0.0311	314	0.0306
423	0.0346	197	0.0269
530	0.0371	-	-
629	0.0402	-	-
817	0.0456	-	-
1008	0.0450	-	-
1158	0.0475	-	-

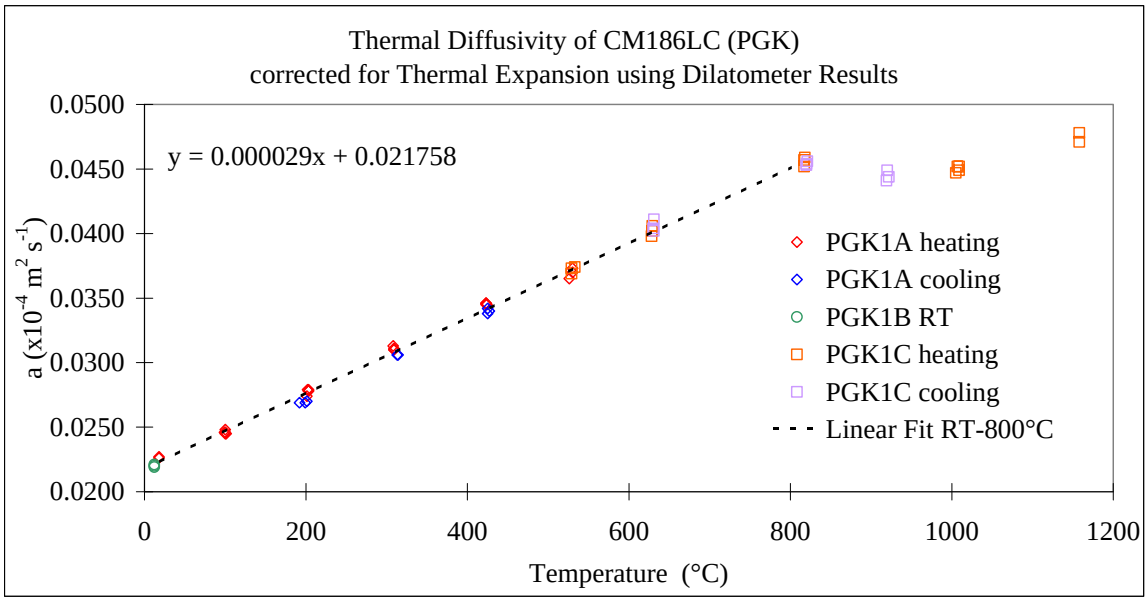

Fitted thermal diffusivity values for PGK

T °C	a, 10^{-4} m^2 s^{-1}
20	0.0223
50	0.0232
100	0.0247
150	0.0261
200	0.0276
250	0.0291
300	0.0305
350	0.0320
400	0.0334
450	0.0349
500	0.0364
550	0.0378
600	0.0393
650	0.0407
700	0.0422
750	0.0437
800	0.0451

Estimated value of thermal diffusivity in the liquid 0.05×10^{-4} m^2 s^{-1}.

A.2.2.4 Thermal expansion and melting behaviour data on CM186LC

1. Solid thermal expansion

Temperature, °C	Fractional length change, ppm	Mean coefficient from 25 °C to temp, 10^{-6} K^{-1}	Expansivity at temperature, 10^{-6} K^{-1}	Density, Mg m^{-3}
25	0	-	-	8.689
50	235	9.4	-	8.683
100	770	10.3	-	8.669
150	1360	10.9	13.6	8.654
200	1980	11.3	13.5	8.638
250	2650	11.8	13.6	8.620
300	3330	12.1	13.7	8.603
350	4010	12.3	13.9	8.586
400	4710	12.6	14.1	8.568
450	5430	12.8	14.4	8.550
500	6150	12.9	14.8	8.532
550	6880	13.1	15.2	8.513
600	7620	13.3	15.7	8.495
650	8400	13.4	16.3	8.475
700	9210	13.6	16.9	8.455
750	10030	13.8	17.6	8.435
800	10880	14.0	18.3	8.414
850	11800	14.3	19.1	8.392
900	12770	14.6	20.0	8.368
950	13810	14.9	21.0	8.343
1000	14940	15.3	22.0	8.316
1050	16160	15.8	23.0	8.287
1100	17500	16.3	24.2	8.256
1150	18970	16.9	25.3	8.221
1200	20600	17.5	26.6	8.183

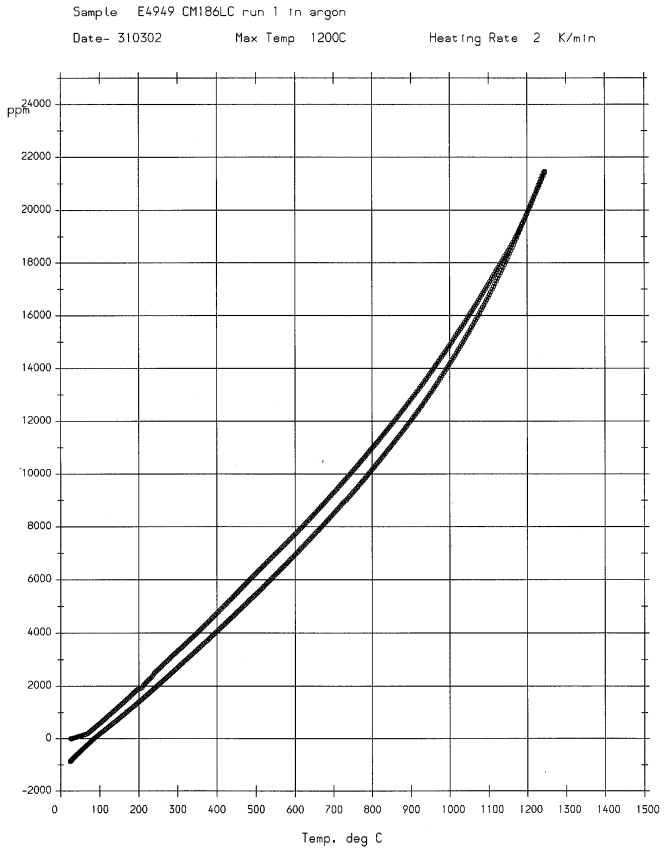
Sample E4949 CM186LC run 1 in argon
Date- 310302
Max Temp 1200C
Heating Rate 2 K/min
ppm
24000
22000
20000
18000
16000
14000
12000
10000
8000
6000
4000
2000
0
-2000
0 100 200 300 400 500 600 700 800 900 1000 1100 1200 1300 1400 1500
Temp. deg C

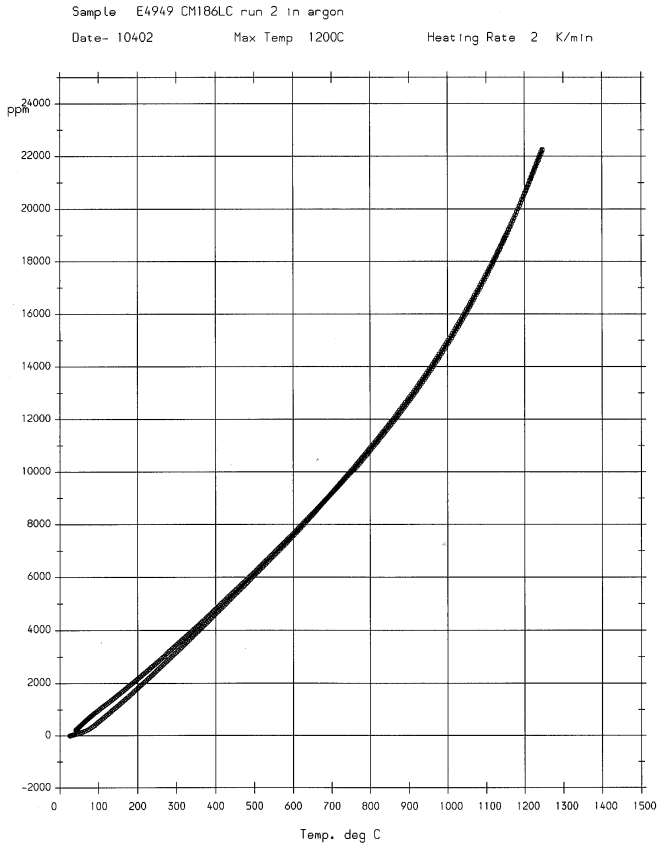
Sample E4949 CM186LC run 2 in argon
Date- 10402
Max Temp 1200C
Heating Rate 2 K/min
ppm
24000
22000
20000
18000
16000
14000
12000
10000
8000
6000
4000
2000
0
-2000
0 100 200 300 400 500 600 700 800 900 1000 1100 1200 1300 1400 1500
Temp. deg C

2. Melting experiment

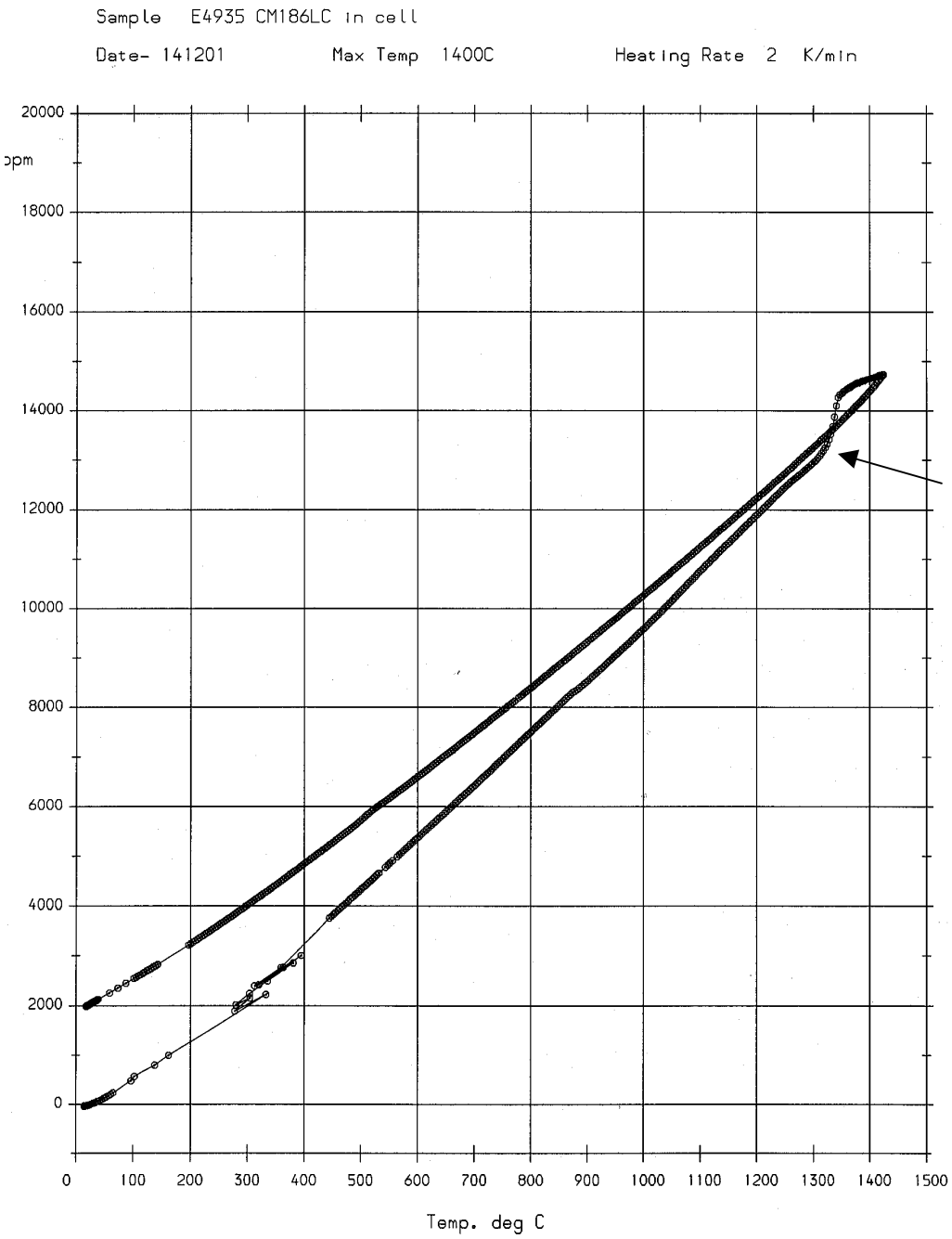

Indistinct melting characteristics. Sample jammed, liquid wicking along pistons.

Suspected onset of melting: 1310 °C
Suspected completion of melting: 1340 °C

However, melting is not a sharply defined effect, and this curve is suspicious.

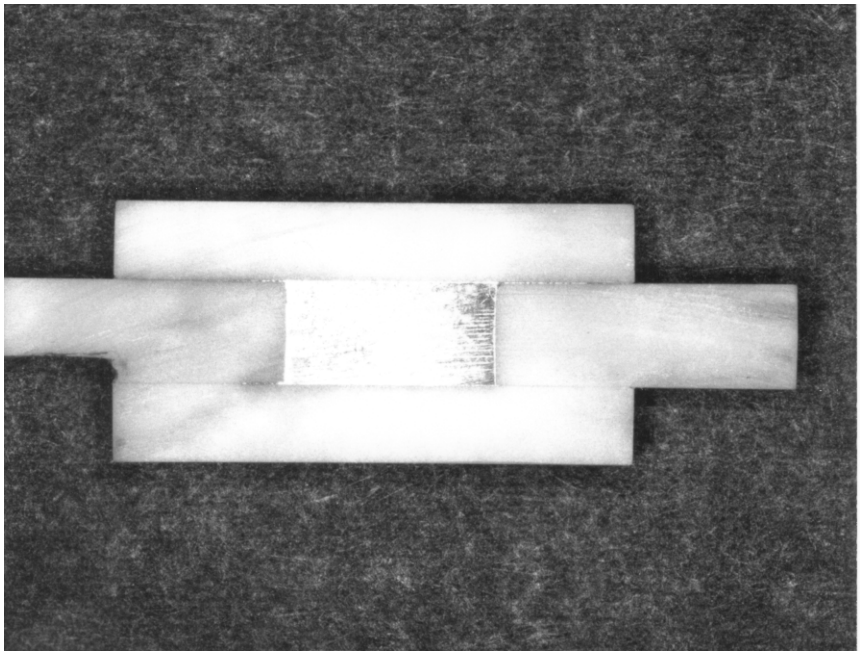

5 mm

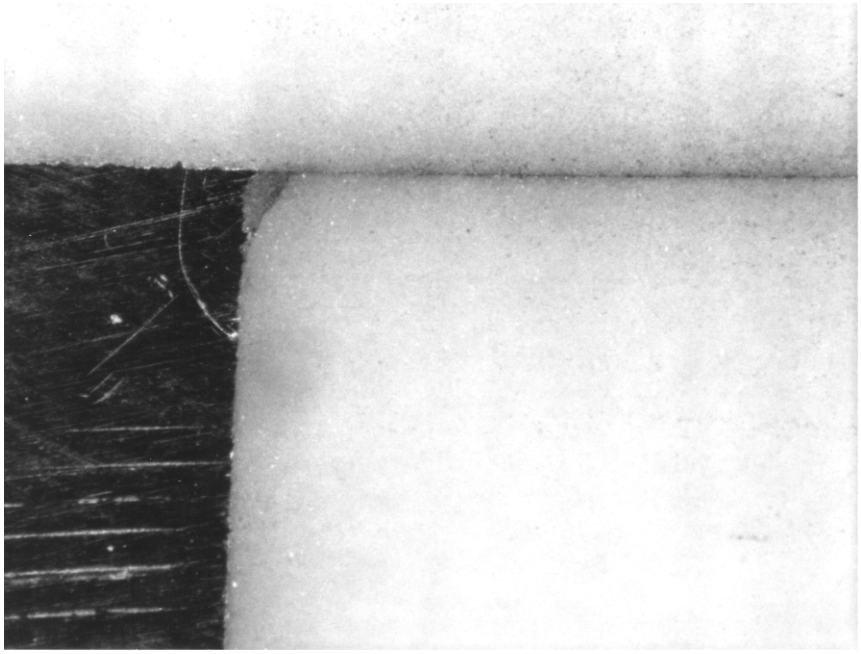

Melt infiltrating down piston/cylinder gap

1 mm

There was clear evidence of the piston/cylinder system leaking. The system could not be disassembled, and so was cut in half lengthways to reveal the problem. This showed that metal had infiltrated along the piston/cylinder gap, in some places to the outside. This reduces the volume of metal between the pistons, and jams the system with reaction products.

Apparent expansion of sample in cell:

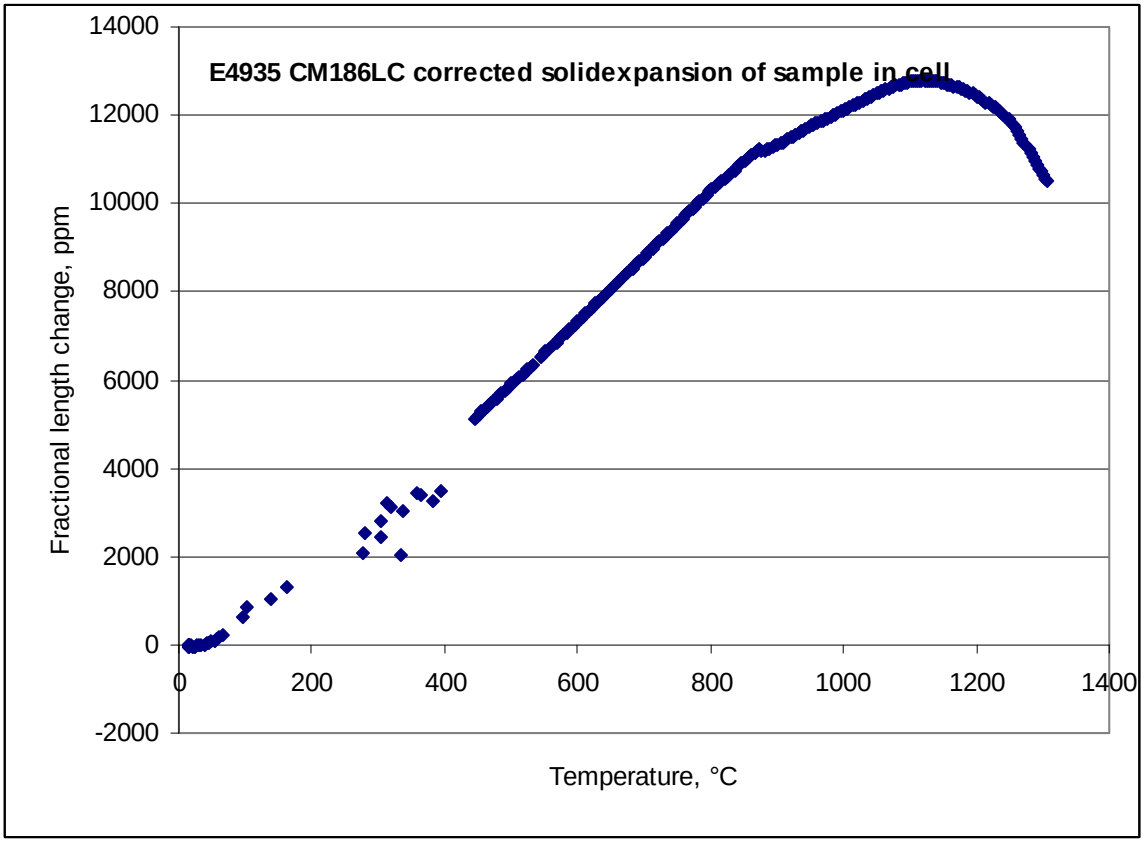

Apparent melting curve:

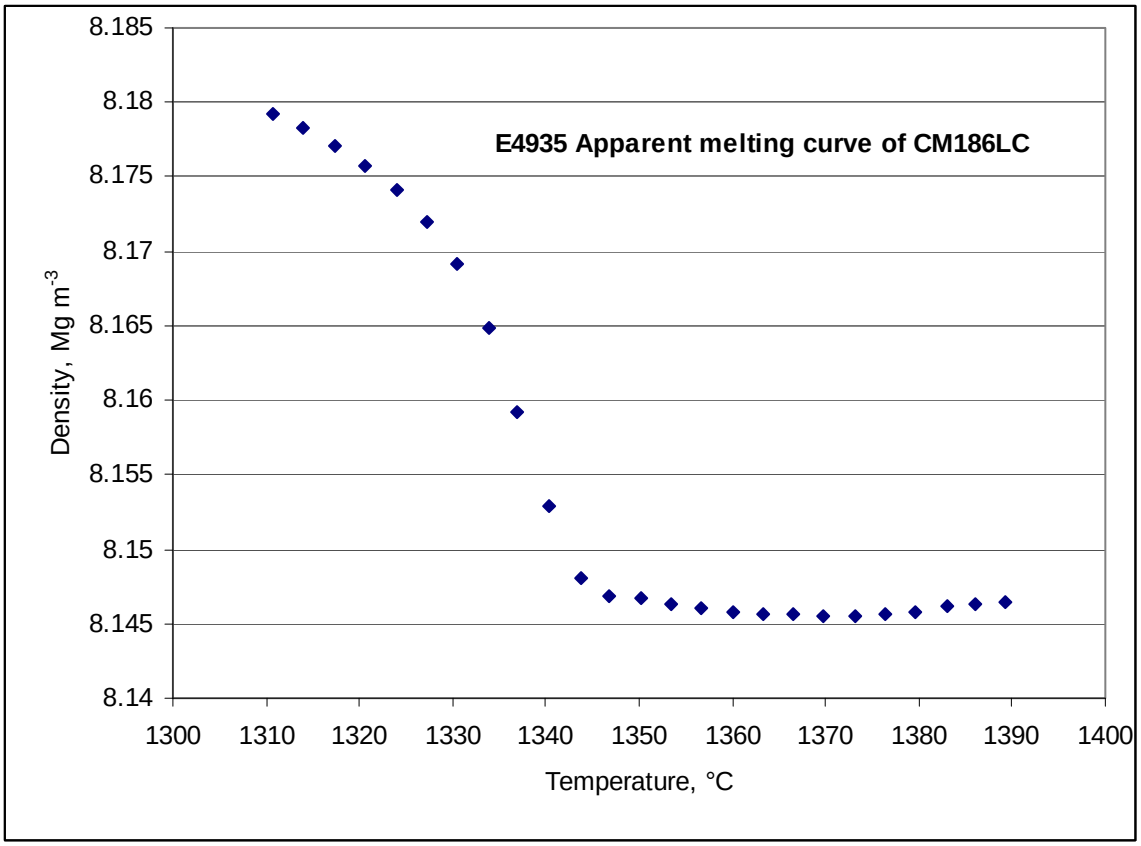

This plot does not show abrupt features like the others. Probably not real.

Apparent density as a function of temperature:

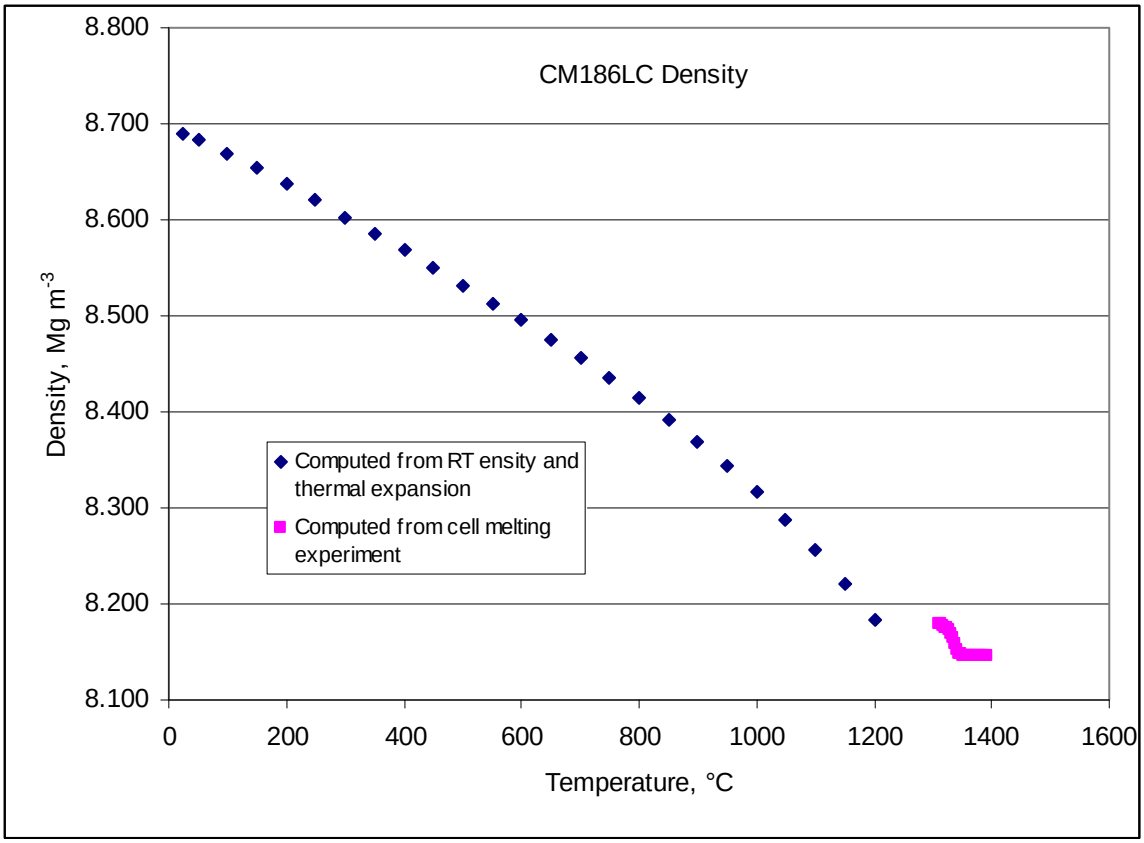

The liquid densities would appear to be overestimated because of leakage and jamming.

CM186LC– density in the mush and liquid from piston dilatometry

Temperature, °C	Density, Mg m^{-3}	
	Mush	Liquid
1300	-	-
1310	8.178	-
1320	8.177	-
1330	8.169	-
1340	8.155	-
1350	-	8.147
1360	-	8.146
1370	-	8.146

(Note these data are likely to be biased high by leakage from the cell. They should be treated with caution, and as indicative of trends only. More probable values are closer to 8.0 Mg m^{-3}).

Second attempt – oxidised sample

Dilatometer output:

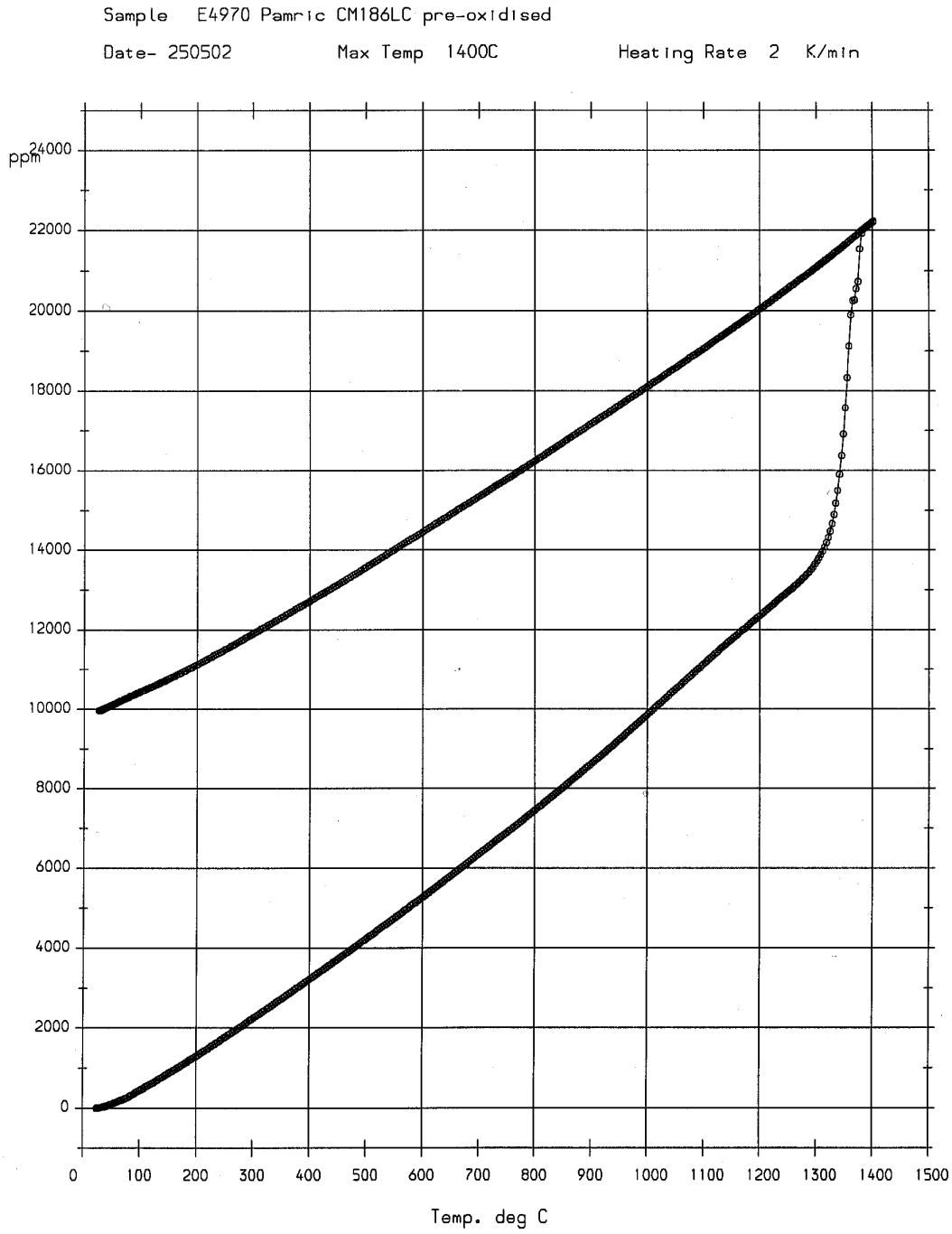

Apparent liquid production temperature	1295°C
Liquidus temperature	1385 °C
Max temp of run	1405°C
Cubical expansion coefficient heating	16.6 x 10^{-6} K^{-1}
Cubical expansion coeff, cooling	17.6 x 10^{-6} K^{-1}

Computed density from cell volume data:

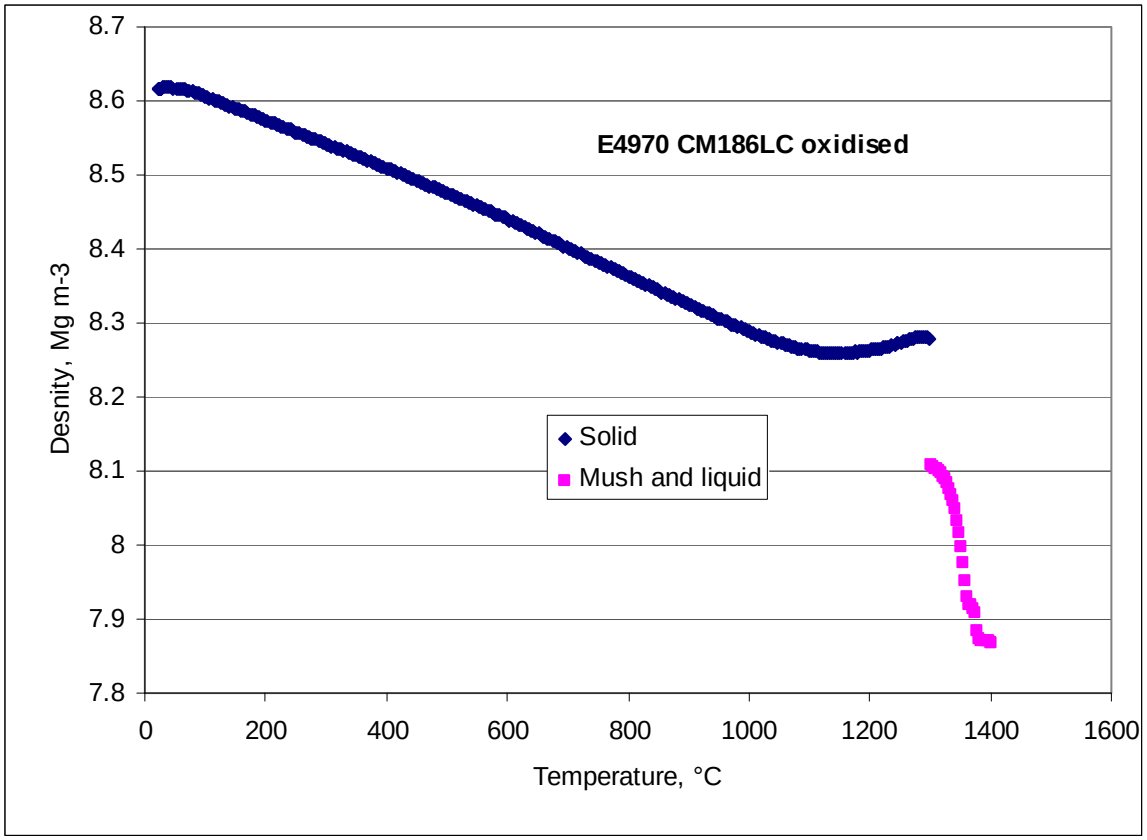

Computed mushy zone and liquid density:

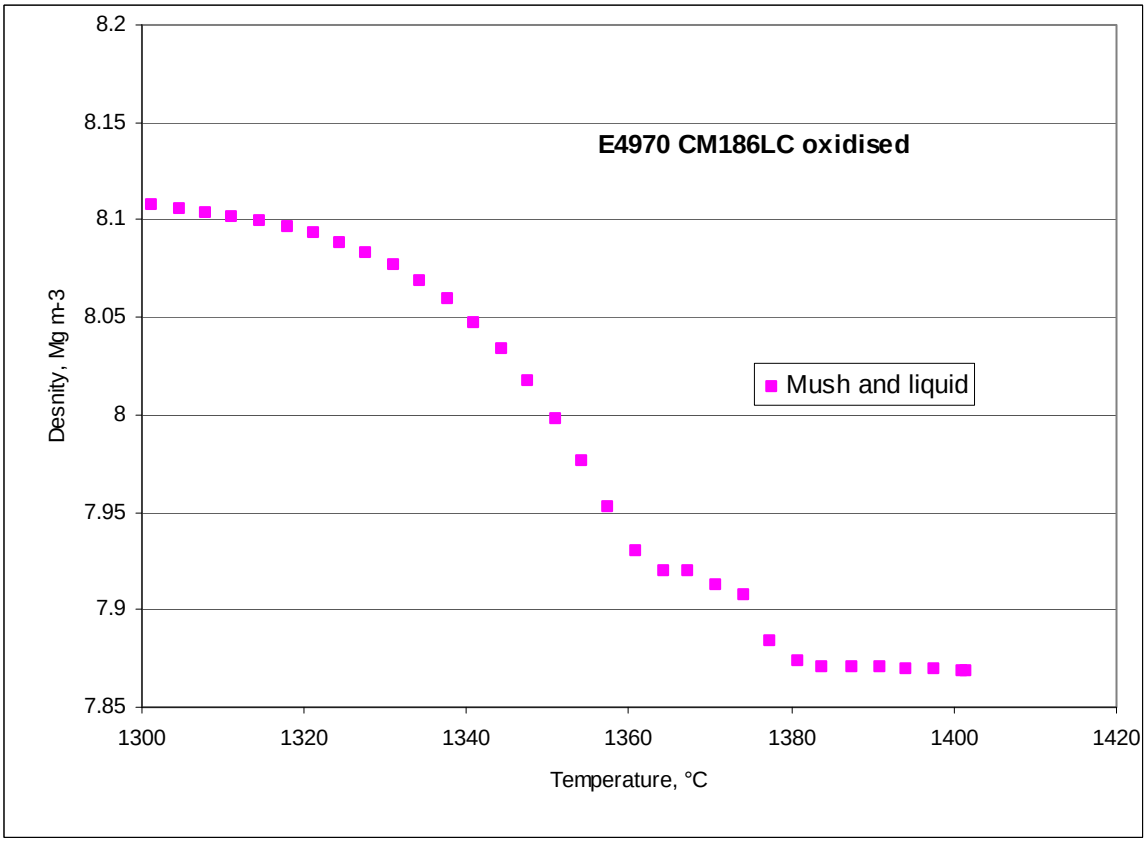

Computed fractional volume change in liquid with temperature:

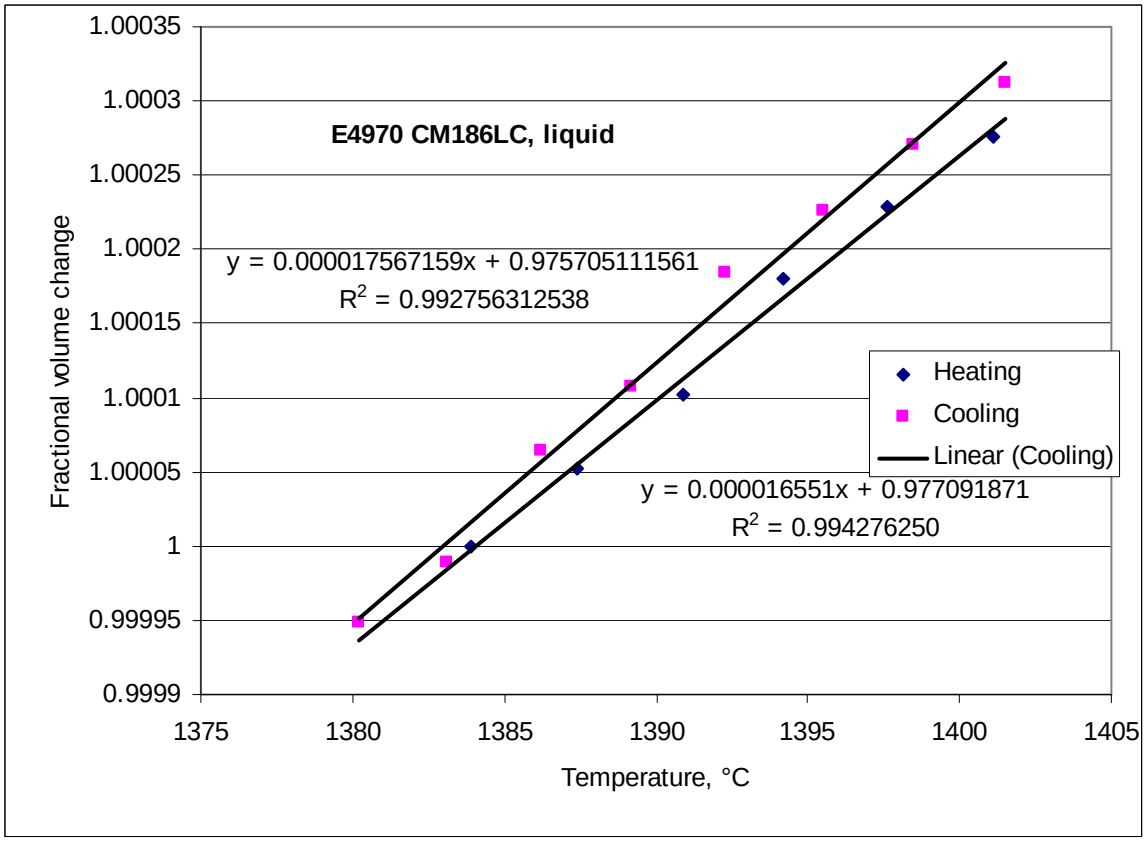

A.2.3 CMSX10 – code PGZ

A.2.3.1 Chemical analysis

Element (%)	CMSX10 (PGZ) Chemical Analysis
Cr	2.3
Co	3.4
Mo	.41
W	5.6
Ta	8.3
Re	6.4
Al	5.78
Ti	0.32
Hf	0.03
Si	<0.03
Mn	<0.01
B	<25 ppm
C	.10
Cu	<0.01
Fe	<0.05
P	<0.005
Zr	<0.001
V	<0.01
Ni	bal

Analysis supplied by Cannon Muskegon

A.2.3.2 Heat capacity, J/g/K and enthalpy, J/g

Specific heat, C_p, J/g/K:

PGZ	860°C	900°C	950°C	1000°C	1050°C	1100°C	1150°C	1200°C	1250°C	1300°C	1350°C	1400°C	1450°C	1500°C
heat 1	0.64	0.64	0.66	0.69	0.74	0.80	0.84	0.93	0.91	1.13	0.89	7.43	0.71	0.62
heat 2	0.64	0.63	0.64	0.68	0.74	0.81	0.83	0.91	0.89	0.99	0.91	6.64	0.65	0.67
heat 3	0.65	0.63	0.64	0.64	0.68	0.75	0.78	0.86	0.87	0.91	0.85	6.13	0.59	0.58
ave	**0.64**	**0.64**	**0.65**	**0.67**	**0.72**	**0.79**	**0.82**	**0.90**	**0.89**	**1.01**	**0.88**	**6.74**	**0.65**	**0.62**
PGZ	**860°C**	**900°C**	**950°C**	**1000°C**	**1050°C**	**1100°C**	**1150°C**	**1200°C**	**1250°C**	**1300°C**	**1350°C**	**1400°C**	**1450°C**	**1500°C**
cool 1	0.63	0.65	0.68	0.72	0.78	0.84	0.91	1.02	1.00	1.05	4.60	0.66	0.62	-
cool 2	0.63	0.65	0.69	0.73	0.78	0.84	0.92	1.03	1.05	0.92	3.70	0.59	0.61	-
cool 3	0.63	0.64	0.68	0.71	0.76	0.82	0.90	0.99	1.05	0.90	3.57	0.6	0.61	-
ave	**0.63**	**0.64**	**0.68**	**0.72**	**0.77**	**0.83**	**0.91**	**1.01**	**1.03**	**0.96**	**3.96**	**0.62**	**0.61**	**-**

CMSX10K PGZ (mass = 175.2mg) solid results Run at 10°C/min
Comparing solid results pre- and post- remelting

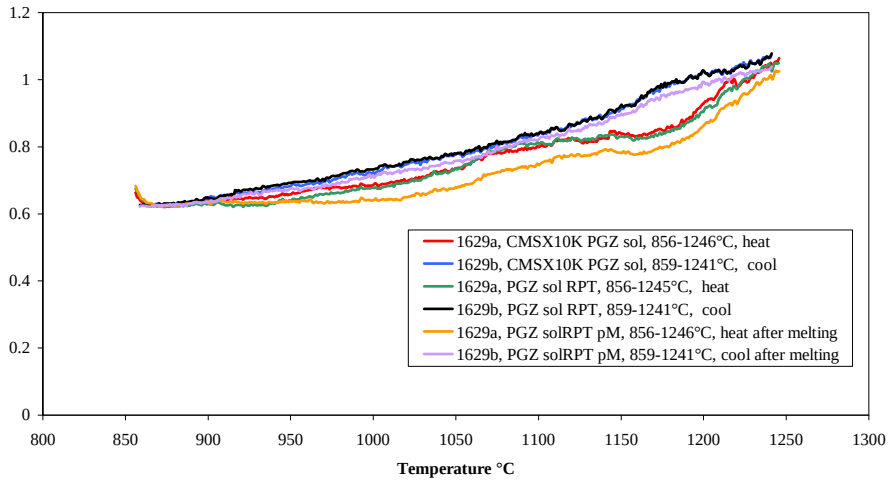

CMSX10K PGZ (mass = 173.2mg)
Run at 10°C/min

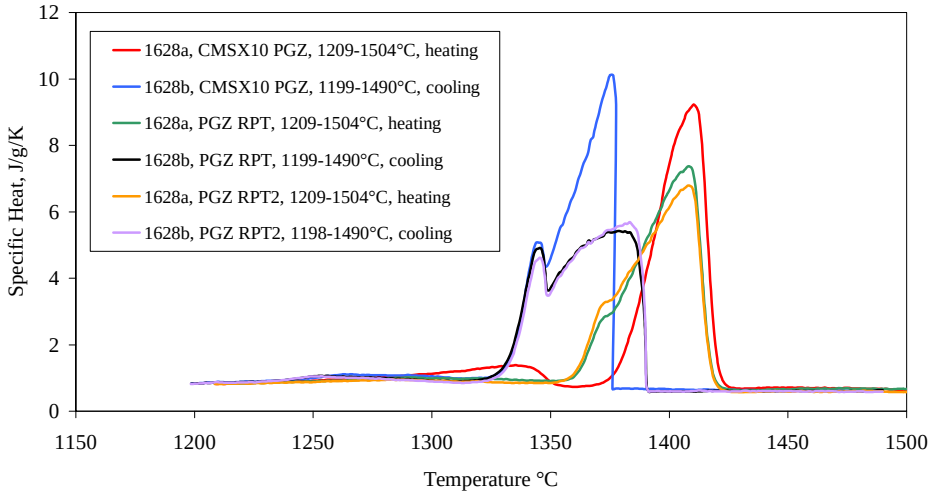

Enthalpy, J/g:

Heating	Solidus, °C	Liquidus, °C	Enthalpy J/g
Heat 1	1362	1428	207.5
Heat 2	1353	1429	206.7
Heat 3	1350	1427	206.9
Ave	**1352**	**1428**	**207.0**
Cooling	**Solidus, °C**	**Liquidus, °C**	**Enthalpy J/g**
Cool 1	1322	1380	234.1
Cool 2	1314	1392	216.1
Cool 3	1313	1392	214.8
Ave	**1316**	**1388**	**221.7**

CMSX10K PGZ (mass = 173.2mg) Run at 10°C/min

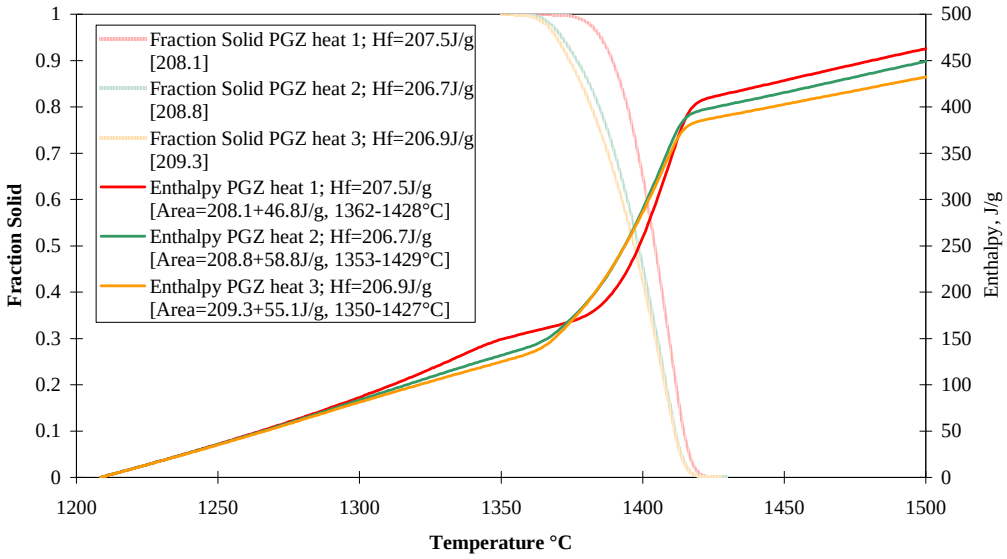

CMSX10K PGZ (mass = 173.2mg) Run at 10°C/min

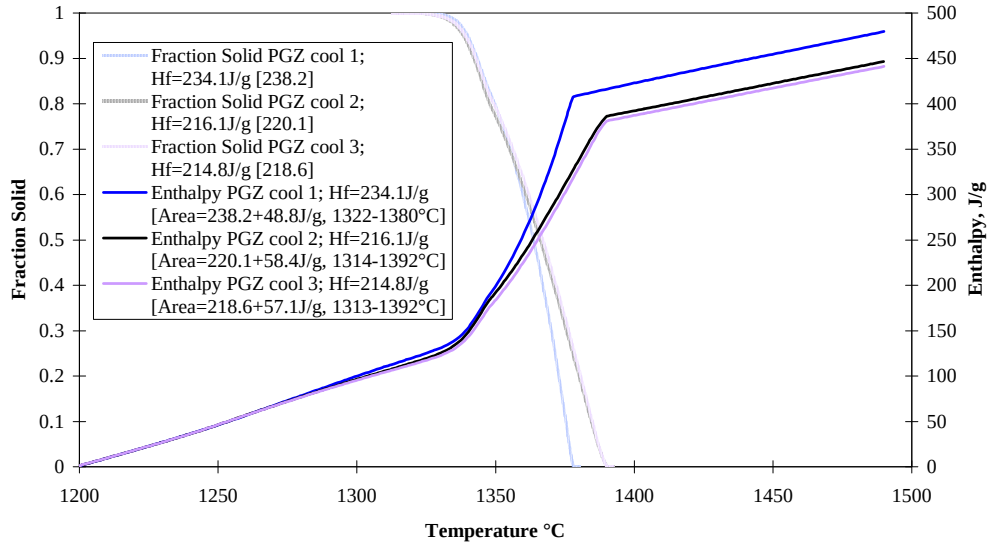

A.2.3.3 Thermal Diffusivity

1. Solid material

Measurements made to a temperature of 735°C. Results corrected for thermal expansion. From room temperature to 735°C the following formula may be used:

Thermal diffusivity, $a = 2.88 \times 10^{-5} T + 0.0237$ [20°C>T<735°C]

Average Measured Solid Thermal Diffusivity Results for PGZ

T, °C (T_1)	PGZ2A Heating	T, °C (T_1)	PGZ2A Cooling
83	0.0260	639	0.0422
312	0.0329	-	-
538	0.0388	-	-
735	0.0449	-	-
T, °C (T_1)	**PGZ3A Heating**	**T, °C (T_1)**	**PGZ2A Cooling**
438	0.0368	-	-

Fitted Solid Thermal Diffusivity Results for PGZ

T, °C	PGZ a, $10^{-4}m^2 s^{-1}$
20	0.0243
50	0.0251
100	0.0266
150	0.0280
200	0.0294
250	0.0309
300	0.0323
350	0.0337
400	0.0352
450	0.0366
500	0.0381
550	0.0395
600	0.0409
650	0.0424
700	0.0438
750	0.0453

2. Preliminary thermal diffusivity of liquid results:

There is good agreement between the measurements carried out using a sapphire cell with previous solid results in solid region.

The results obtained at 1350°C are either in the mushy region or on solid material, the results at 1400°C are definitely in the liquid, and the results obtained between these two points are in the mush. Unfortunately the sapphire crucible cracked at some point on cooling, so cannot use this same sample for repeat measurements.

Sample was oxidised during measurements, with areas of the oxide remaining attached to both the base and the lid of the crucible once the sample had been removed. This prompts the question as to whether to pre-oxidise samples.

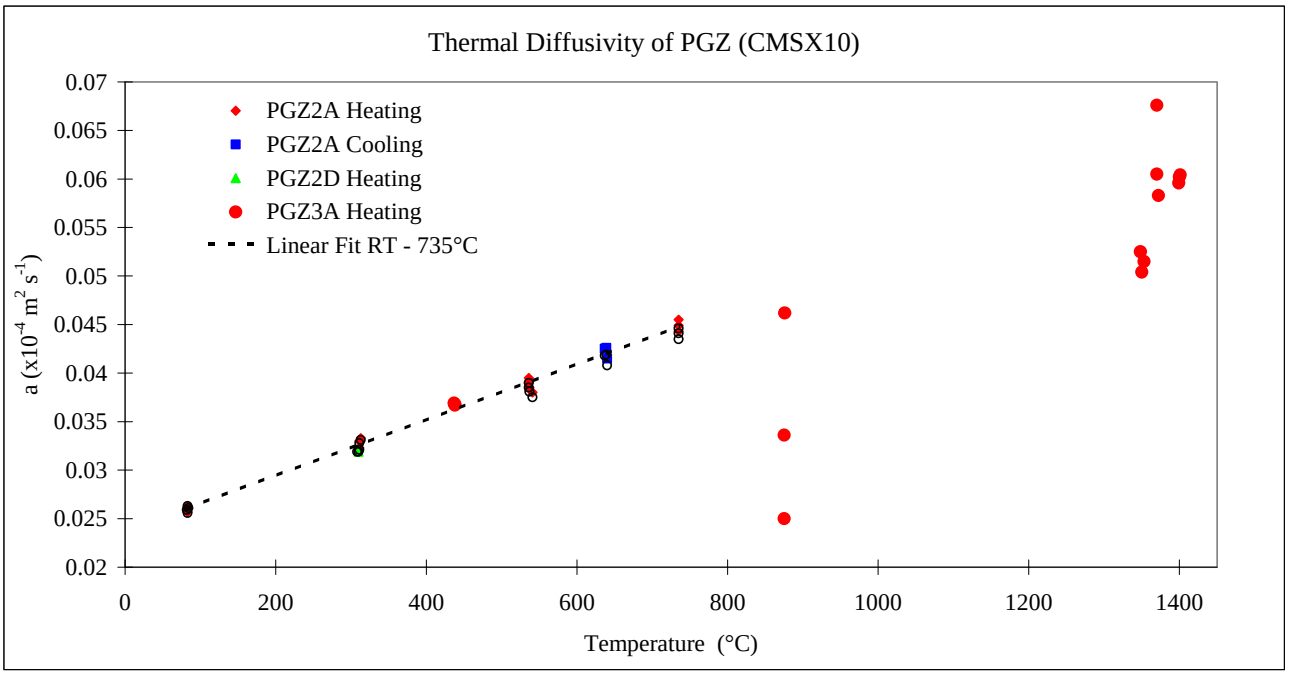

Value for thermal diffusivity in the liquid 0.06 x 10^{-4} m^2 s^{-1}

Measured Thermal Diffusivity Results in transition regions (showing spread of results and average):

T (°C)	PGZ3A Heating a, $10^{-4}m^2 s^{-1}$	T (°C)	PGZ3A Cooling a, $10^{-4}m^2 s^{-1}$
875	0.0336	1372	0.0583
876	0.0462	1370	0.0605
875	0.0250	1370	0.0676
875	**0.0349**	**1371**	**0.0621**
1400	0.0602	1353	0.0515
1399	0.0596	1348	0.0525
1401	0.0604	1350	0.0504
1400	**0.0601**	**1350**	**0.0515**

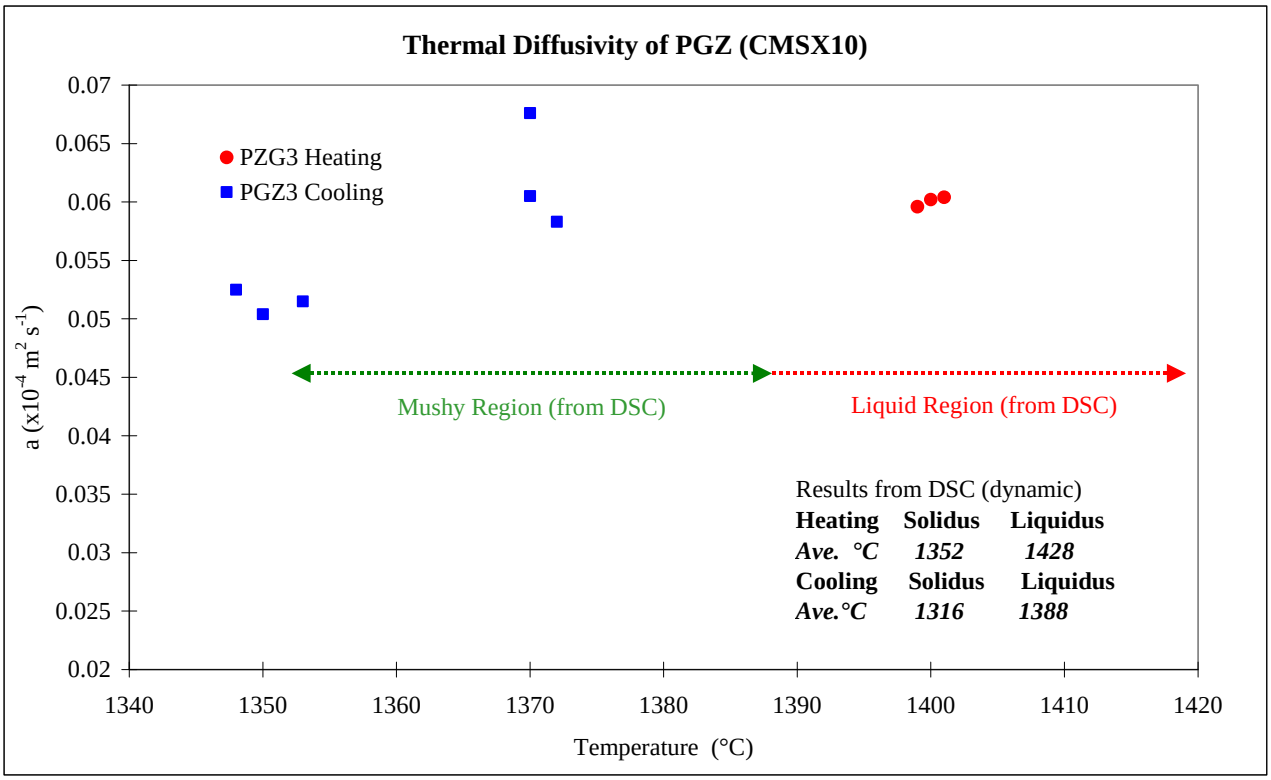

A.2.3.4 Thermal expansion and melting behaviour data on CMSX10

1. Solid thermal expansion

Temperature, °C	Fractional length change, ppm	Mean coefficient from 25 °C to temp, 10^{-6} K^{-1}	Expansivity at temperature, 10^{-6} K^{-1}	Density, Mg m^{-3}
25	0	-	10.2	9.046
50	245	9.8	10.4	9.039
100	850	11.3	10.9	9.023
150	1475	11.8	11.4	9.006
200	2110	12.1	11.9	8.989
250	2760	12.3	12.4	8.972
300	3420	12.4	12.9	8.954
350	4100	12.6	13.3	8.936
400	4780	12.7	13.8	8.918
450	5480	12.9	14.3	8.900
500	6190	13.0	14.8	8.881
550	6900	13.1	15.3	8.863
600	7640	13.3	15.7	8.843
650	8400	13.4	16.2	8.824
700	9190	13.6	16.7	8.803
750	9990	13.8	17.2	8.783
800	10810	13.9	17.7	8.762
850	11670	14.1	18.1	8.740
900	12570	14.4	18.6	8.717
950	13510	14.6	19.1	8.694
1000	14500	14.9	19.6	8.669
1050	15540	15.2	20.1	8.643
1100	16650	15.5	20.6	8.616
1150	17850	15.9	21.0	8.586
1200	19140	16.3	21.5	8.555

Cannon Muskegon website gives 9.05 Mg m^{-3} for RT density.

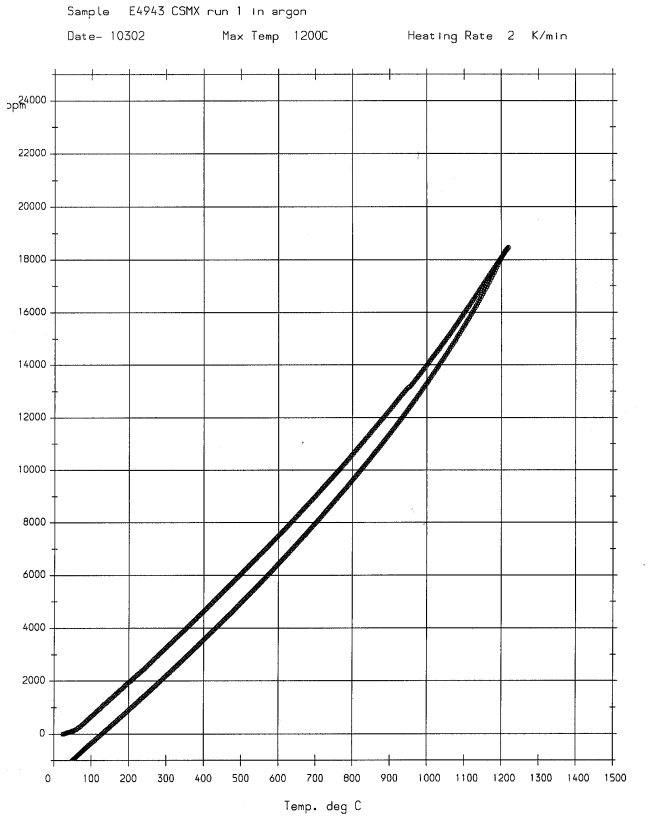
Sample E4943 CSMX run 1 in argon
Date- 10302
Max Temp 1200C
Heating Rate 2 K/min
ppm
24000
22000
20000
18000
16000
14000
12000
10000
8000
6000
4000
2000
0
0 100 200 300 400 500 600 700 800 900 1000 1100 1200 1300 1400 1500
Temp. deg C

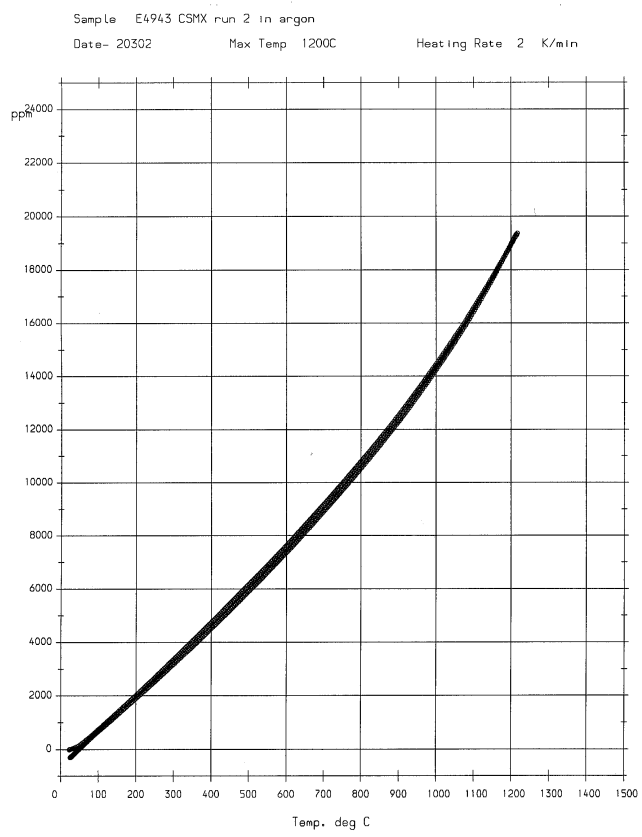
Sample E4943 CSMX run 2 in argon
Date- 20302
Max Temp 1200C
Heating Rate 2 K/min
ppm
24000
22000
20000
18000
16000
14000
12000
10000
8000
6000
4000
2000
0
0 100 200 300 400 500 600 700 800 900 1000 1100 1200 1300 1400 1500
Temp. deg C

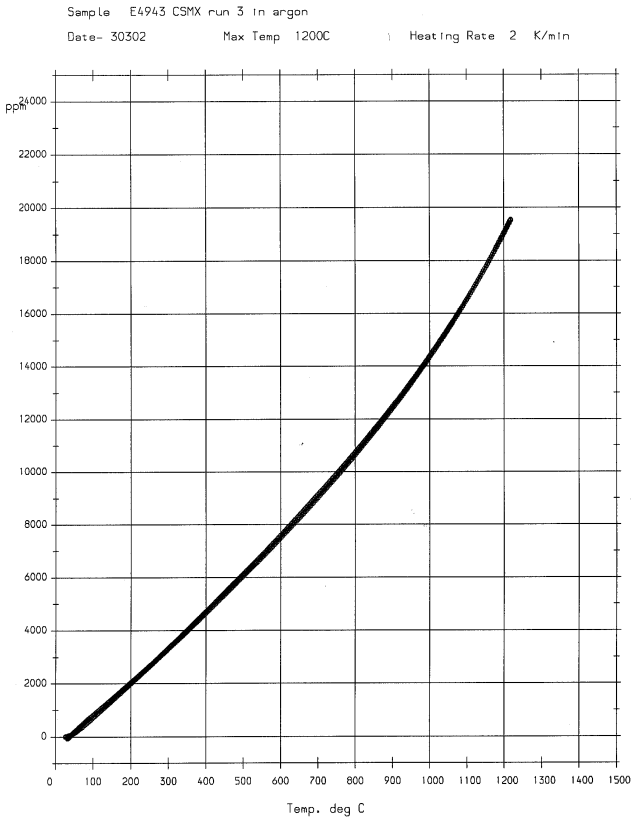

Thermal expansion plots for three consecutive cycles – note slight offset in first run, and smooth trace with no obvious phase changes.

2. Melting experiments

Raw trace:

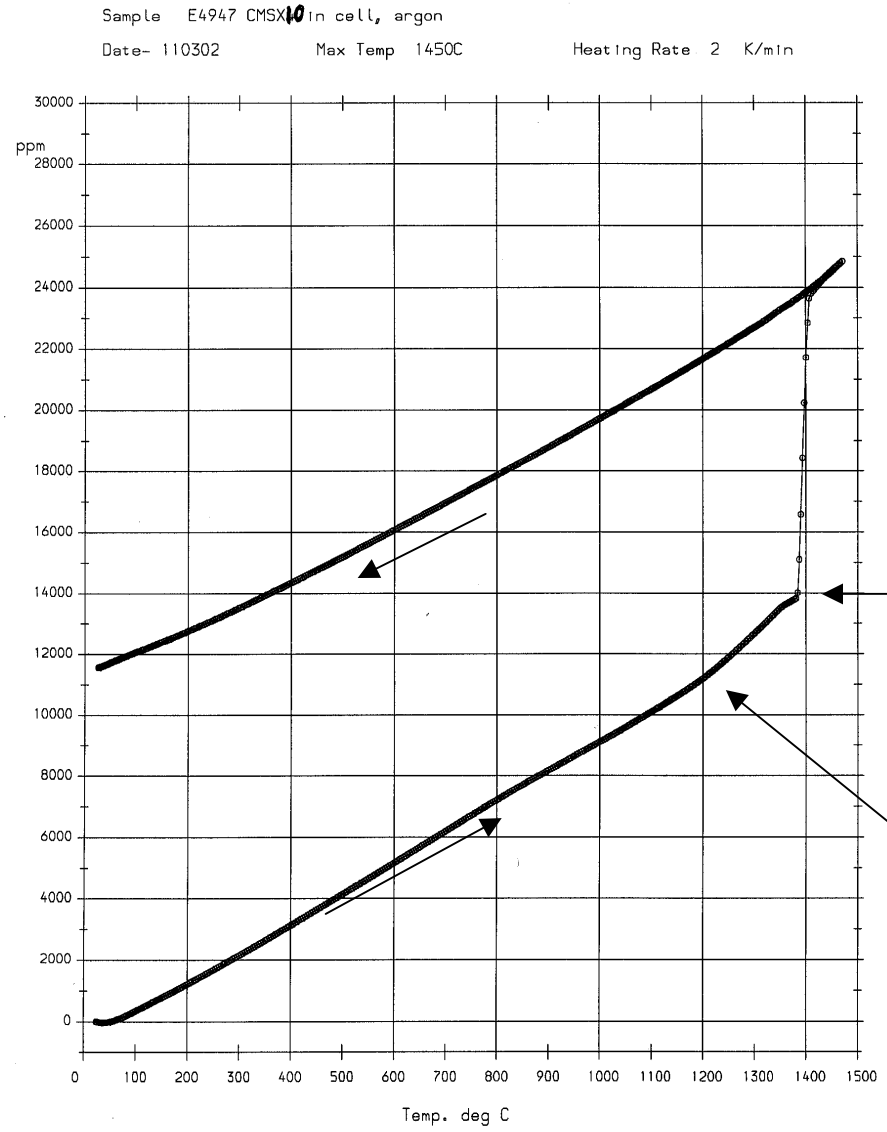

Sharp rise = onset of melting collapse; end of melting process = liquid only.
Cell jams on cooling

No phase change to 1200 °C

Apparent liquid production temperature: 1386 °C
Liquidus temperature: 1405 °C

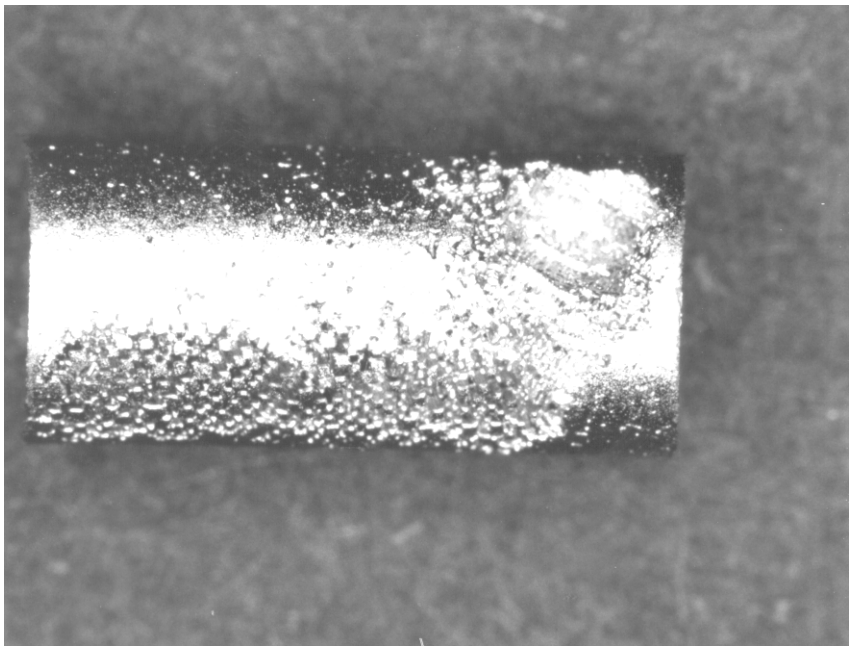

CMSX10 sample after running in cell – note 'sucking in' due to lack of feeding.

2 mm

Apparent solid linear expansion of sample in cell (corrected for expansion of pistons):

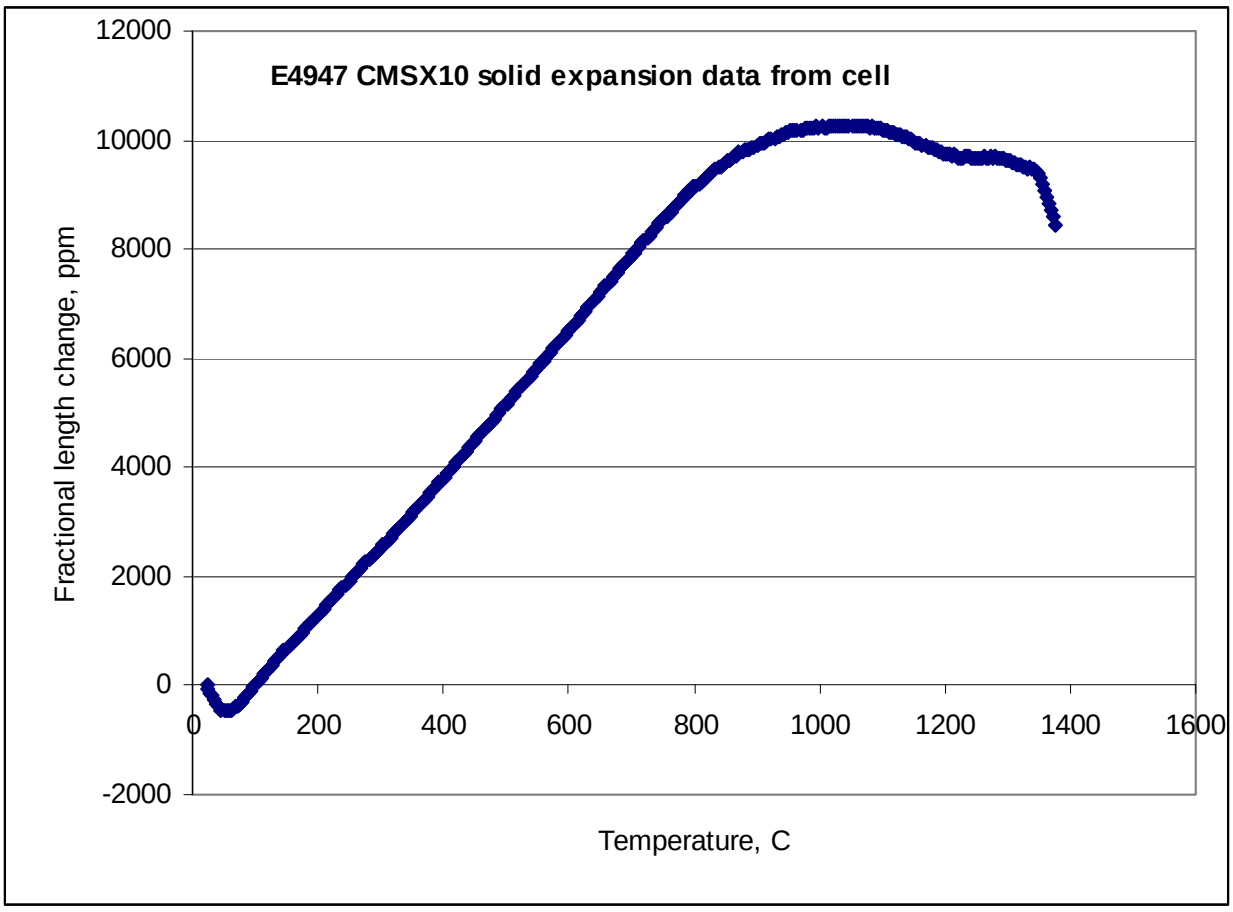

Apparent contraction at high temperatures may be due to softening under push-rod force.

Apparent mushy zone and liquid density during heating assuming no leakage:

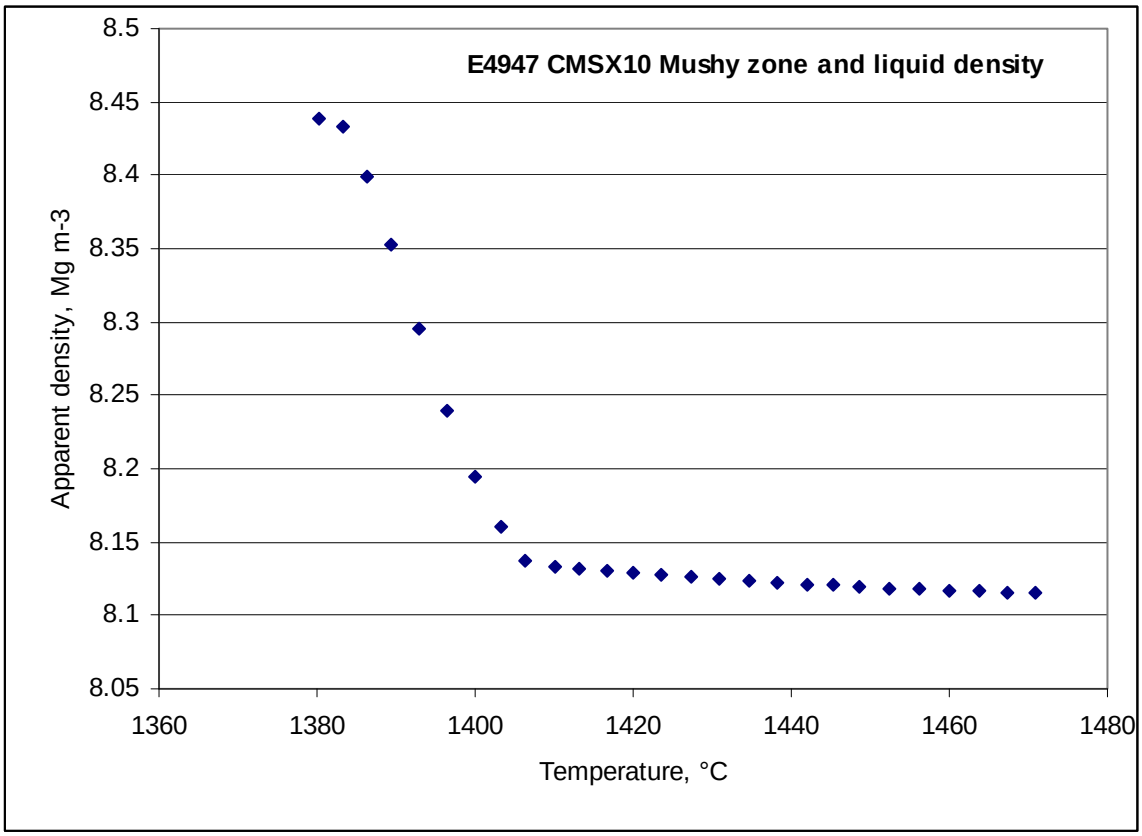

.

Fractional volume change from liquidus temperature:

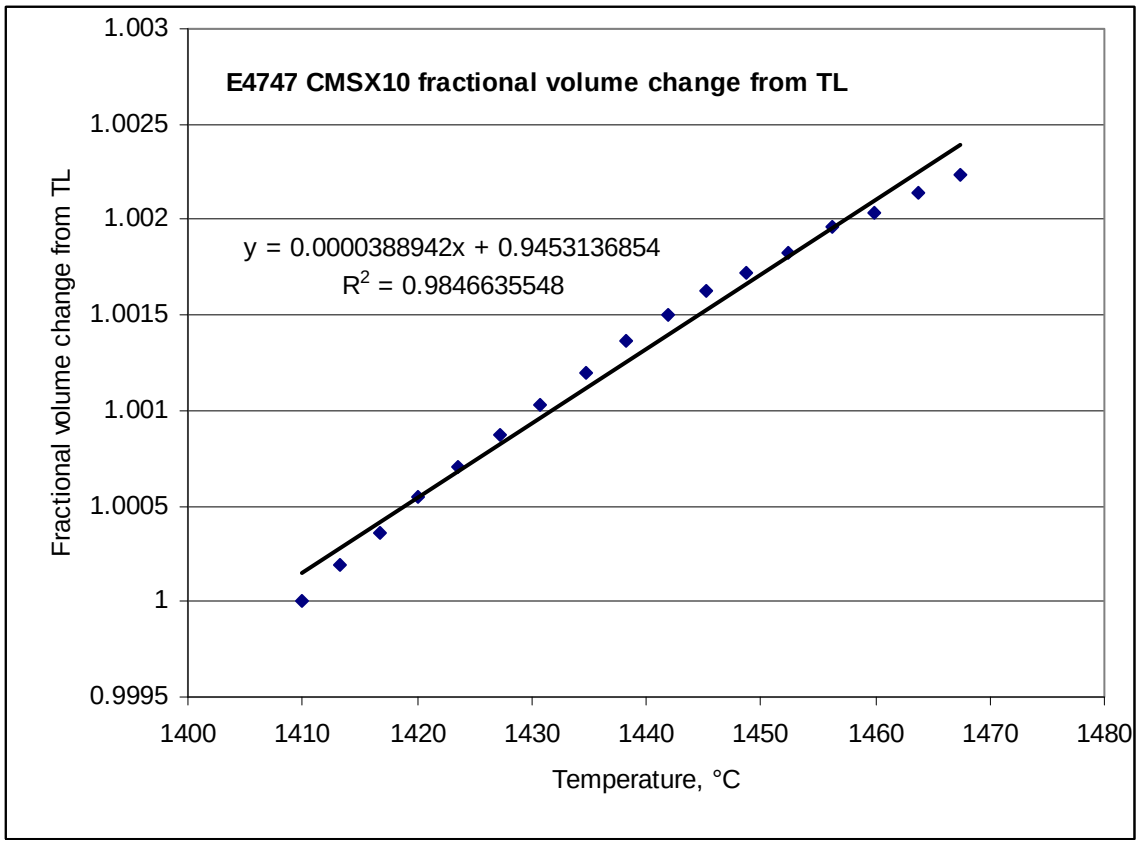

Cubical expansion of liquid = 39 x 10^{-6} K^{-1}, but at start closer to 50 x 10^{-6} K^{-1}.

Apparent density through the mush:

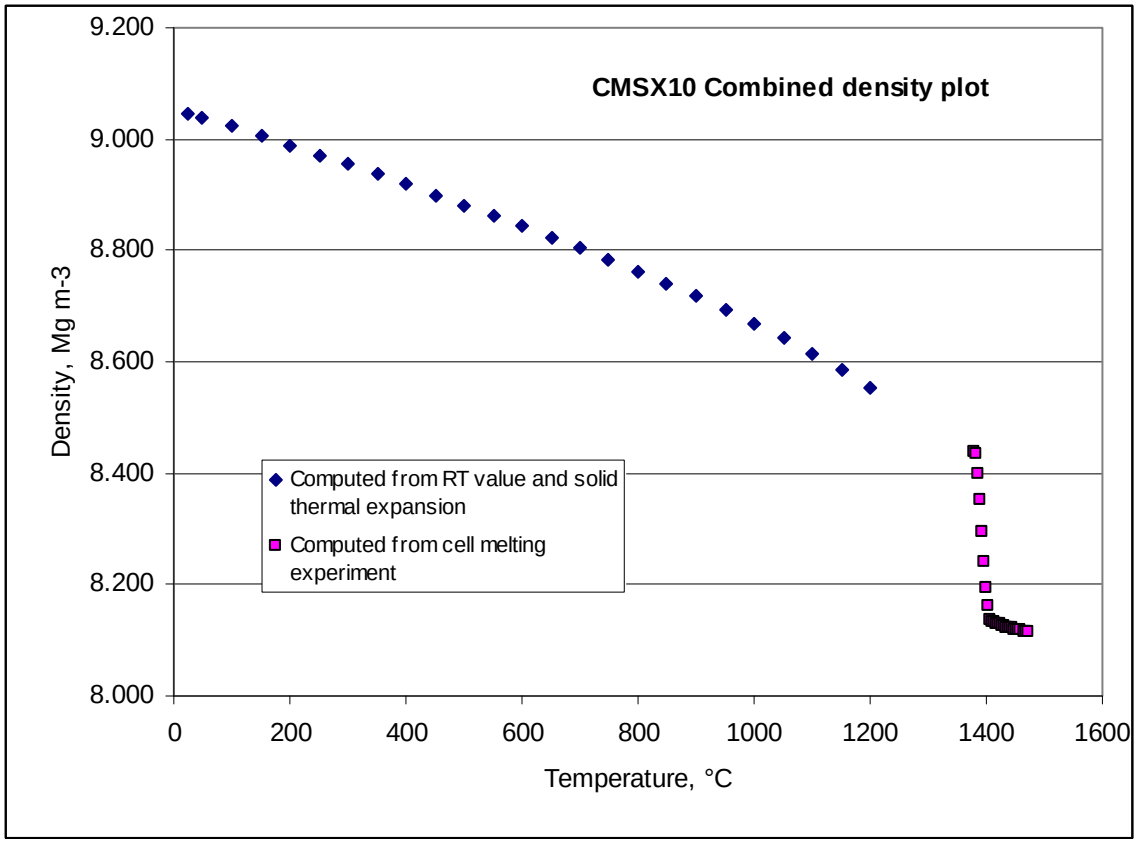

The gap in this plot is due to experimental limitations of the two methods.

CMSX10 – density in the mush and liquid from piston dilatometry:

Temperature, °C	Density, Mg m^{-3}	
	Mush	Liquid
1380	8.442	-
1390	8.338	-
1400	8.192	-
1410	-	8.133
1420	-	8.129
1430	-	8.126

A.2.4 Rene 80 – code PHC

Element (%)	PHC (Rene 80)	Typical Rene 80
Cr	13.9	14
Co	9.6	9.5
Mo	4.05	4
Al	2.95	3
Ti	4.95	5
C	-	0.17
B	.013	0.015
Zr	.030	0.003
Ni	Balance	bal.
Re	<.05	-
Ta	<.10	-
W	3.9	-
V	<.01	-
Si	.03	-
Mn	.02	-
Cb	<.05	-
Cu	<.10	-
Fe	.16	-
Hf	<.05	-
P	<.005	-

Analysis supplied by Cannon Muskegon

A.2.4.2 Thermal Diffusivity

From room temperature until 800°C the equation can be used.

Thermal diffusivity, $a = 2.59 \times 10^{-5} T + 0.0271$ [20°C>T<800°C]

Average measured values for Thermal Diffusivity for PHC (from at least three measurements)

T (°C)	PHC1A Heating	T (°C)	PHC1A Cooling
19	0.0277	21	0.0274
104	0.0297	-	-
317	0.0358	-	-
504	0.0404	-	-
704	0.0464	-	-
T (°C)	**PHC1B Heating**		
898	0.0493	-	-
1089	0.0492	-	-

Fitted Thermal Diffusivity Results for PHC

T (°C)	PHC a, $10^{-4} m^2 s^{-1}$
20	0.0277
50	0.0284
100	0.0297
150	0.0310
200	0.0323
250	0.0336
300	0.0349
350	0.0362
400	0.0375
450	0.0388
500	0.0401
550	0.0414
600	0.0427
650	0.0440
700	0.0453
750	0.0466
800	0.0479

Thermal diffusivity values for liquid PHC from at least three measurements.

T, °C	PHC2B Heating
413	0.0353
912	0.0440
1067	0.0448
1170	0.0454
1449	0.0446

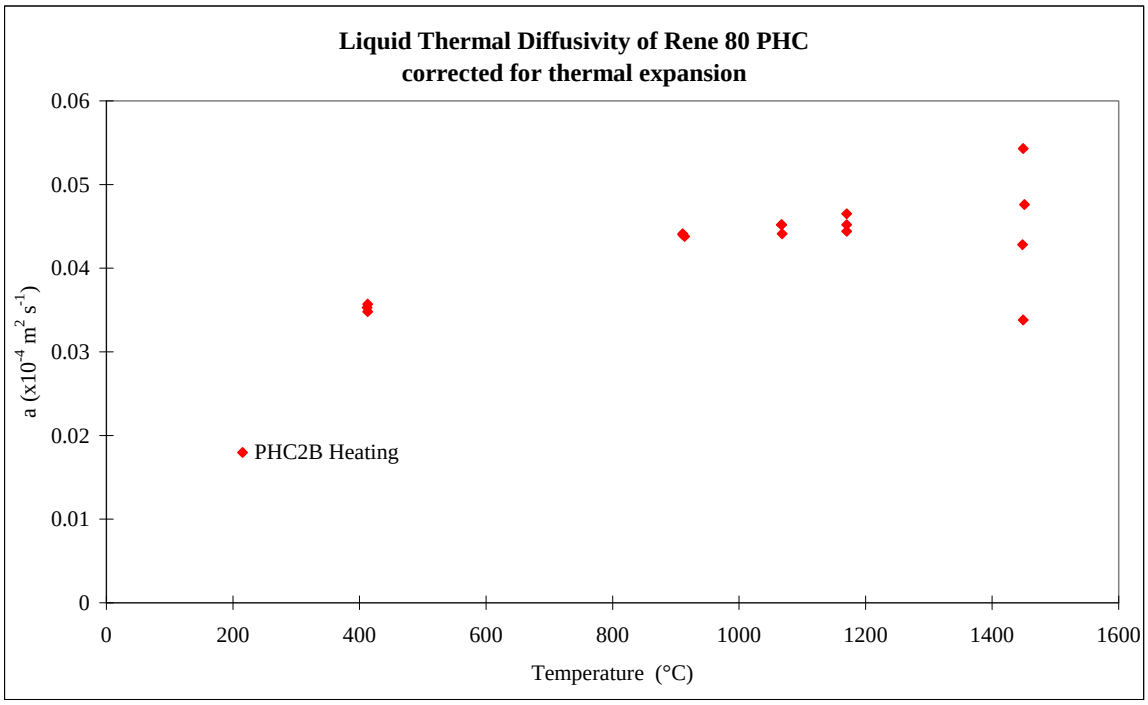

The results at 1450°C show extreme scatter. This is probably due to the sample not being completely liquid, and the laser energy is partially being absorbed to facilitate the transition. Estimated value for the thermal diffusivity of PHC in the liquid 0.05 $m^2 s^{-1}$.

A.2.4.3 Heat capacity, J/g/K and enthalphy, J/g

Heat capacity, J/g/K:

Heating	1000°C	1050°C	1100°C	1150°C	1200°C	1250°C	1300°C	1350°C	1400°C
heat 1	0.81	0.87	0.99	-	-	-	-	-	-
heat 2	0.82	0.87	0.99	1.27	0.80	1.07	5.42	1.04	1.01
heat 1	0.85	0.92	1.06	1.18	0.73	0.98	5.58	0.78	0.78
heat 2	0.91	0.95	1.08	1.11	0.79	1.12	4.12	0.76	0.80
heat 3	0.93	1.02	1.18	1.05	0.70	1.01	4.60	0.72	0.77
ave	**0.86**	**0.93**	**1.06**	**1.15**	**0.75**	**1.05**	**4.93**	**0.83**	**0.84**
Cooling	**1000°C**	**1050°C**	**1100°C**	**1150°C**	**1200°C**	**1250°C**	**1300°C**	**1350°C**	**1400°C**
cool 1	0.83	0.95	1.38	1.02	1.14	3.55	5.29	0.89	-
cool 2	0.83	0.95	1.46	-	-	-	-	-	-
cool 1	0.91	1.03	1.42	0.90	1.01	3.26	4.87	0.80	-
cool 2	0.90	1.03	1.38	0.90	1.03	3.24	5.47	0.81	-
cool 3	0.92	1.05	1.53	0.93	1.03	3.17	5.44	0.81	-
ave	**0.88**	**1.00**	**1.43**	**0.94**	**1.05**	**3.31**	**5.27**	**0.83**	**-**

Rene 80 PHC (mass = 156.6mg)
Run at 10°C/min ***after*** melting

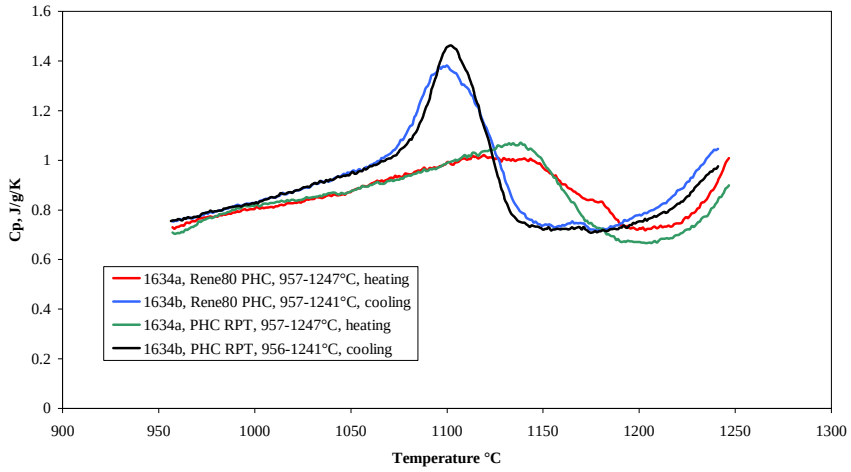

Rene 80 PHC (mass = 156.6 mg)
Run at 10.0°C/min

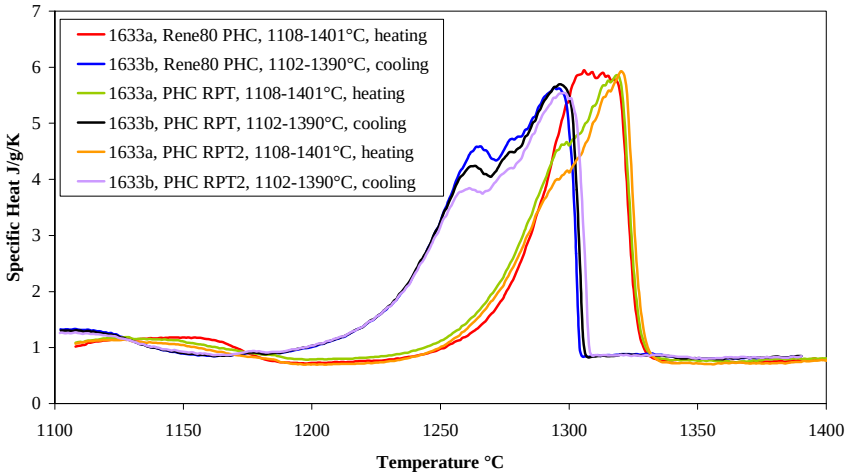

Heating	Solidus, °C	Liquidus, °C	Enthalpy J/g
heat 2	1209	1338	221.2
heat 1	1200	1335	206.9
heat 2	1215	1340	206
heat 3	1224	1338	200.7
ave	**1212**	**1338**	**208.7**
Cooling	**Solidus, °C**	**Liquidus, °C**	**Enthalpy J/g**
cool 1	1168	1308	260.9
cool 1	1169	1308	246.5
cool 2	1168	1308	248.7
cool 3	1166	1310	242.7
ave	**1168**	**1309**	**249.7**

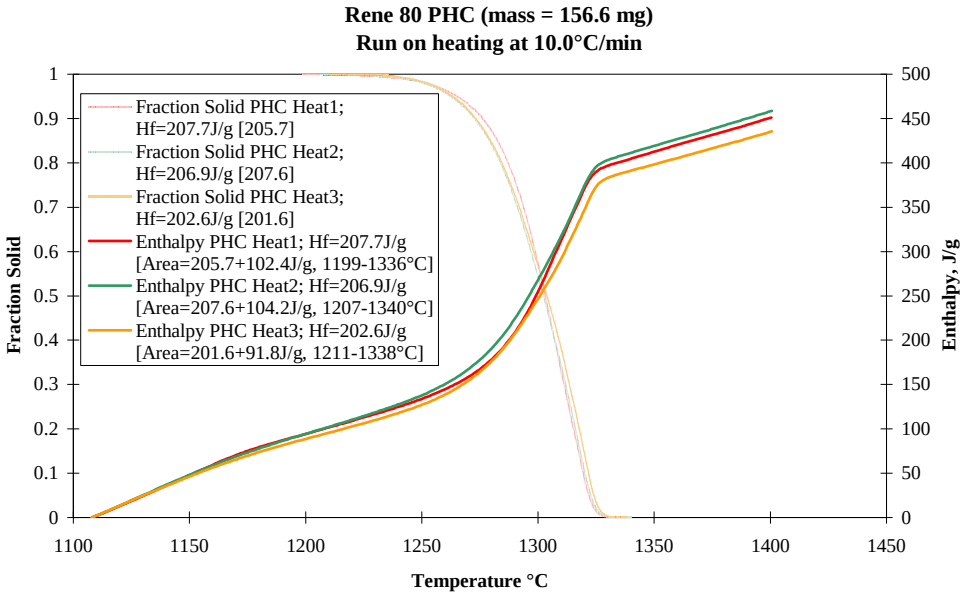

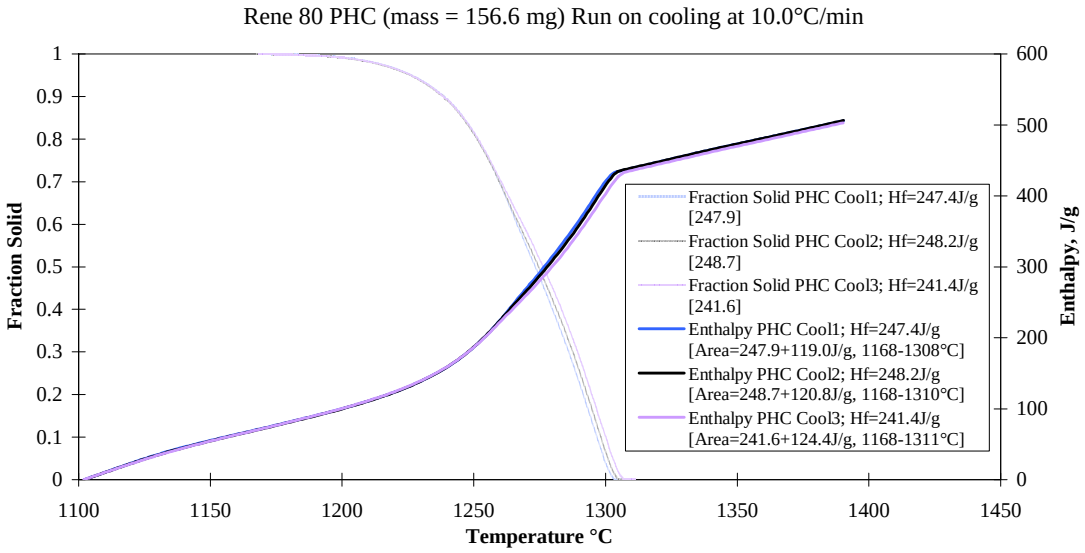

A.2.4.4 Thermal expansion and melting behaviour data on Rene 80

1. Solid thermal expansion

Temperature, °C	Fractional length change, ppm	Mean coefficient from 25 °C to temp, 10^{-6} K^{-1}	Expansivity at temperature, 10^{-6} K^{-1}	Density, Mg m^{-3}
25	0	-	-	8.130
50	240	9.6	11.3	8.124
100	850	11.3	12.5	8.109
150	1490	11.9	12.6	8.094
200	2110	12.1	13.2	8.079
250	2810	12.5	13.9	8.062
300	3500	12.7	13.9	8.046
350	4200	12.9	14.2	8.029
400	4920	13.1	14.5	8.012
450	5650	13.3	14.7	7.994
500	6390	13.5	15.0	7.977
550	7150	13.6	15.7	7.959
600	7960	13.8	16.5	7.940
650	8800	14.1	17.0	7.921
700	9660	14.3	17.4	7.901
750	10540	14.5	18.3	7.881
800	11490	14.8	19.5	7.859
850	12490	15.1	20.7	7.836
900	13560	15.5	22.3	7.812
950	14720	15.9	24.7	7.786
1000	16030	16.4	27.6	7.757
1050	17480	17.1	31.1	7.725
1100	19140	17.8	37.6	7.689
1150	21240	18.9	-	7.643
1200	22740	19.4	-	7.611

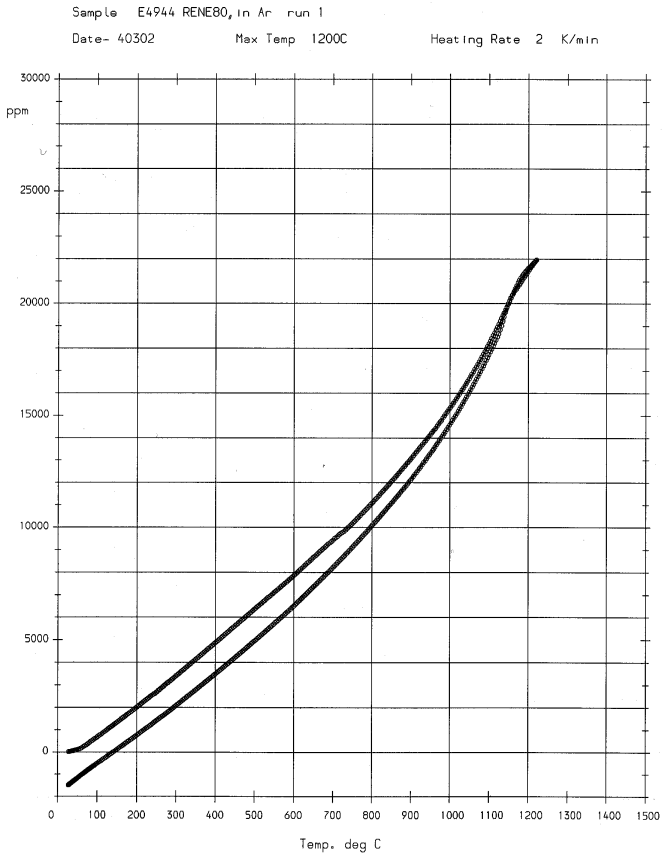
Sample E4944 RENE80, In Ar run 1
Date- 40302
Max Temp 1200C
Heating Rate 2 K/min
ppm
30000
25000
20000
15000
10000
5000
0
0 100 200 300 400 500 600 700 800 900 1000 1100 1200 1300 1400 1500
Temp. deg C

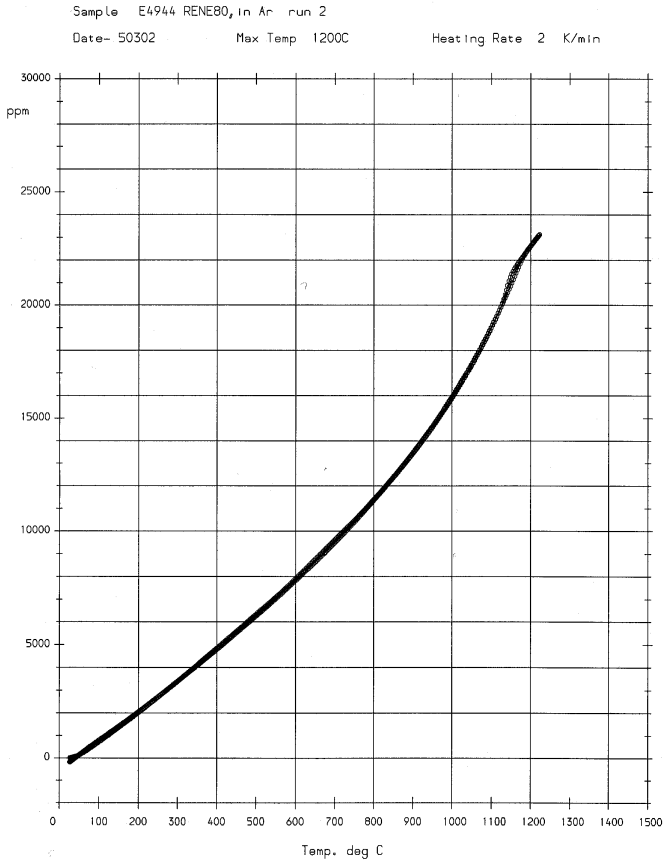
Sample E4944 RENE80, In Ar run 2
Date- 50302
Max Temp 1200C
Heating Rate 2 K/min
ppm
30000
25000
20000
15000
10000
5000
0
0 100 200 300 400 500 600 700 800 900 1000 1100 1200 1300 1400 1500
Temp. deg C

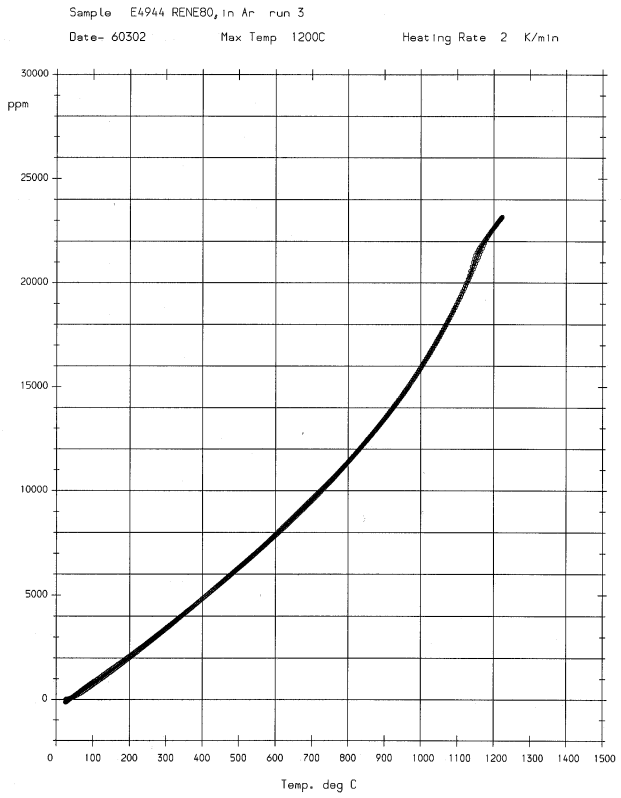

Thermal expansion runs on solid. Note small offset in first run. Note also slight kink at about 1170 °C. This results in poor curve-fitting in this region, so no expansivity data have been computed.

2. Melting experiments

2.1 Raw trace

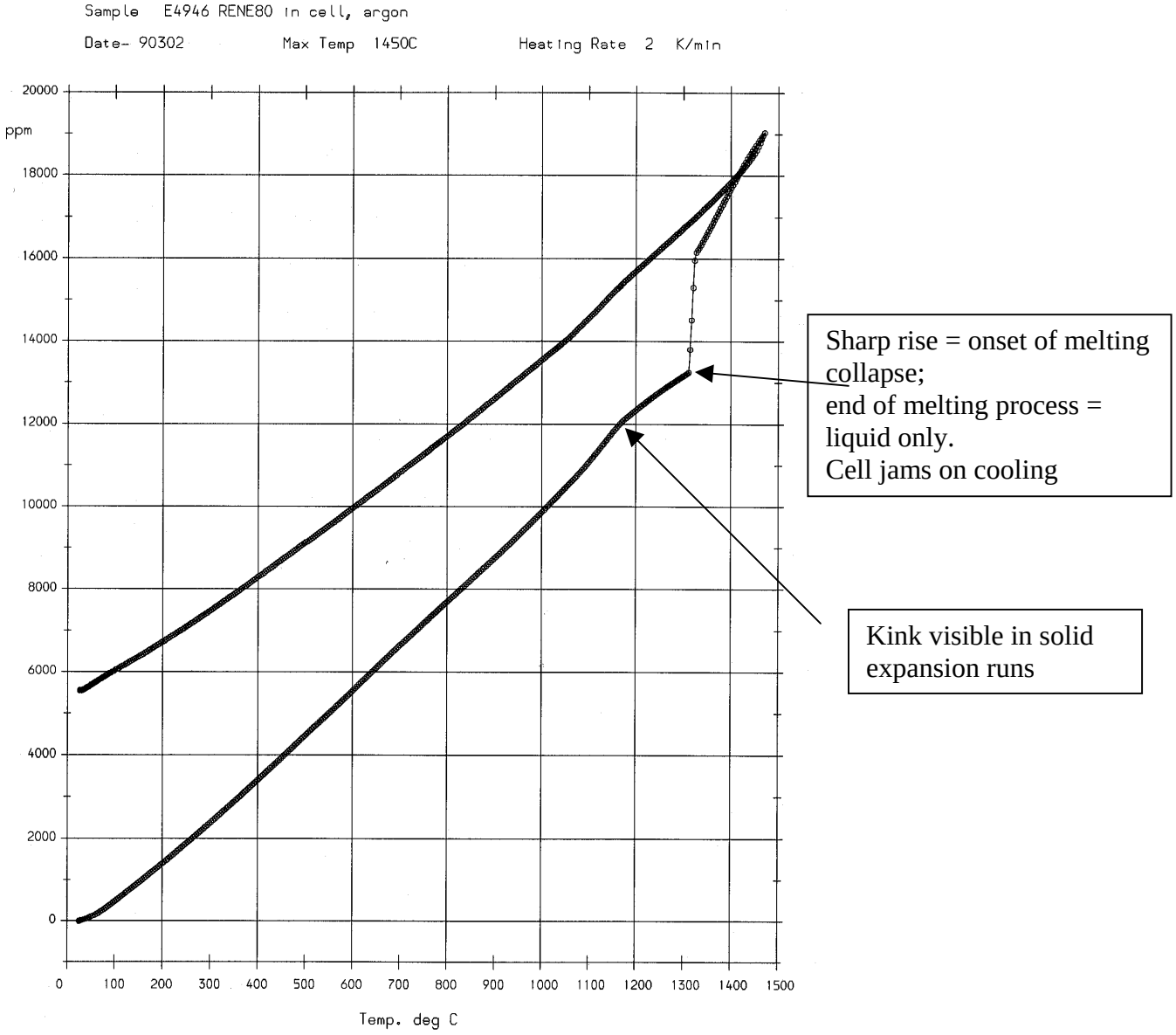

Apparent liquid production temperature: 1300°C
Liquidus temperature: 1320°C

No image of melted sample – stuck inside cell.

Apparent solid expansion of sample in cell:

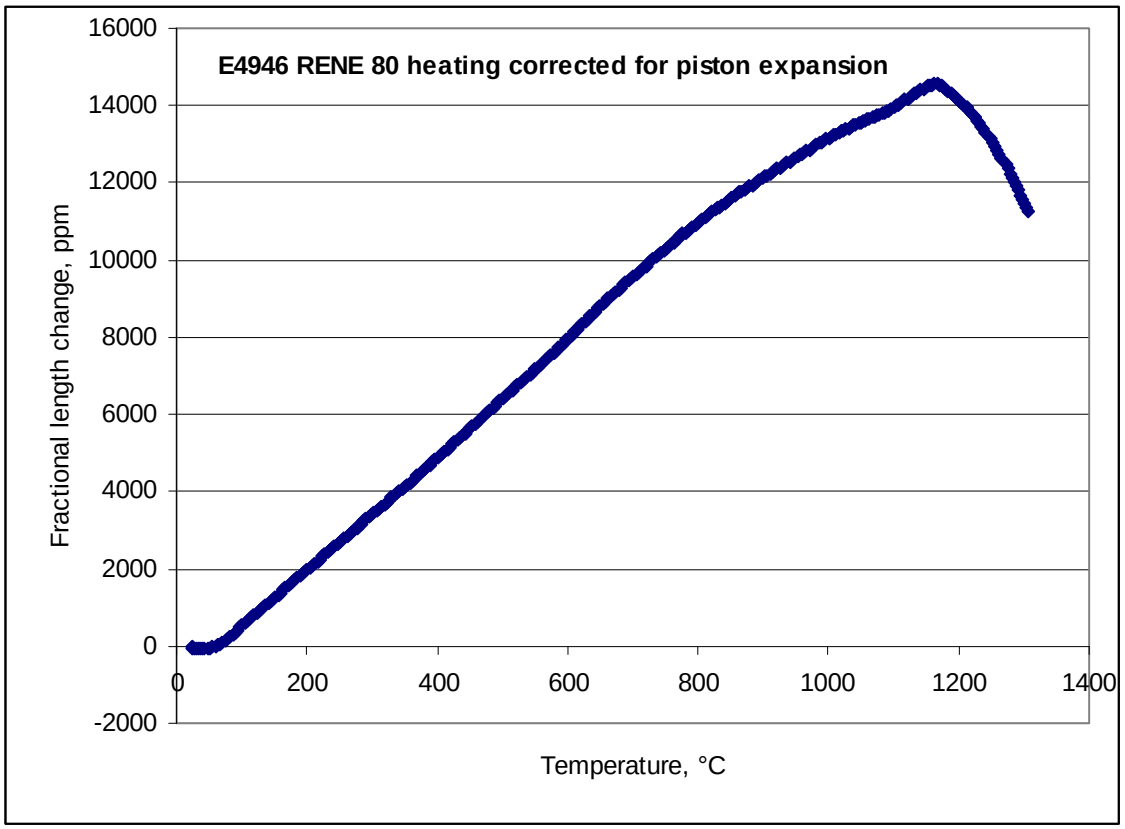

The sample appears to soften and collapse above 1200 °C.

Mushy zone and liquid density computed from cell data during heating:

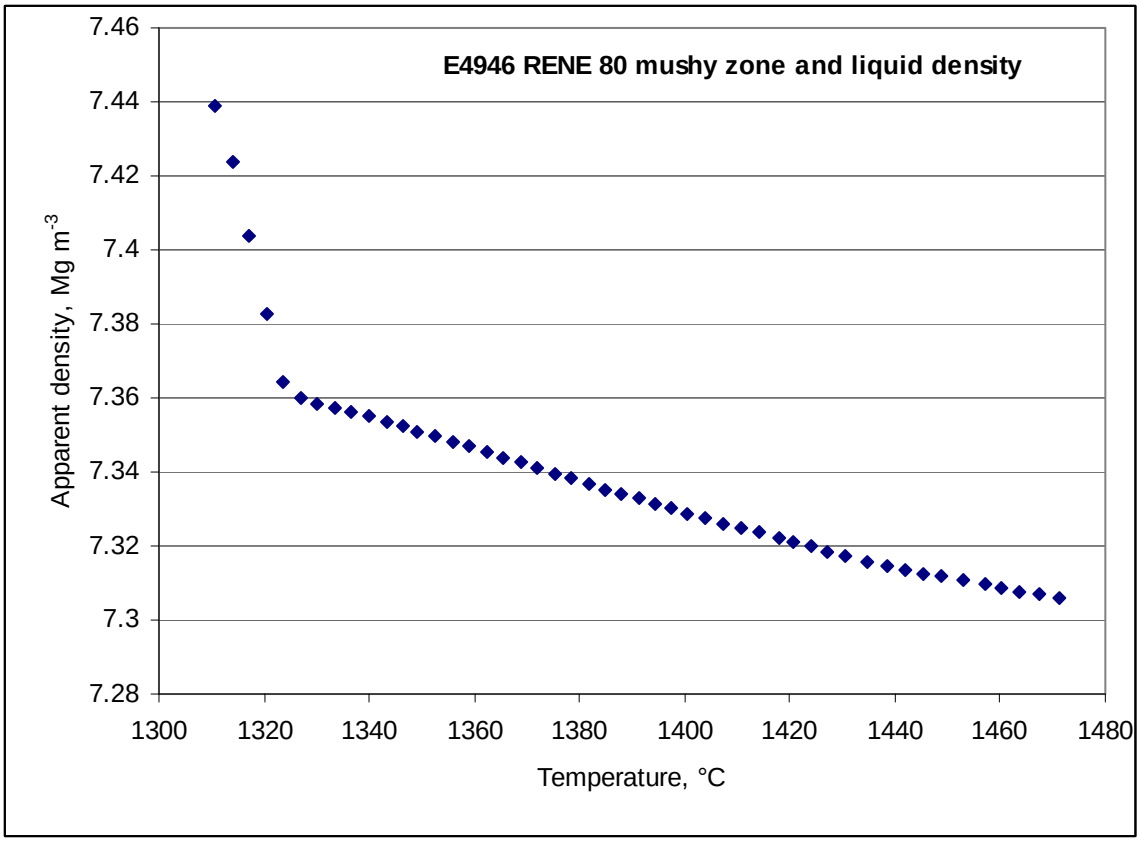

Fractional volume change as a function of temperature from the liquidus temperature:

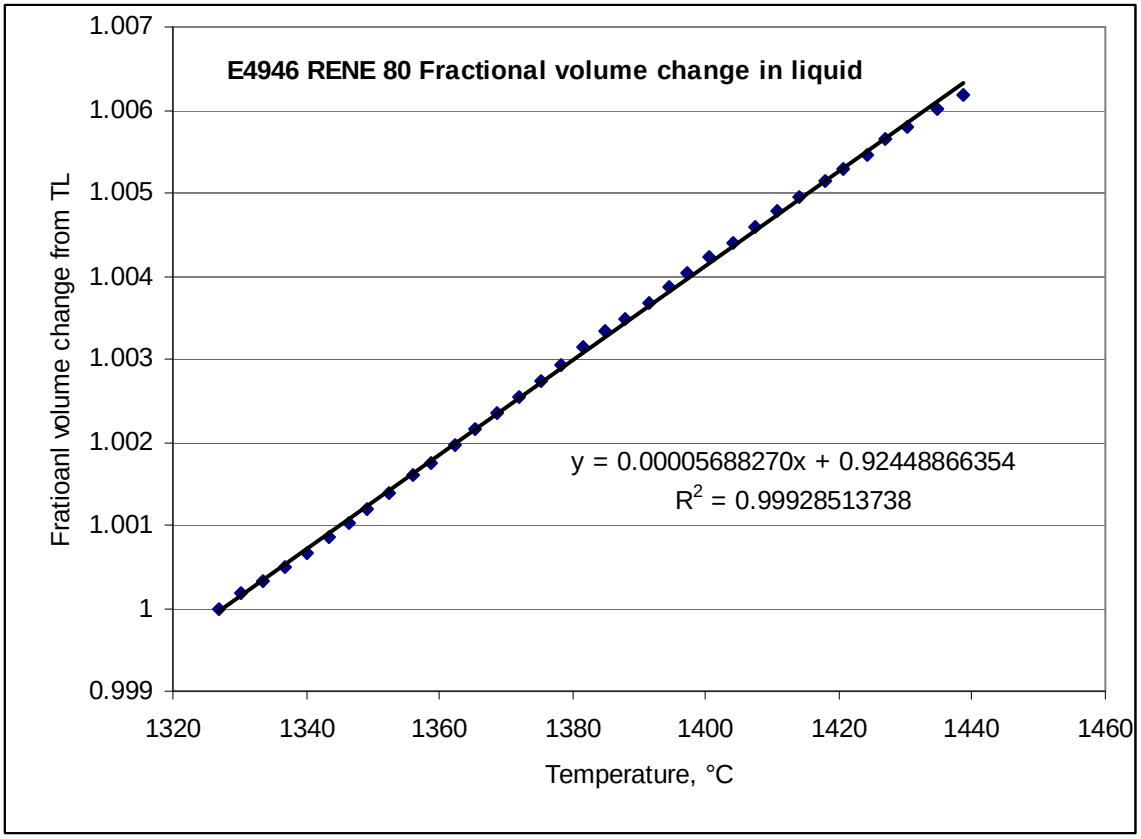

A straightline fit to the data gives a cubical expansion coefficient of 57 x 10^{-6} K^{-1}.

Density versus temperature plot for both solid and liquid densities:

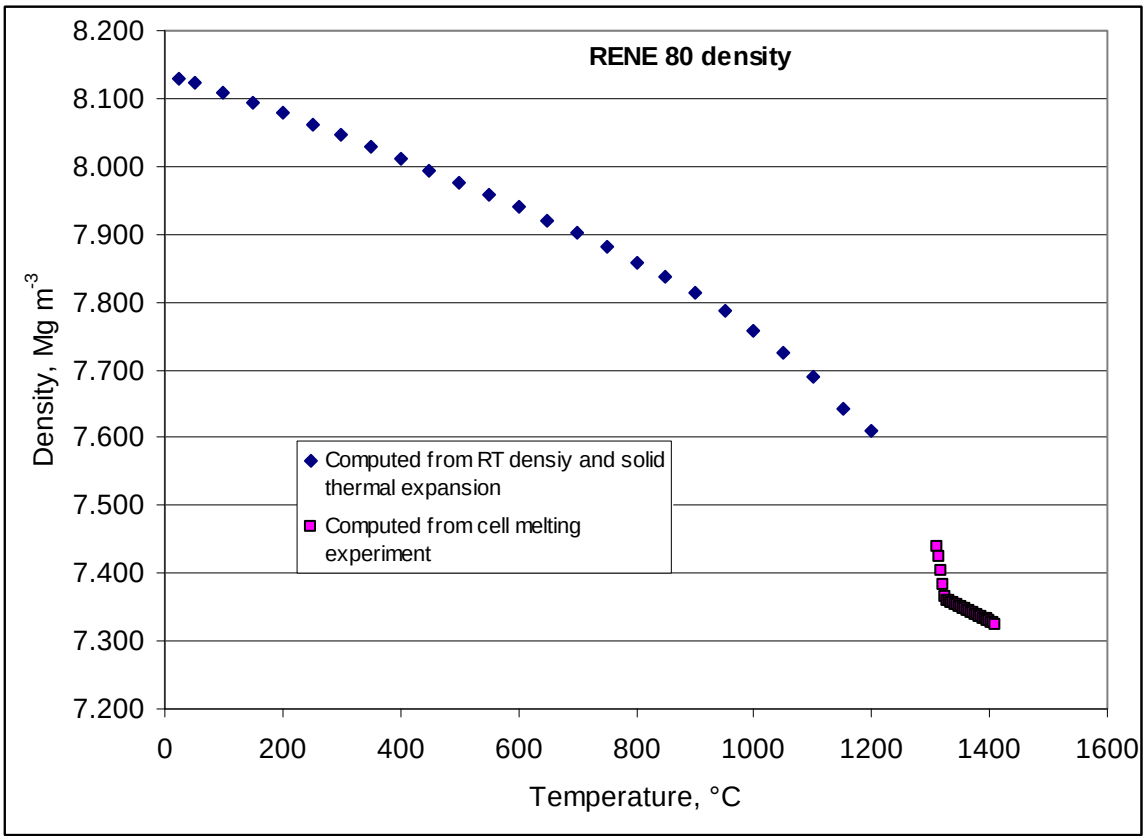

RENE 80– density in the mush and liquid from piston dilatometry

Temperature, °C	Density, Mg m^{-3}	
	Mush	Liquid
1310	7.444	-
1320	7.387	-
1330	-	7.359
1340	-	7.355
1350	-	7.351
1360	-	7.346
1370	-	7.342
1380	-	7.338
1390	-	7.333
1400	-	7.329
1410	-	7.325

A.3 MOULD MATERIALS

A.3.1 Mould types

Mould code	Type (main structure, not facecoats)	Supplier
PGB	Zircon-water/molochite stucco	1
PGC	Fused silica-water/Cerametal 05-1 stucco	1
PGD	Dual system (molochite-colloidal silica/fused silica-sodium silicate)/Cerametal 05-1 stucco	1
PGF	Non-disclosable	2
PGL	Alumina –based	3
PGM	Alumina –based	4
PGN	Zircon/silica slurry with molochite stucco	5
PHG	Non-disclosable?	6

A.3.2 Mould density and porosity

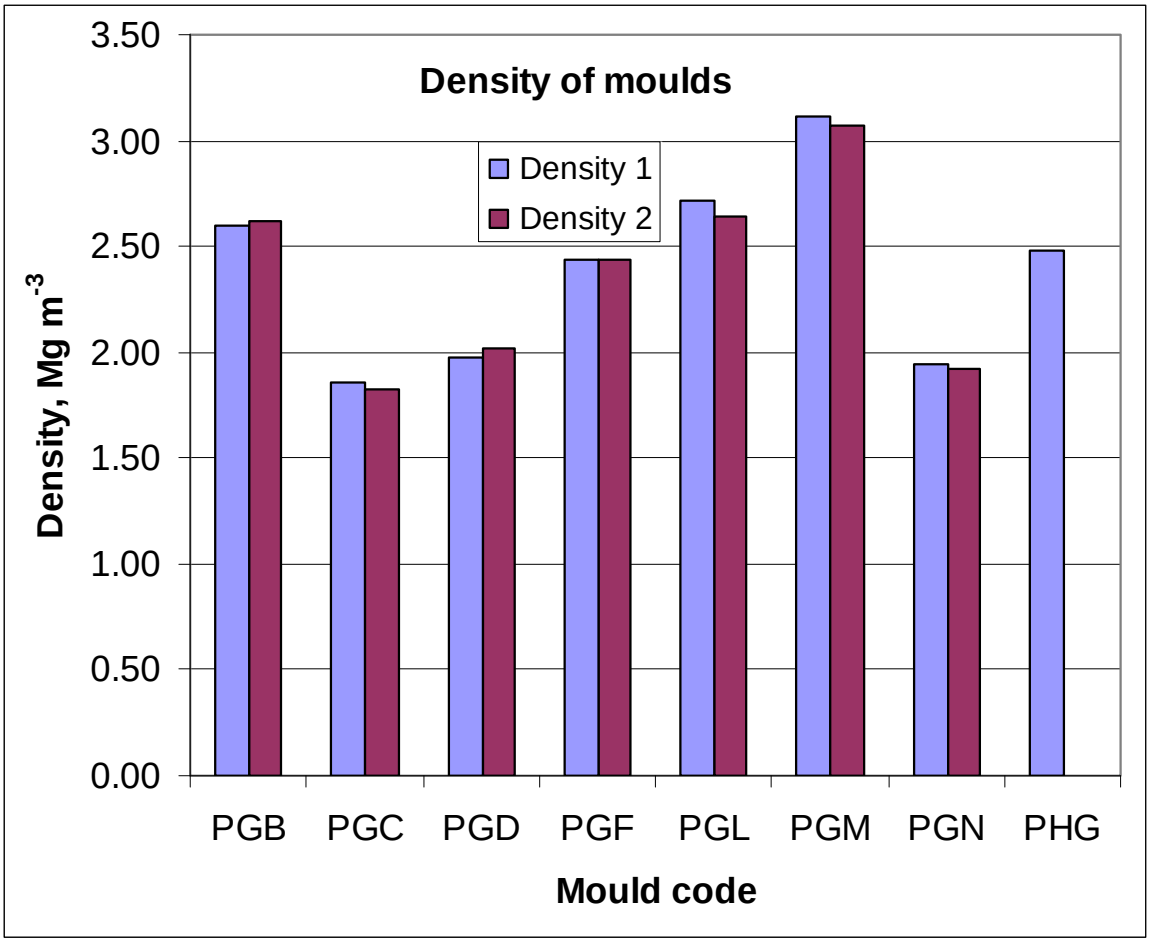

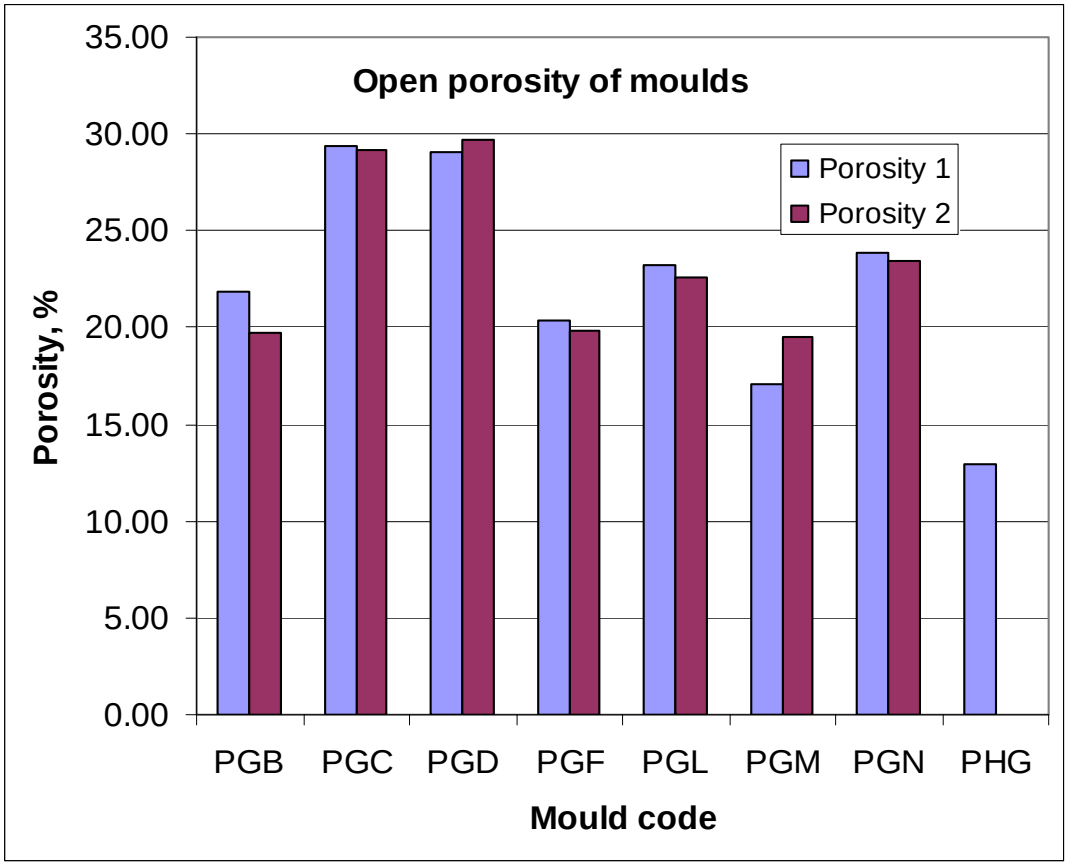

A.3.3 Shrinkage on firing

To understand behaviour in thermal expansion runs, shrinkage tests were performed. Small squares/ rectangles of each mould cut, and dimensions measured before and after heating to 1430 °C for 1 h in air. Data given for average length and width fractional shrinkages.

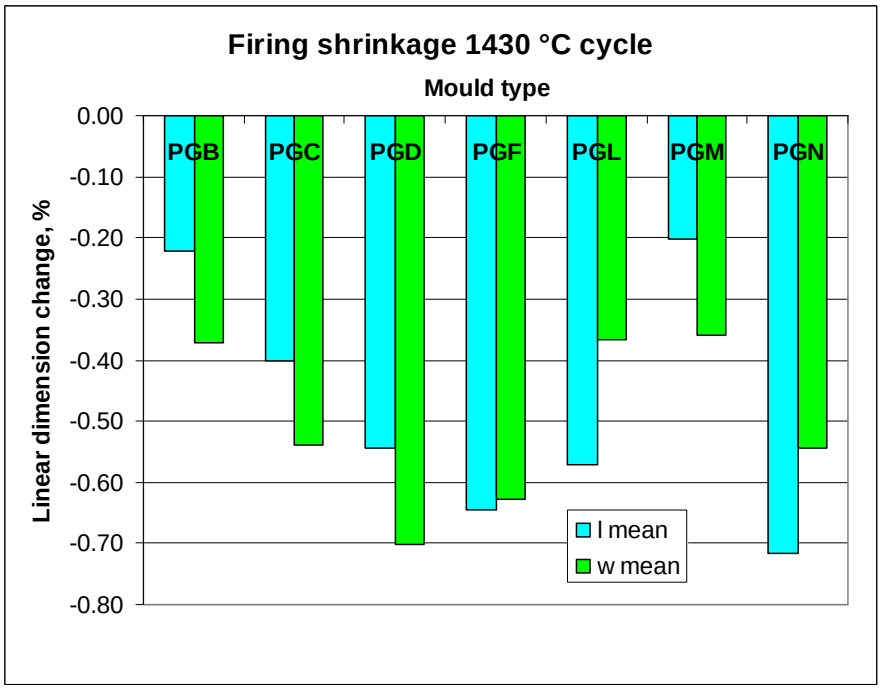

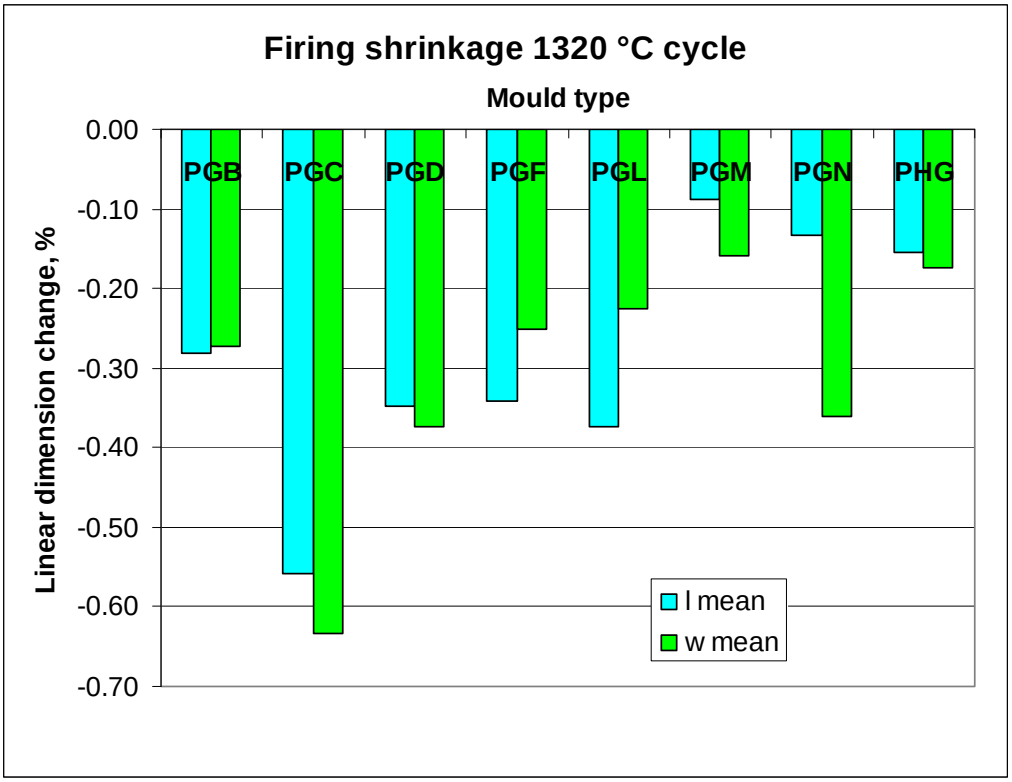

While generally larger, the dilatometer shrinkages are ranked approximately the same as the unstressed firing shrinkages.

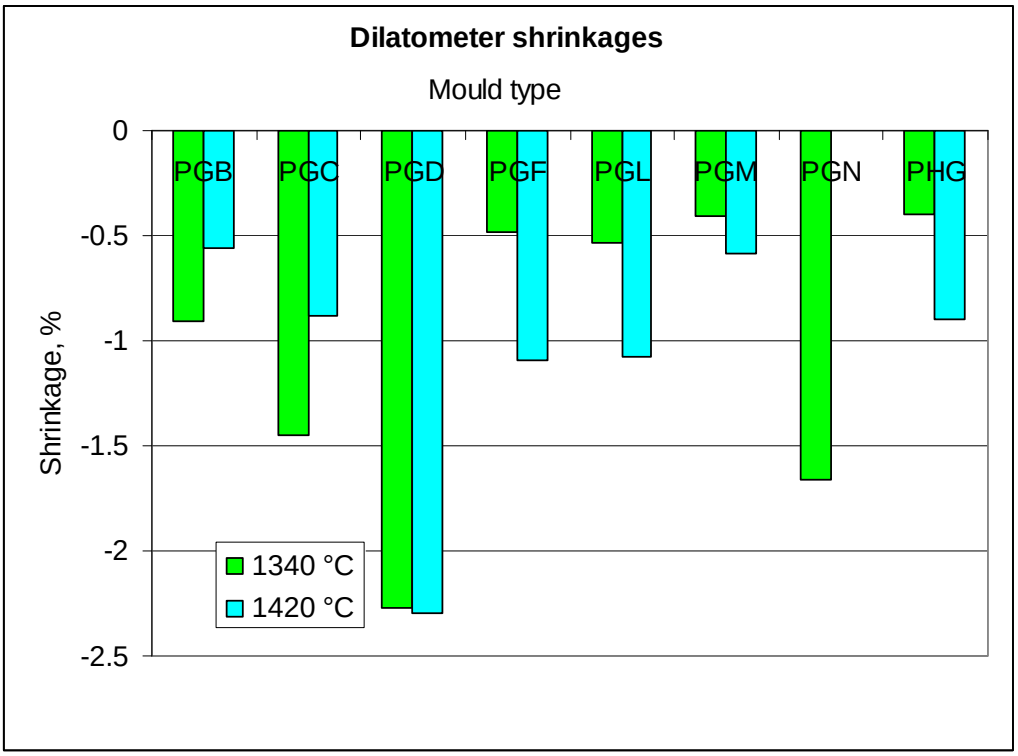

A.3.4. Thermal expansion

The general trend is that the higher the temperature, the larger the net shrinkage.

A.3.4.1 Mould PGB

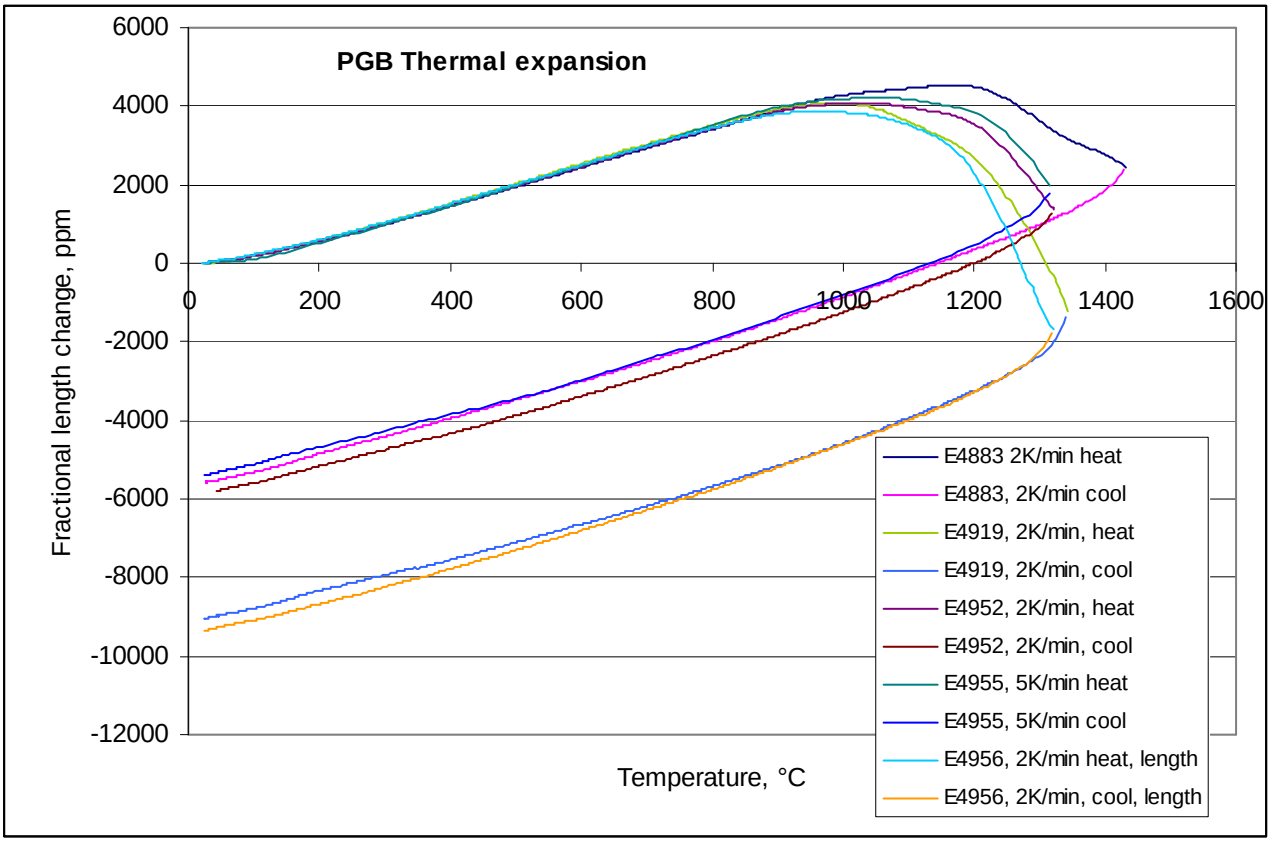

Run 1, across the width (heating rate 2 K/min)**:**

E4882	RT Density:	2.61 Mg m^{-3}	Offset:	5580 ppm	
Temp. range, °C	Expansion coeff., 10^{-6} K^{-1}		Temp., °C	Density, Mg m^{-3}	
	Heat	Vool		Heat	Cool
			25	2.610	2.654
25-100	2.7	3.5	100	2.608	2.652
25-200	3.3	4.2	200	2.605	2.648
25-300	3.6	4.3	300	2.602	2.645
25-400	3.9	4.4	400	2.599	2.641
25-500	4.1	4.4	500	2.595	2.638
25-600	4.2	4.5	600	2.591	2.634
25-700	4.3	4.6	700	2.587	2.630
25-800	4.4	4.6	800	2.583	2.626
25-900	4.5	4.9	900	2.579	2.620
25-1000	4.4	4.8	1000	2.577	2.617
25-1100	4.1	4.9	1100	2.576	2.613
25-1200	3.8	5.0	1200	2.575	2.608
25-1300	2.9	5.1	1300	2.581	2.603
25-1400	2.0	5.4	1400	2.589	2.596
T max, °C	1430				

Run 2, across the width (heating rate 2 K/min)**:**

E4919	RT density:	2.61 Mg m^{-3}	Offset:	9050 ppm	
Temp. range, °C	Expansion coeff., 10^{-6} K^{-1}		Temp., °C	Density. Mg m^{-3}	
	Heat	Cool		Heat	Cool
			25	2.610	2.682
25-100	3.5	3.5	100	2.608	2.680
25-200	3.4	4.1	200	2.605	2.676
25-300	3.7	4.0	300	2.602	2.673
25-400	4.0	4.0	400	2.598	2.670
25-500	4.3	4.1	500	2.594	2.667
25-600	4.4	4.2	600	2.590	2.663
25-700	4.5	4.3	700	2.586	2.659
25-800	4.3	4.3	800	2.584	2.656
25-900	4.5	4.5	900	2.579	2.651
25-1000	4.2	4.6	1000	2.578	2.646
25-1100	3.4	4.7	1100	2.582	2.642
25-1200	2.3	4.9	1200	2.589	2.636
25-1300	0.3	5.3	1300	2.607	2.629
T max, °C	1336				

Run 3, across width (heating rate 2 K/min)**:**

E4952	RT density:	2.61 Mg m^{-3}	Offset:	5800 ppm	
Temp. range, °C	Expansion coeff., 10^{-6} K^{-1}		Temp., °C	Density, Mg m^{-3}	
	Heat	Cool		Heat	Cool
			25	2.610	2.656
25-100	2.4	3.3	100	2.609	2.654
25-200	3.1	3.9	200	2.606	2.651
25-300	3.6	4	300	2.602	2.647
25-400	3.9	4	400	2.599	2.644
25-500	4.1	4.1	500	2.595	2.640
25-600	4.3	4.3	600	2.591	2.636
25-700	4.4	4.4	700	2.587	2.632
25-800	4.4	4.5	800	2.583	2.628
25-900	4.4	4.6	900	2.580	2.624
25-1000	4.2	4.7	1000	2.578	2.620
25-1100	3.7	4.8	1100	2.579	2.615
25-1200	3	5	1200	2.583	2.610
25-1300	-1.4	4.9	1300	2.624	2.607
T max, °C	1320				

Run 4, across width:

E4955	RT density:	2.61 Mg m^{-3}	Offset:	5400 ppm	
Temp. range, °C	Expansion coefficient, 10^{-6} K^{-1}		Temp., °C	Density, Mg m^{-3}	
	Heat	Cool		Heat	Cool
			25	2.610	2.653
25-100	-1.3	3.6	100	2.611	2.651
25-200	3	4.1	200	2.606	2.647
25-300	3.6	4.1	300	2.602	2.644
25-400	3.9	4.1	400	2.599	2.641
25-500	4.2	4.1	500	2.594	2.637
25-600	4.3	4.2	600	2.591	2.634
25-700	4.5	4.3	700	2.586	2.630
25-800	4.6	4.5	800	2.582	2.625
25-900	4.5	4.6	900	2.579	2.621
25-1000	4.3	4.7	1000	2.577	2.617
25-1100	3.9	4.8	1100	2.577	2.612
25-1200	3.3	5	1200	2.580	2.607
25-1300	1.8	5.4	1300	2.592	2.599
T max, °C	1320				

Run 1, parallel to length:

E4956	RT density:	2.61 Mg m^{-3}	Offset:	9330 ppm	
Temp. range, °C	Expansion coeff., 10^{-6} K^{-1}		Temp., °C	Density, Mg m^{-3}	
	Heat	Cool		Heat	Cool
			25	2.610	2.684
25-100	2.9	3.2	100	2.608	2.683
25-200	3.4	3.7	200	2.605	2.679
25-300	3.8	3.9	300	2.602	2.676
25-400	4	4.1	400	2.598	2.672
25-500	4.2	4.3	500	2.594	2.668
25-600	4.4	4.4	600	2.590	2.664
25-700	4.4	4.5	700	2.587	2.660
25-800	4.4	4.6	800	2.583	2.656
25-900	4.3	4.7	900	2.581	2.652
25-1000	4	4.8	1000	2.580	2.647
25-1100	3.3	5	1100	2.582	2.642
25-1200	2	5.1	1200	2.592	2.637
25-1300	-0.8	5.5	1300	2.618	2.629
T max, °C	1320				

A.3.4.2 Mould PGC

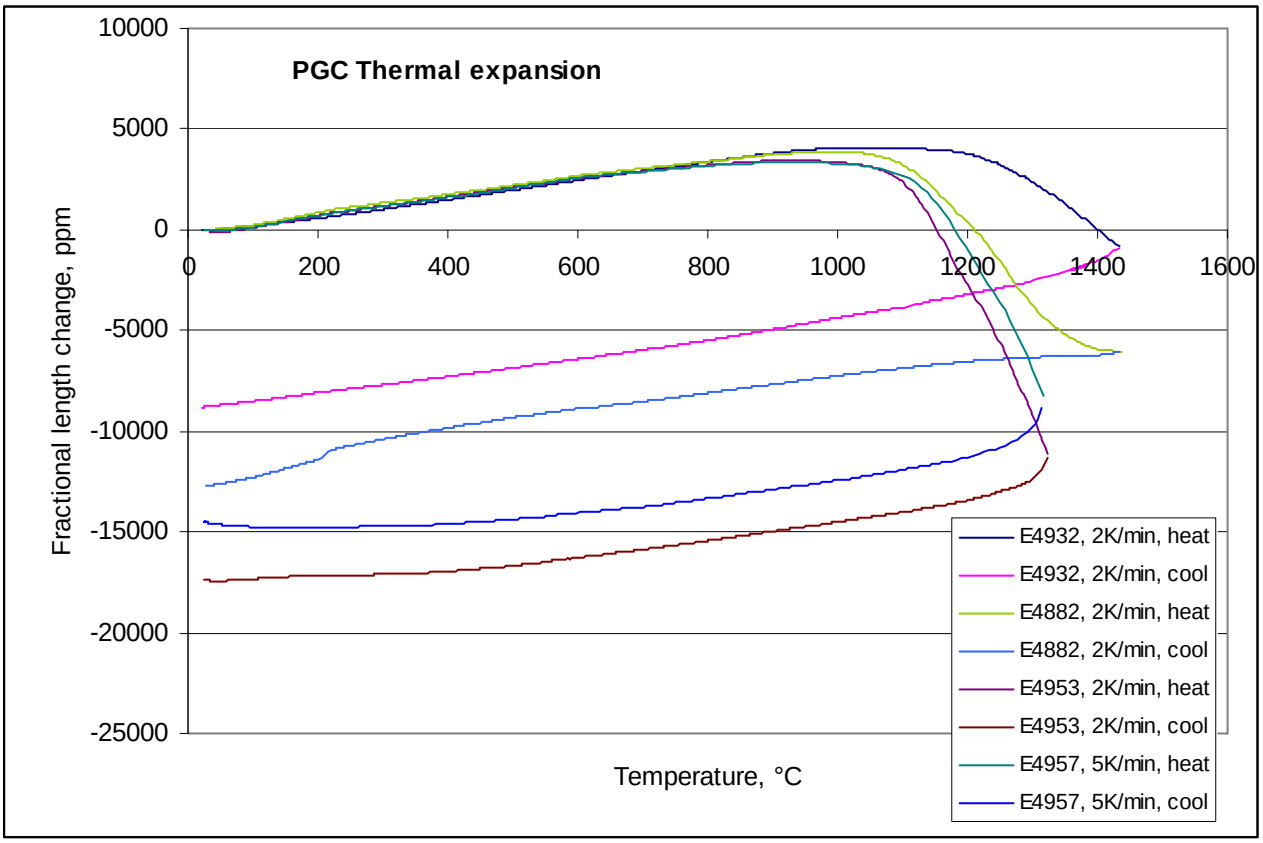

Run 1, across width(heating rate 2 K/min):

E4883	**RT density:**	**1.84 Mg m^{-3}**	**Offset:**	**12730 ppm**	
Temp. range, °C	**Expansion coeff., 10^{-6} K^{-1}**		**Temp., °C**	**Density, Mg m^{-3}**	
	Heat	**Cool**		**Heat**	**Cool**
			25	1.840	1.912
25-100	2.9	6.0	100	1.839	1.910
25-200	3	7.6	200	1.837	1.904
25-300	4.8	8.5	300	1.833	1.899
25-400	4.7	7.7	400	1.830	1.896
25-500	4.7	7.2	500	1.828	1.893
25-600	4.7	6.7	600	1.825	1.890
25-700	4.5	6.2	700	1.823	1.888
25-800	4.4	6.0	800	1.821	1.886
25-900	4.3	5.8	900	1.819	1.883
25-1000	4	5.6	1000	1.819	1.881
25-1100	3	5.5	1100	1.822	1.879
25-1200	0.3	5.3	1200	1.838	1.877
25-1300	-2.9	5.0	1300	1.861	1.876
25-1400	-4.3	4.7	1400	1.873	1.876
T max, °C	1430				

Run 2 across width(heating rate 2 K/min):

E4932	RT density:	1.84 Mg m^{-3}	Offset:	8790 ppm	
Temp. range, °C	Expansion coeff., 10^{-6} K^{-1}		Temp., °C	Density, Mg m^{-3}	
	Heat	Cool		Heat	Cool
			25	1.840	1.889
25-100	2.5	3.7	100	1.839	1.888
25-200	3.3	4.1	200	1.837	1.885
25-300	3.7	4	300	1.834	1.883
25-400	4	4	400	1.832	1.881
25-500	4.2	4.1	500	1.829	1.878
25-600	4.3	4.1	600	1.826	1.876
25-700	4.3	4.2	700	1.824	1.873
25-800	4.4	4.3	800	1.821	1.871
25-900	4.3	4.4	900	1.819	1.868
25-1000	4.2	4.5	1000	1.818	1.865
25-1100	3.8	4.6	1100	1.818	1.862
25-1200	3.2	4.8	1200	1.819	1.858
25-1300	1.9	4.9	1300	1.827	1.854
25-1400	0.0	5.3	1400	1.840	1.849
T max, °C	1433				

Run 3, across width (heating rate 2 K/min):

E4953	RT density:	1.84 Mg m^{-3}	Offset:	17400 ppm	
Temp. range, °C	Expansion coeff., 10^{-6} K^{-1}		Temp., °C	Density, Mg m^{-3}	
	Heat	Cool		Heat	Cool
			25	1.840	1.939
25-100	-1.3	0.4	100	1.841	1.939
25-200	4	1.1	200	1.836	1.938
25-300	4.3	1	300	1.833	1.938
25-400	4.4	1.1	400	1.831	1.937
25-500	4.4	1.4	500	1.829	1.936
25-600	4.5	1.9	600	1.826	1.933
25-700	4.3	2.2	700	1.824	1.931
25-800	4.1	2.5	800	1.823	1.928
25-900	3.9	2.7	900	1.821	1.926
25-1000	3.4	2.9	1000	1.822	1.923
25-1100	2.2	3.1	1100	1.827	1.920
25-1200	-2.3	3.3	1200	1.855	1.917
25-1300	-7.2	3.9	1300	1.892	1.911
T max, °C	1320				

Run 4, across width (heating rate 5 K/min)**:**

E4957	**RT density:**	**1.84 Mg m^{-3}**	**Offset:**	**14500 ppm**	
Temp. range, °C	**Expansion coeff., 10^{-6} K^{-1}**		**Temp., °C**	**Density, Mg m^{-3}**	
	Heat	**Cool**		**Heat**	**Cool**
			25	1.840	1.922
25-100	-1.5	-3.3	100	1.841	1.924
25-200	4.1	-1.4	200	1.836	1.924
25-300	4.2	-0.8	300	1.834	1.924
25-400	4.2	-0.3	400	1.831	1.923
25-500	4.3	0.2	500	1.829	1.922
25-600	4.5	0.8	600	1.826	1.920
25-700	4.3	1.1	700	1.824	1.918
25-800	4.1	1.5	800	1.823	1.916
25-900	3.8	1.8	900	1.822	1.913
25-1000	3.4	2.1	1000	1.822	1.911
25-1100	2.5	2.4	1100	1.825	1.908
25-1200	-0.9	2.7	1200	1.846	1.904
25-1300	-5.4	3.7	1300	1.879	1.895
T max, °C	1320				

A.3.4.3 Mould PGD

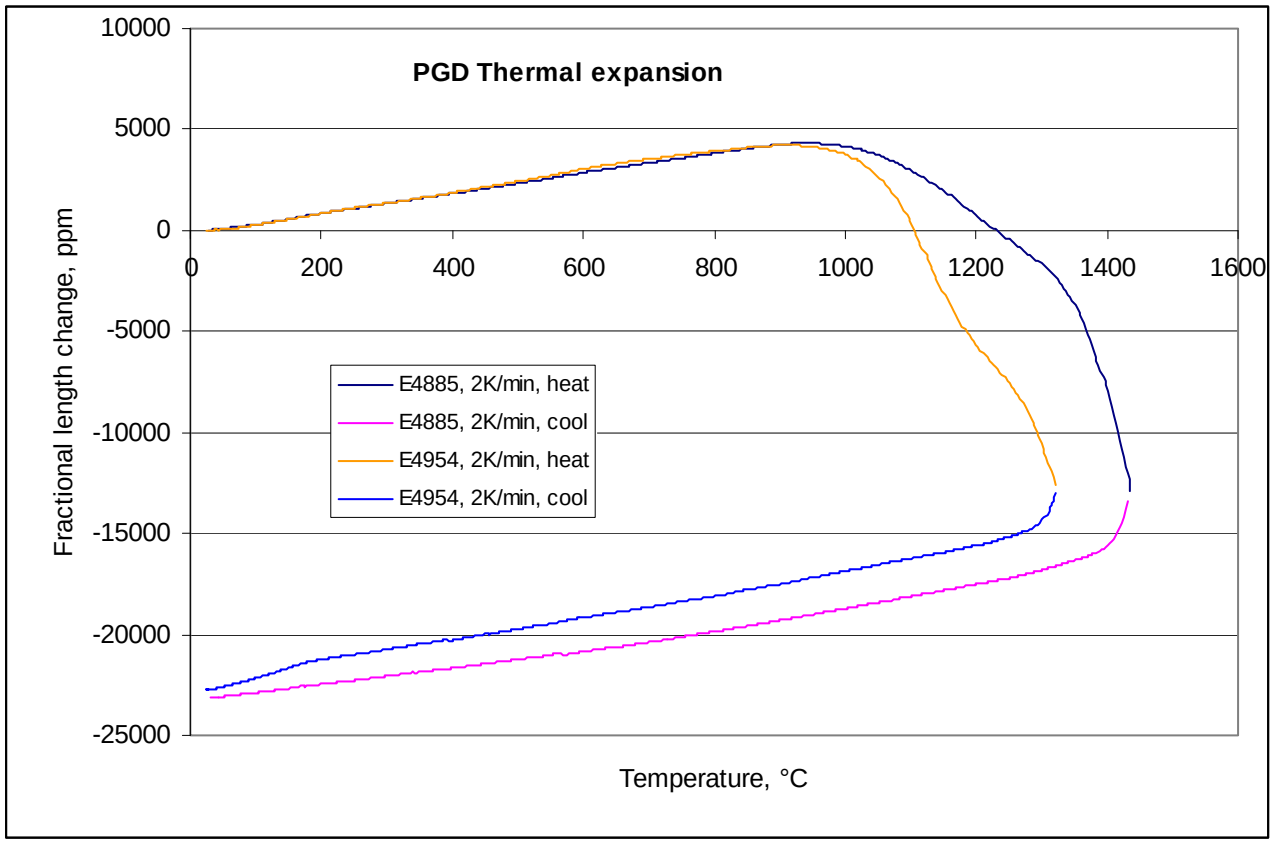

Run 1 (heating rate 2 k/min):

E4885	**RT density:**	**2.00 Mg m^{-3}**	**Offset:**	**23000 ppm**	
Temp. range, °C	**Expansion coeff., 10^{-6} K^{-1}**		**Temp., °C**	**Density, Mg m^{-3}**	
	Heat	**Cool**		**Heat**	**Cool**
			25	2.000	2.078
25-100	3.5	3.9	100	1.998	2.077
25-200	4.9	4	200	1.995	2.074
25-300	4.9	4	300	1.992	2.072
25-400	4.9	4	400	1.989	2.069
25-500	4.9	4.1	500	1.986	2.066
25-600	5	4	600	1.983	2.064
25-700	5	4.1	700	1.980	2.061
25-800	4.9	4.3	800	1.977	2.058
25-900	4.9	4.4	900	1.974	2.055
25-1000	4.3	4.6	1000	1.975	2.051
25-1100	2.7	4.7	1100	1.983	2.047
25-1200	0.6	4.8	1200	1.996	2.044
25-1300	-1.3	5	1300	2.010	2.039
25-1400	-2.7	5.6	1400	2.022	2.031
T max, °C	1430				

Run 2, (heating rate 2 K/min)

E4885	RT density:	2.00 Mg m^{-3}	Offset:	22700 ppm	
Temp. range, °C	Expansion coeff., 10^{-6} K^{-1}		Temp., °C	Density, Mg m^{-3}	
	Heat	Cool		Heat	Cool
			25	2.000	2.143
25-100	3.5	7.2	100	1.998	2.139
25-200	4.9	8.4	200	1.995	2.133
25-300	4.9	7.2	300	1.992	2.130
25-400	5	6.5	400	1.989	2.127
25-500	5.1	6.2	500	1.986	2.124
25-600	5.3	6.2	600	1.982	2.120
25-700	5.2	6	700	1.979	2.117
25-800	5.1	6	800	1.976	2.113
25-900	4.8	6	900	1.975	2.109
25-1000	3.9	6	1000	1.977	2.105
25-1100	0.4	6	1100	1.997	2.102
25-1200	-4.8	6.1	1200	2.034	2.097
25-1300	-8.2	6.5	1300	2.064	2.090
T max, °C	1320				

A.3.4.4 Mould PGF

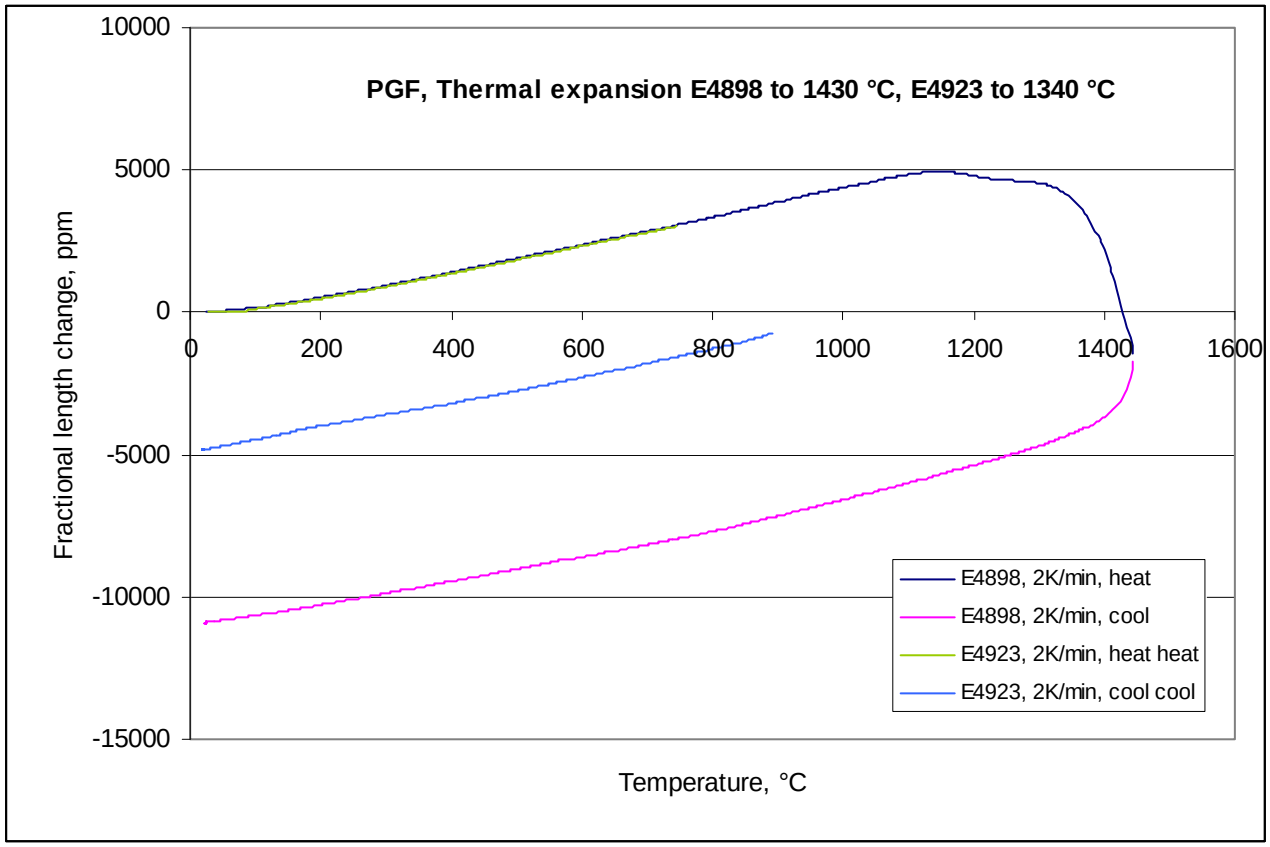

Run 1 (Heating rate 2 K/min):

E4898	RT density:	2.44 Mg m^{-3}	Offset:	10892 ppm	
Temp. range, °C	Expansion coeff., 10^{-6} K^{-1}		Temp., °C	Density, Mg m^{-3}	
	Heat	Cool		Heat	Cool
			25	2.440	2.521
25-100	2.3	3.2	100	2.439	2.520
25-200	3	3.5	200	2.436	2.517
25-300	3.4	3.7	300	2.433	2.514
25-400	3.7	3.8	400	2.430	2.511
25-500	4	3.9	500	2.426	2.508
25-600	4.1	4	600	2.423	2.504
25-700	4.2	4	700	2.419	2.501
25-800	4.3	4.1	800	2.416	2.498
25-900	4.4	4.3	900	2.412	2.493
25-1000	4.5	4.4	1000	2.408	2.489
25-1100	4.5	4.6	1100	2.405	2.484
25-1200	4.1	4.7	1200	2.405	2.480
25-1300	3.6	4.9	1300	2.407	2.475
25-1400	1.6	5.2	1400	2.424	2.468
T max, °C	1430				

Run 2 (heating rate 2K/min):

E4923	**RT density:**	**2.44 Mg m^{-3}**	**Offset:**	**4800 ppm**	
Temp. range, °C	**Expansion coeff., 10^{-6} K^{-1}**		**Temp., °C**	**Density, Mg m^{-3}**	
	Heat	**Cool**		**Heat**	**Cool**
			25	2.440	2.521
25-100	1.7	4.1	100	2.439	2.519
25-200	2.7	4.6	200	2.437	2.515
25-300	3.3	4.4	300	2.433	2.512
25-400	3.6	4.3	400	2.430	2.509
25-500	3.9	4.3	500	2.426	2.506
25-600	4	4.4	600	2.423	2.502
25-700	4.2	4.4	700	2.419	2.499
25-800	-	4.5	800	-	2.495
25-900	Data lost due to thermocouple problem				
25-1000					
25-1100					
25-1200					
25-1300					
T max, °C	1340				

A.3.4.5 Mould PGL

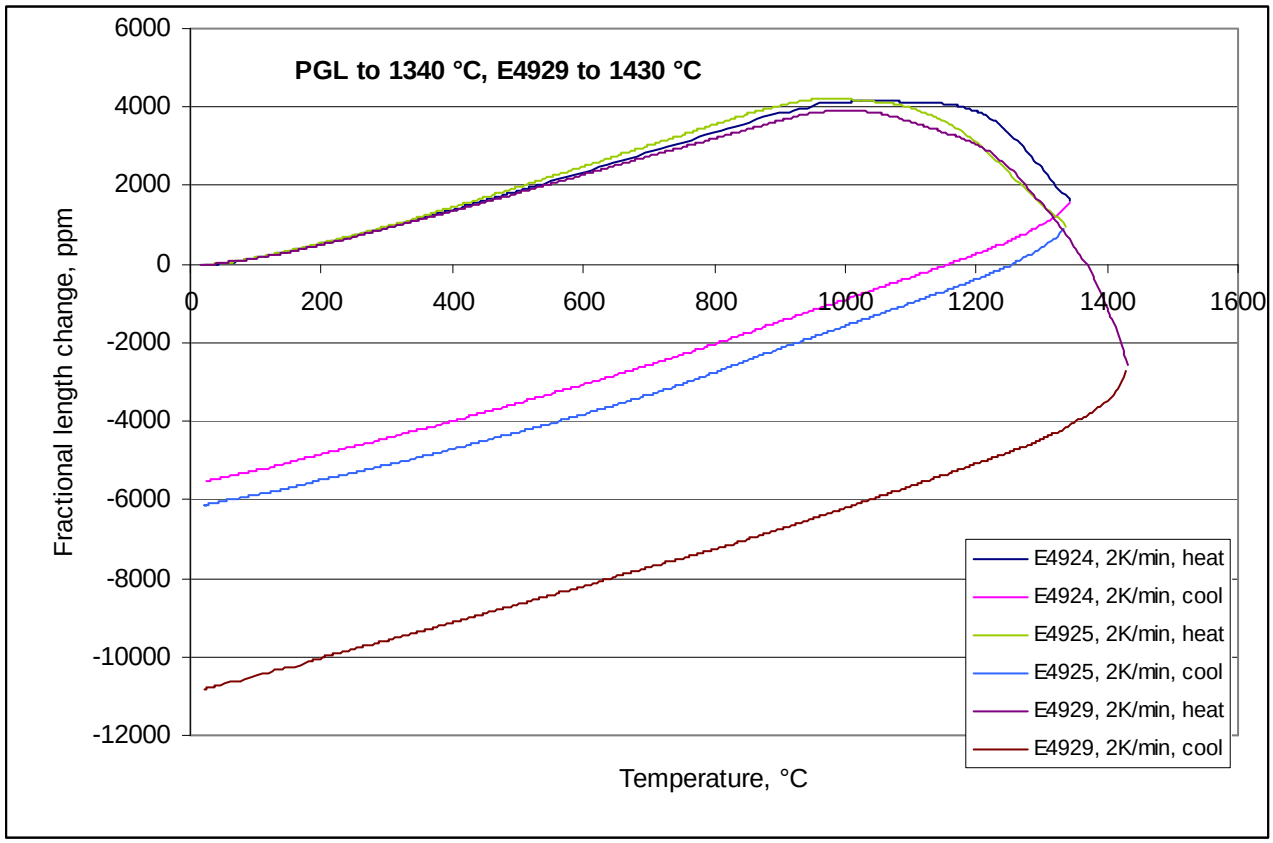

Run 1 (heating rate 2 K/min):

E4924	**RT density:**	**2.68 Mg m^{-3}**	**Offset:**	**5530 ppm**	
Temp. range, °C	**Expansion coeff., 10^{-6} K^{-1}**		**Temp., °C**	**Density, Mg m^{-3}**	
	Heat	**Cool**		**Heat**	**Cool**
			25	2.680	2.725
25-100	2	3.6	100	2.679	2.723
25-200	2.9	3.9	200	2.676	2.719
25-300	3.4	4	300	2.672	2.716
25-400	3.7	4.1	400	2.669	2.712
25-500	3.9	4.2	500	2.665	2.709
25-600	4.1	4.3	600	2.661	2.705
25-700	4.2	4.4	700	2.657	2.701
25-800	4.3	4.5	800	2.653	2.697
25-900	4.4	4.6	900	2.649	2.692
25-1000	4.2	4.7	1000	2.647	2.688
25-1100	3.8	4.8	1100	2.647	2.683
25-1200	3.3	4.9	1200	2.649	2.678
25-1300	1.9	5.1	1300	2.661	2.672
T max, °C	1344				

Run 2 (heating rate 2 K/min)

E4925	RT density:	2.68 Mg m^{-3}	Offset:	6117 ppm	
Temp. range, °C	Expansion coeff., 10^{-6} K^{-1}		Temp., °C	Density, Mg m^{-3}	
	Heat	Cool		Heat	Cool
			25	2.680	2.730
25-100	2.1	3.2	100	2.679	2.728
25-200	3	3	200	2.676	2.725
25-300	3.5	3.6	300	2.672	2.722
25-400	3.8	3.8	400	2.669	2.718
25-500	4.1	3.9	500	2.664	2.715
25-600	4.3	4	600	2.660	2.711
25-700	4.5	4.1	700	2.656	2.707
25-800	4.6	4.3	800	2.652	2.703
25-900	4.6	4.5	900	2.648	2.698
25-1000	4.3	4.7	1000	2.647	2.693
25-1100	3.7	4.8	1100	2.648	2.688
25-1200	2.6	4.9	1200	2.656	2.683
25-1300	1.2	5.1	1300	2.668	2.677
T max, °C	1336				

Run 3 (heating rate 2 K/min):

E4929	RT density:	2.68 Mg m^{-3}	Offset:	10800 ppm	
Temp. range, °C	Expansion coeff., 10^{-6} K^{-1}		Temp., °C	Density, Mg m^{-3}	
	Heat	Cool		Heat	Cool
			25	2.680	2.769
25-100	2	4.4	100	2.679	2.766
25-200	2.9	4.4	200	2.676	2.762
25-300	3.3	4.4	300	2.673	2.759
25-400	3.6	4.5	400	2.669	2.755
25-500	3.8	4.5	500	2.666	2.751
25-600	4	4.5	600	2.662	2.747
25-700	4.1	4.6	700	2.658	2.743
25-800	4.1	4.6	800	2.655	2.739
25-900	4.2	4.6	900	2.651	2.736
25-1000	4	4.7	1000	2.649	2.731
25-1100	3.4	4.8	1100	2.651	2.726
25-1200	2.6	4.9	1200	2.656	2.721
25-1300	1.2	5	1300	2.668	2.716
25-1400	-0.8	5.3	1400	2.689	2.709
T max, °C	1431				

A.3.4.6 Mould PGM

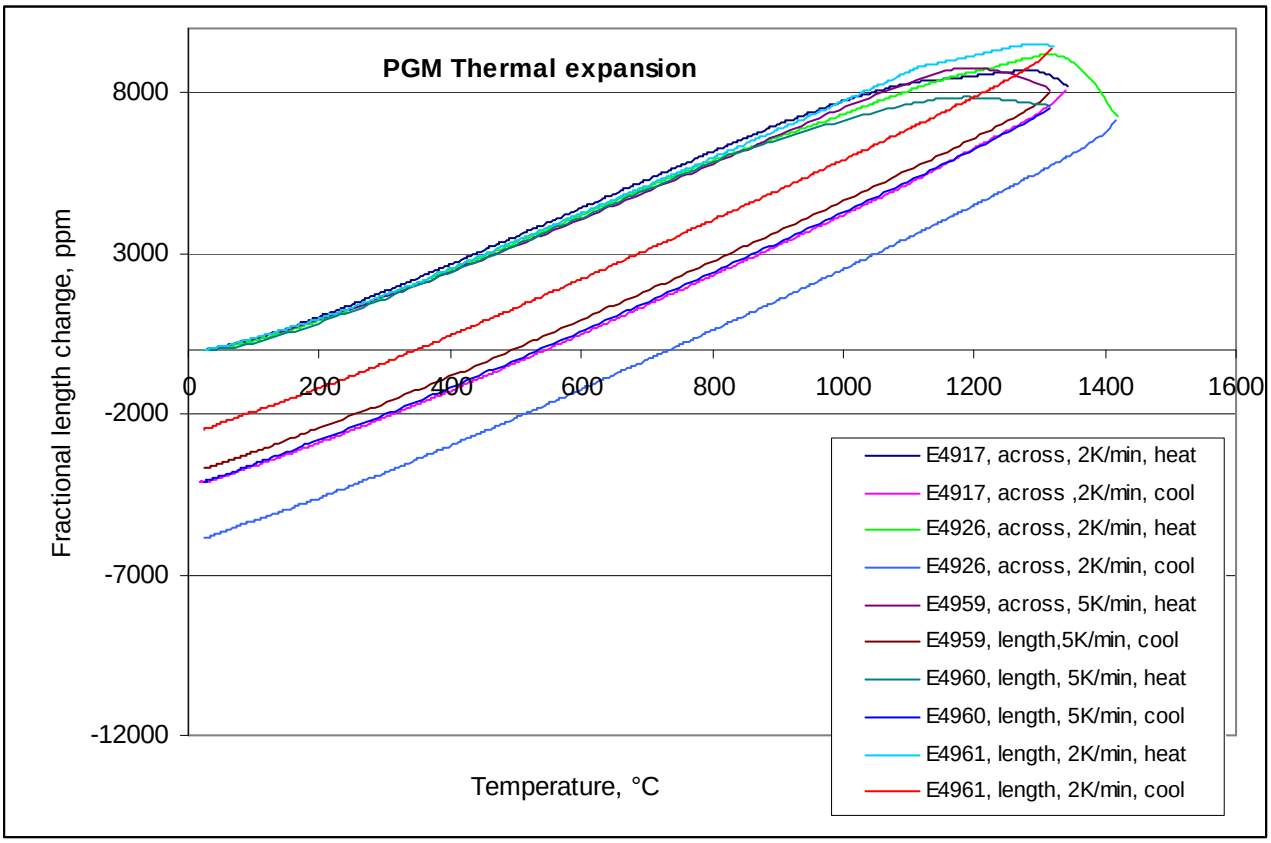

Run 1 across width (heating rate 2 K/min):

E4917	**RT density:**	**3.095 Mg m^{-3}**	**Offset:**	**4113 ppm**	
Temp. range, °C	**Expansion coeff., 10^{-6} K^{-1}**		**Temp., °C**	**Density, Mg m^{-3}**	
	Heat	**Cool**		**Heat**	**Cool**
			25	3.095	3.134
25-100	4.3	6.5	100	3.092	3.129
25-200	5.8	6.9	200	3.086	3.122
25-300	6.6	7.3	300	3.078	3.115
25-400	7.1	7.5	400	3.070	3.107
25-500	7.4	7.8	500	3.063	3.099
25-600	7.7	8	600	3.054	3.091
25-700	7.8	8.1	700	3.047	3.083
25-800	7.9	8.3	800	3.039	3.074
25-900	8	8.4	900	3.031	3.065
25-1000	7.9	8.5	1000	3.025	3.057
25-1100	7.7	8.6	1100	3.019	3.048
25-1200	7.3	8.8	1200	3.017	3.038
25-1300	6.8	9	1300	3.016	3.028
T max, °C	1342				

Run 2 across width (heating rate 2 K/min):

E4926	RT density:	3.095 Mg m^{-3}	Offset:	5874 ppm	
Temp. range, °C	Expansion coeff., 10^{-6} K^{-1}		Temp., °C	Density, Mg m^{-3}	
	Heat	Cool		Heat	Cool
			25	3.095	3.150
25-100	3.5	7.3	100	3.093	3.145
25-200	5.1	7.1	200	3.087	3.138
25-300	6.0	7.5	300	3.080	3.131
25-400	6.6	7.7	400	3.072	3.123
25-500	7.0	7.9	500	3.064	3.115
25-600	7.3	8.1	600	3.056	3.107
25-700	7.5	8.2	700	3.048	3.098
25-800	7.6	8.4	800	3.041	3.089
25-900	7.6	8.5	900	3.034	3.081
25-1000	7.5	8.6	1000	3.028	3.072
25-1100	7.5	8.7	1100	3.021	3.063
25-1200	7.4	8.8	1200	3.016	3.054
25-1300	7.2	8.9	1300	3.011	3.045
25-1400	5.7	9.2	1400	3.023	3.034
T max °C	1419				

Run 3 across width (heating rate 5 K/min):

E4959	RT density:	3.095 Mg m^{-3}	Offset:	3700 ppm	
Temp. range, °C	Expansion coeff., 10^{-6} K^{-1}		Temp., °C	Density, Mg m^{-3}	
	Heat	Cool		Heat	Cool
			25	3.095	3.130
25-100	4.8	6.5	100	3.092	3.125
25-200	5.5	7.2	200	3.086	3.118
25-300	6	7.4	300	3.080	3.111
25-400	6.5	7.6	400	3.072	3.103
25-500	6.8	7.6	500	3.065	3.096
25-600	7.1	8	600	3.057	3.087
25-700	7.3	8.2	700	3.050	3.078
25-800	7.5	8.3	800	3.042	3.070
25-900	7.6	8.4	900	3.034	3.062
25-1000	7.7	8.5	1000	3.026	3.053
25-1100	7.7	8.6	1100	3.019	3.044
25-1200	7.5	8.7	1200	3.015	3.036
25-1300	6.5	8.9	1300	3.019	3.025
T max, °C	1320				

Run 4 along length (heating rate 5 K/min):

E4960	**RT density:**	**3.095 Mg m^{-3}**	**Offset:**	**4100 ppm**	
Temp. range, °C	**Expansion coeff., 10^{-6} K^{-1}**		**Temp., °C**	**Density, Mg m^{-3}**	
	Heat	**Cool**		**Heat**	**Cool**
			25	3.095	3.133
25-100	2.9	6.9	100	3.093	3.129
25-200	4.8	7.4	200	3.087	3.121
25-300	5.8	7.5	300	3.080	3.114
25-400	6.4	7.7	400	3.073	3.106
25-500	6.8	7.9	500	3.065	3.098
25-600	7.2	8.1	600	3.057	3.090
25-700	7.4	8.3	700	3.049	3.081
25-800	7.5	8.4	800	3.042	3.073
25-900	7.5	8.5	900	3.035	3.064
25-1000	7.3	8.6	1000	3.030	3.056
25-1100	7.1	8.7	1100	3.025	3.047
25-1200	6.7	8.8	1200	3.023	3.038
25-1300	6	10.5	1300	3.025	3.011
T max, °C	1320				

Run 5 along length (heating rate 2 K/min):

E4961	**RT density:**	**3.095 Mg m^{-3}**	**Offset:**	**2500 ppm**	
Temp. range, °C	**Expansion coeff., 10^{-6} K^{-1}**		**Temp., °C**	**Density, Mg m^{-3}**	
	Heat	**Cool**		**Heat**	**Cool**
			25	3.095	3.118
25-100	4.8	7.2	100	3.092	3.113
25-200	5.5	7.2	200	3.086	3.107
25-300	6.2	7.5	300	3.079	3.099
25-400	6.7	7.7	400	3.072	3.091
25-500	7.1	7.9	500	3.064	3.083
25-600	7.4	8.1	600	3.056	3.075
25-700	7.6	8.3	700	3.048	3.066
25-800	7.7	8.4	800	3.040	3.058
25-900	7.8	8.5	900	3.032	3.050
25-1000	7.9	8.6	1000	3.025	3.041
25-1100	8	8.7	1100	3.017	3.032
25-1200	7.8	8.8	1200	3.011	3.024
25-1300	7.5	9	1300	3.008	3.013
T max, °C	1320				

A.3.4.7 Mould PGN

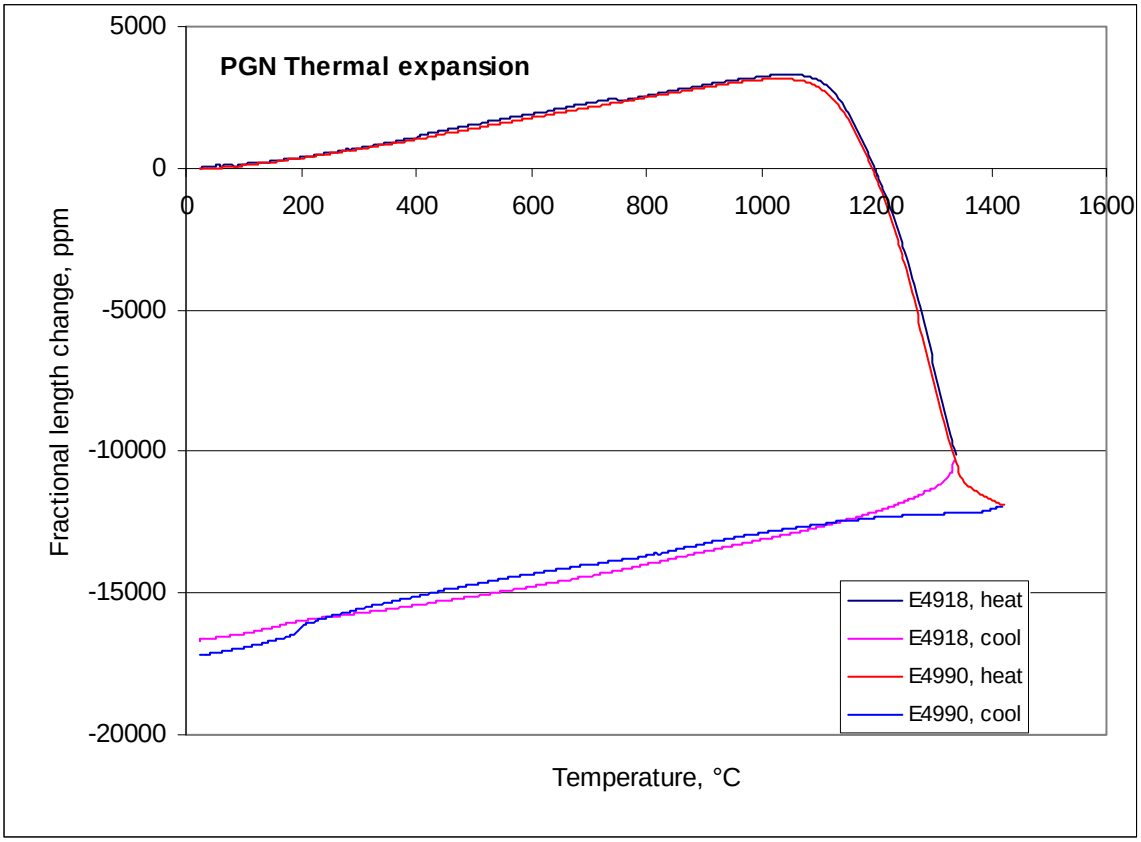

Run 1 across width (heating rate 2 K/min):

E4918	**RT density:**	**1.935 Mg m^{-3}**	**Offset:**	**16640 ppm**	
Temp. range, °C	**Expansion coeff., 10^{-6} K^{-1}**		**Temp., °C**	**Density, Mg m^{-3}**	
	Heat	**Cool**		**Heat**	**Cool**
			25	1.935	2.035
25-100	1.9	2.7	100	1.934	2.034
25-200	2.2	3.8	200	1.933	2.031
25-300	2.5	3.3	300	1.931	2.029
25-400	2.9	3.3	400	1.929	2.027
25-500	3.2	3.2	500	1.926	2.026
25-600	3.3	3.2	600	1.924	2.024
25-700	3.4	3.3	700	1.922	2.021
25-800	3.3	3.4	800	1.920	2.019
25-900	3.3	3.5	900	1.918	2.016
25-1000	3.3	3.6	1000	1.916	2.014
25-1100	2.9	3.7	1100	1.917	2.011
25-1200	-0.1	3.8	1200	1.936	2.008
25-1300	-5.5	4.2	1300	1.976	2.003
T max, °C	1340				

Run 2 across width (heating rate 2 K/min):

E4990	**RT density:**	**1.935 Mg m^{-3}**	**Offset:**	**17200 ppm**	
Temp. range, °C	**Expansion coeff., 10^{-6} K^{-1}**		**Temp., °C**	**Density, Mg m^{-3}**	
	Heat	**Cool**		**Heat**	**Cool**
			25	1.935	2.038
25-100	1.3	3.6	100	1.934	2.037
25-200	2.1	5.4	200	1.933	2.033
25-300	2.4	5.9	300	1.931	2.028
25-400	2.7	5.5	400	1.929	2.026
25-500	2.9	5.3	500	1.927	2.023
25-600	3.1	5	600	1.925	2.021
25-700	3.2	4.8	700	1.923	2.019
25-800	3.2	4.5	800	1.921	2.017
25-900	3.3	4.5	900	1.918	2.014
25-1000	3.2	4.4	1000	1.917	2.012
25-1100	2.6	4.3	1100	1.919	2.010
25-1200	-0.3	4.1	1200	1.937	2.009
25-1300	-6	3.9	1300	1.980	2.008
25-1400	-8.5	3.7	1400	2.004	2.008
T max, °C	1420				

A.3.4.8 Mould PHG

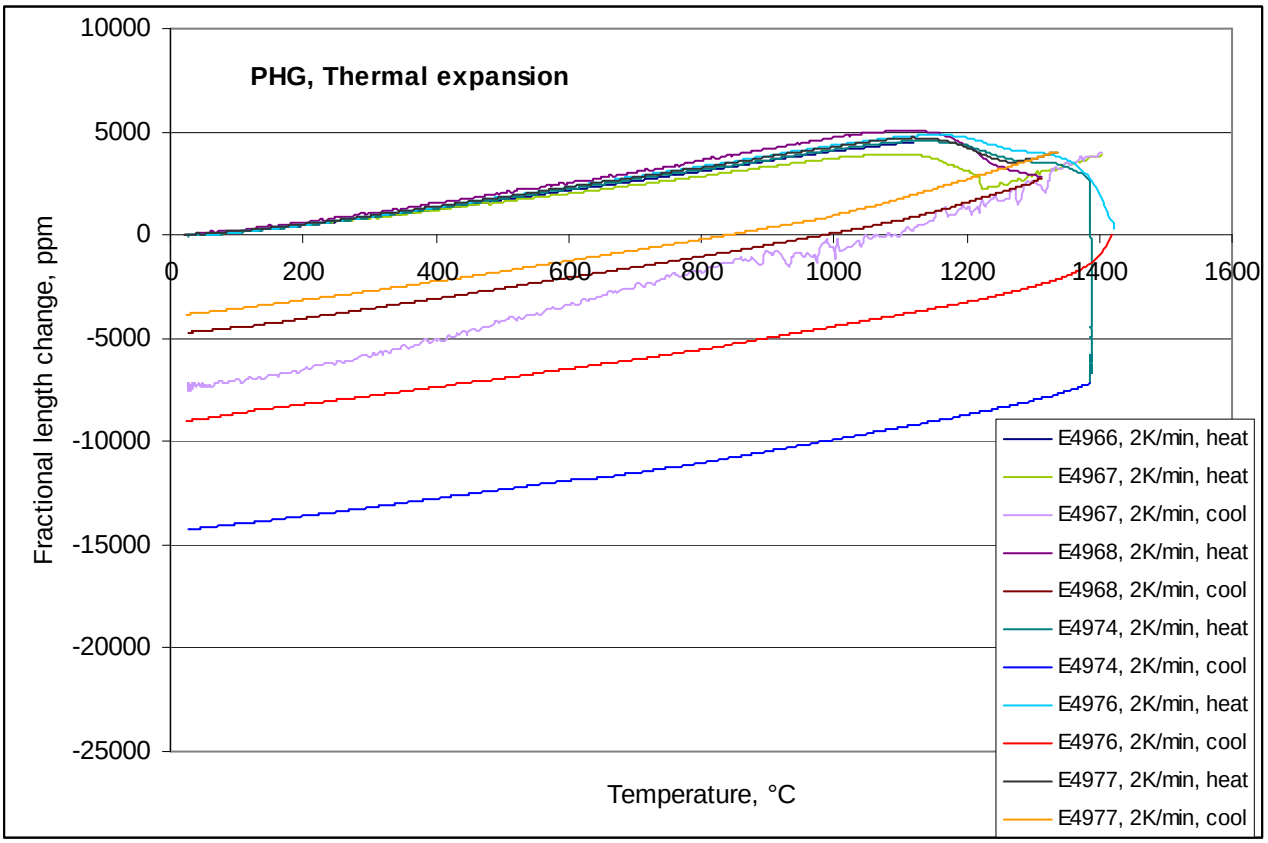

Run 2 across width (heating rate 2 K/min):

E4966	**RT density:**	**2.476 Mg m^{-3}**	**Offset:**	**n/a**	
Temp. range, °C	**Expansion coeff., 10^{-6} K^{-1}**		**Temp., °C**	**Density, Mg m^{-3}**	
	Heat	**Cool**		**Heat**	**Cool**
			25	2.476	-
25-100	1.9	-	100	2.475	-
25-200	2.6	-	200	2.473	-
25-300	3.1	-	300	2.470	-
25-400	3.3	-	400	2.467	-
25-500	3.6	-	500	2.463	-
25-600	3.8	-	600	2.460	-
25-700	3.7	-	700	2.458	-
25-800	4	-	800	2.453	-
25-900	4.1	-	900	2.450	-
25-1000	4.2	-	1000	2.446	-
25-1100	4.1	-	1100	2.444	-
25-1200	no data	-	1200	-	-
25-1300	-	-	1300	-	-
T max, °C	1320				

Run 3 across width (heating rate 2 K/min):

E4967	RT Density:	2.476 Mg m^{-3}	Offset,	- ppm	
Temp. range, °C	Expansion coeff., 10^{-6} K^{-1}		Temp., °C	Density, Mg m^{-3}	
	Heat	Cool		Heat	Cool
			25	2.476	-
25-100	2	-	100	2.475	-
25-200	2.7	-	200	2.472	-
25-300	3	-	300	2.470	-
25-400	3.2	-	400	2.467	-
25-500	3.3	-	500	2.464	-
25-600	3.5	-	600	2.461	-
25-700	3.6	-	700	2.458	-
25-800	3.7	-	800	2.455	-
25-900	3.8	-	900	2.451	-
25-1000	2.8	-	1000	2.456	-
25-1100	3.6	-	1100	2.447	-
25-1200	2.6	-	1200	2.453	-
25-1300	no data	-	1300	-	
T max, °C	1320				

Run 4 across width (heating rate 2 K/min):

E4968	RT density:	2.476 Mg m^{-3}	Offset:	4700 ppm	
Temp. range, °C	Expansion coeff., 10^{-6} K^{-1}		Temp., °C	Density, Mg m^{-3}	
	Heat	Cool		Heat	Cool
			25	2.476	2.511
25-100	2.5	3.5	100	2.475	2.509
25-200	3.3	3.8	200	2.472	2.506
25-300	3.8	4.2	300	2.468	2.503
25-400	4.2	4.3	400	2.464	2.499
25-500	4.3	4.5	500	2.461	2.495
25-600	4.4	4.6	600	2.457	2.491
25-700	4.5	4.7	700	2.454	2.487
25-800	4.6	4.7	800	2.450	2.484
25-900	4.8	4.6	900	2.445	2.481
25-1000	4.8	4.9	1000	2.442	2.476
25-1100	4.7	5	1100	2.439	2.471
25-1200	3.7	5.3	1200	2.444	2.465
25-1300	2.3	5.7	1300	2.454	2.457
T max, °C	1320				

Run 5 across width (heating rate 2 K/min):

E4974	RT density:	2.476 Mg m^{-3}	Offset:	14300 ppm	
Temp. range, °C	Expansion coeff., 10^{-6} K^{-1}		Temp., °C	Density, Mg m^{-3}	
	Heat	Cool		Heat	Cool
			25	2.476	2.585
25-100	1.7	3.9	100	2.475	2.583
25-200	2.6	3.9	200	2.473	2.580
25-300	3.1	4	300	2.470	2.577
25-400	3.5	4.1	400	2.466	2.573
25-500	3.7	4.1	500	2.463	2.570
25-600	3.9	4.2	600	2.459	2.567
25-700	4	4.1	700	2.456	2.564
25-800	4.1	4.2	800	2.453	2.560
25-900	4.2	4.4	900	2.449	2.556
25-1000	4.2	4.5	1000	2.446	2.552
25-1100	4.2	4.6	1100	2.443	2.547
25-1200	3.7	4.7	1200	2.444	2.543
25-1300	2.8	4.9	1300	2.450	2.537
T max, °C	1320				

Run 6, across width (heating rate 2 K/min, long hold at 1380 °C)

E4976	RT density:	2.476 Mg m^{-3}	Offset:	16640 ppm	
Temp. range, °C	Expansion coeff., 10^{-6} K^{-1}		Temp., °C	Density, Mg m^{-3}	
	Heat	Cool		Heat	Cool
			25	2.476	2.604
25-100	1.7	4.5	100	2.475	2.601
25-200	2.7	4.5	200	2.472	2.598
25-300	3.3	4.3	300	2.469	2.595
25-400	3.6	4.3	400	2.466	2.591
25-500	3.9	4.3	500	2.462	2.588
25-600	4.1	4.4	600	2.459	2.584
25-700	4.2	4.4	700	2.455	2.581
25-800	4.3	4.5	800	2.451	2.577
25-900	4.4	4.6	900	2.448	2.573
25-1000	4.5	4.7	1000	2.444	2.568
25-1100	4.4	4.8	1100	2.441	2.564
25-1200	4	4.9	1200	2.441	2.559
25-1300	3.1	5.1	1300	2.447	2.554
25-1400	1.4	5.8	1400	2.462	2.543
T max, °C	1380				

Run 7 across width (heating rate 2 K/min)

E4977	RT density:	2.476 Mg m^{-3}	Offset:	3800 ppm	
Temp. range, °C	Expansion coeff., 10^{-6} K^{-1}		Temp., °C	Density, Mg m^{-3}	
	Heat	Cool		Heat	Cool
			25	2.476	2.504
25-100	2.5	3.6	100	2.475	2.502
25-200	3	3.9	200	2.472	2.499
25-300	3.4	4	300	2.469	2.496
25-400	3.7	4.2	400	2.466	2.493
25-500	3.9	4.4	500	2.462	2.489
25-600	4	4.5	600	2.459	2.485
25-700	4.1	4.6	700	2.456	2.481
25-800	4.2	4.7	800	2.452	2.477
25-900	4.3	4.8	900	2.448	2.473
25-1000	4.4	4.9	1000	2.444	2.469
25-1100	4.3	5.2	1100	2.442	2.463
25-1200	3.6	5.5	1200	2.445	2.457
25-1300	2.9	5.9	1300	2.449	2.449
T max, °C	1320				

A.3.5 Heat capacity J/g/K

Note: Values obtained on cooling only

Mould PGB

PGB	550°C	600°C	650°C	700°C	750°C	800°C	850°C	900°C
cool 1	0.92	0.95	0.98	1.02	1.03	1.05	1.07	1.09
cool 2	0.92	0.94	0.97	0.99	1.01	1.03	1.05	1.07
cool 3	0.92	0.94	0.97	0.99	1.00	1.01	1.04	1.06
ave	**0.92**	**0.94**	**0.97**	**1.00**	**1.00**	**1.03**	**1.06**	**1.08**

PGB	950°C	1000°C	1050°C	1100°C	1150°C	1200°C	1250°C	1300°C
cool 1	1.10	1.10	1.10	1.10	1.11	1.12	1.14	1.10
cool 2	1.09	1.10	1.11	1.11	1.10	1.12	1.11	1.08
cool 3	1.06	1.07	1.08	1.08	1.08	1.09	1.15	1.16
ave	**1.08**	**1.09**	**1.10**	**1.10**	**1.10**	**1.11**	**1.13**	**1.11**

Mould - PGC

PGC	550°C	600°C	650°C	700°C	750°C	800°C	850°C	900°C
cool 1	0.92	0.95	0.98	1.00	1.03	1.05	1.07	1.09
cool 2	0.92	0.94	0.97	0.99	1.01	1.03	1.05	1.08
cool 3	0.92	0.94	0.97	0.99	1.00	1.02	1.04	1.06
ave	**0.92**	**0.94**	**0.97**	**0.99**	**1.01**	**1.03**	**1.06**	**1.08**

PGC	950°C	1000°C	1050°C	1100°C	1150°C	1200°C	1250°C	1300°C
cool 1	1.10	1.10	1.10	1.10	1.11	1.12	1.13	1.10
cool 2	1.09	1.10	1.11	1.11	1.11	1.12	1.11	1.07
cool 3	1.06	1.07	1.08	1.08	-	-	-	-
ave	**1.08**	**1.09**	**1.10**	**1.10**	**1.11**	**1.12**	**1.12**	**1.09**

Mould - PGD

Heat capacity

PGD	550°C	600°C	650°C	700°C	750°C	800°C	850°C	900°C
cool 1	1.12	1.17	1.19	1.24	1.26	1.29	1.34	1.37
cool 2	1.13	1.17	1.19	1.26	1.28	1.33	1.35	1.37
cool 3	1.13	1.17	1.21	1.24	1.29	1.30	1.38	1.39
ave	**1.12**	**1.17**	**1.20**	**1.25**	**1.28**	**1.31**	**1.36**	**1.38**

PGD	950°C	1000°C	1050°C	1100°C	1150°C	1200°C	1250°C	1300°C
cool 1	1.40	1.43	1.42	1.42	1.42	1.40	1.39	1.36
cool 2	1.40	1.40	1.40	1.38	1.35	1.32	1.34	1.30
cool 3	1.37	1.39	1.38	1.36	1.36	1.34	1.33	1.28
ave	**1.39**	**1.41**	**1.40**	**1.39**	**1.38**	**1.35**	**1.35**	**1.31**

Mould - PGF

Heat capacity

PGF	550°C	600°C	650°C	700°C	750°C	800°C	850°C	900°C
cool 1	1.01	1.05	1.07	1.10	1.12	1.14	1.18	1.19
cool 2	1.02	1.06	1.10	1.14	1.17	1.19	1.23	1.25
cool 3	0.98	1.03	1.05	1.08	1.08	1.09	1.12	1.12
ave	**1.00**	**1.05**	**1.07**	**1.11**	**1.13**	**1.14**	**1.18**	**1.19**

PGF	950°C	1000°C	1050°C	1100°C	1150°C	1200°C	1250°C	1300°C
cool 1	1.21	1.23	1.23	1.29	1.28	1.23	1.21	1.12
cool 2	1.25	1.25	1.23	1.24	1.22	1.18	1.16	1.11
cool 3	1.13	1.11	1.11	1.14	1.19	1.17	1.36	1.09
ave	**1.19**	**1.20**	**1.19**	**1.22**	**1.23**	**1.19**	**1.24**	**1.11**

Mould - PGL

Heat capacity

PGL	550°C	600°C	650°C	700°C	750°C	800°C	850°C	900°C
cool 1	0.93	0.97	1.00	1.03	1.09	1.12	1.14	1.17
cool 2	0.87	0.90	0.96	0.97	0.97	0.99	0.97	0.98
cool 3	0.84	0.88	0.89	0.92	0.97	0.93	1.00	1.01
ave	**0.88**	**0.92**	**0.95**	**0.97**	**0.99**	**1.01**	**1.04**	**1.05**

PGL	950°C	1000°C	1050°C	1100°C	1150°C	1200°C	1250°C	1300°C
cool 1	1.18	1.15	1.18	1.17	1.20	1.14	1.12	1.06
cool 2	0.93	0.93	1.03	1.02	1.03	0.98	1.03	0.96
cool 3	0.98	0.97	1.01	1.10	1.16	1.08	1.03	0.94
ave	**1.03**	**1.01**	**1.08**	**1.10**	**1.13**	**1.07**	**1.06**	**0.99**

Variations in Cp influenced by sintering of material.

Mould - PGM

Heat capacity

PGM	550°C	600°C	650°C	700°C	750°C	800°C	850°C	900°C
cool 1	1.00	1.02	1.05	1.07	1.09	1.09	1.12	1.12
cool 2	0.99	1.03	1.05	1.06	1.08	1.09	1.11	1.12
ave	**1.00**	**1.03**	**1.05**	**1.07**	**1.08**	**1.09**	**1.12**	**1.12**

PGM	950°C	1000°C	1050°C	1100°C	1150°C	1200°C	1250°C	1300°C
cool 1	1.12	1.12	1.10	1.09	1.09	1.06	1.07	1.03
cool 2	1.11	1.11	1.10	1.09	1.09	1.05	1.04	1.02
ave	**1.12**	**1.12**	**1.10**	**1.09**	**1.09**	**1.06**	**1.06**	**1.03**

Mould - PGN

Heat capacity

PGN	550°C	600°C	650°C	700°C	750°C	800°C	850°C	900°C
cool 1	1.06	1.12	1.17	1.23	1.27	1.30	1.33	1.32
cool 2	1.06	1.11	1.17	1.24	1.13	1.13	1.35	1.37
cool 3	1.06	1.12	1.17	1.21	1.23	1.24	1.26	1.28
ave	**1.06**	**1.12**	**1.17**	**1.23**	**1.21**	**1.22**	**1.31**	**1.32**

PGN	950°C	1000°C	1050°C	1100°C	1150°C	1200°C	1250°C	1300°C
cool 1	1.31	1.29	1.26	1.24	1.30	1.28	1.24	1.11
cool 2	1.33	1.32	1.26	1.22	1.13	1.10	1.18	1.13
cool 3	1.23	1.25	1.26	1.25	1.23	1.20	1.19	1.14
ave	**1.29**	**1.29**	**1.26**	**1.23**	**1.22**	**1.19**	**1.20**	**1.13**

Theoretical specific heats, after Kubashewski

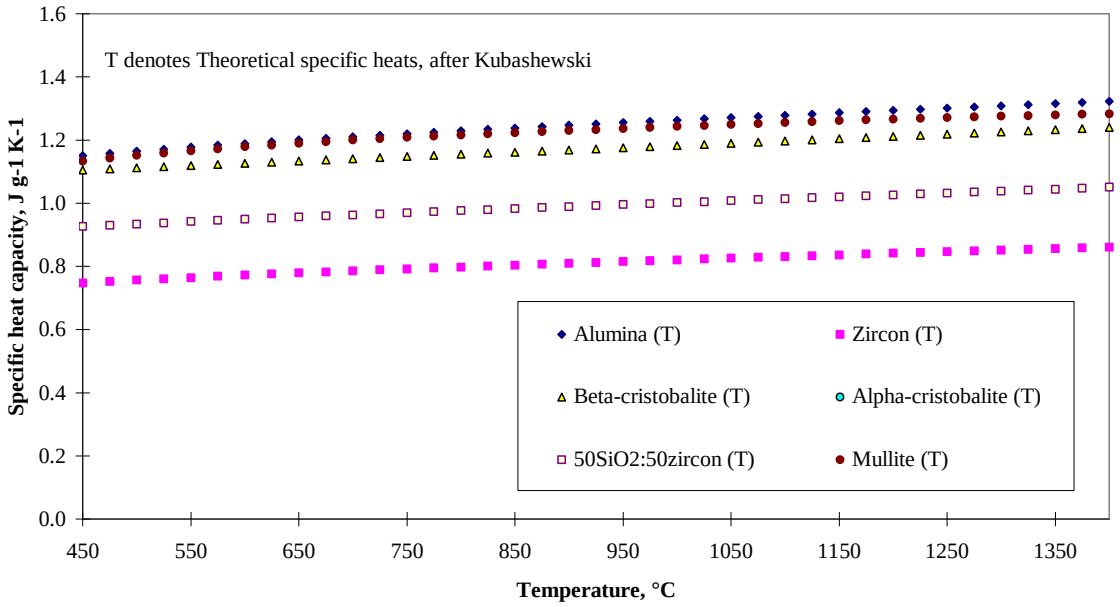

Mould Materials
Run on cooling at 10°C/min from 1350°C to 500°C

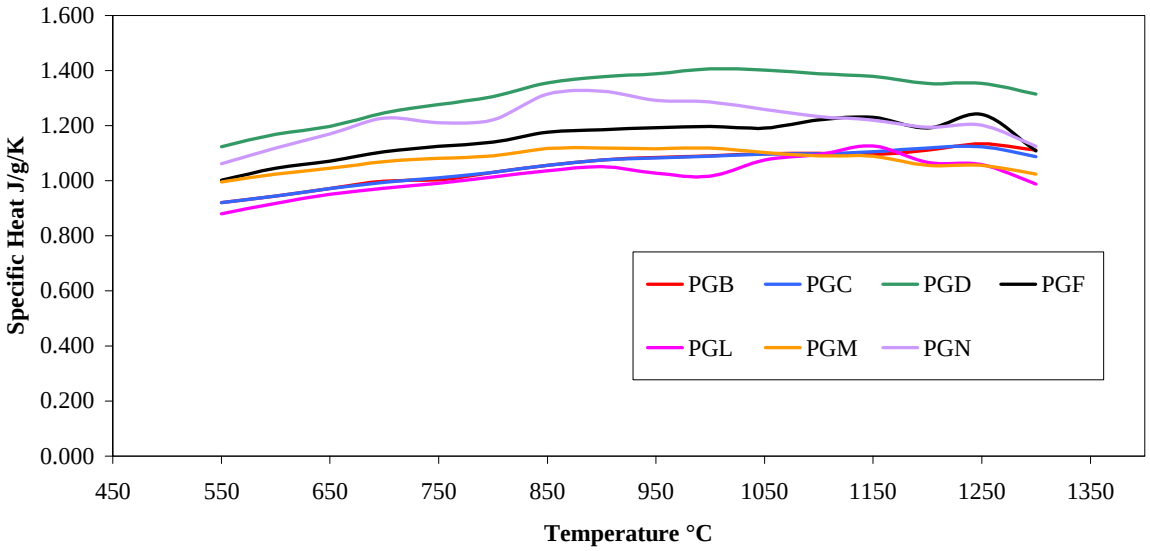

A.3.6 Thermal Diffusivity

Average values for a from at least three measurements ($10^{-4}m^2\ s^{-1}$)

Mould PGB

T (°C)	PGB1 Heating	T (°C)	PGB1 Cooling
12	0.0082	1492	0.0067
24	0.0080	1402	0.0069
210	0.0062	1202	0.0072
498	0.0054	998	0.0077
883	0.0051	703	0.0086
894	0.0052	13	0.0172
1084	0.0051	-	-
1308	0.0054	-	-
1491	0.0064	-	-

Mould PGC

T (°C)	PGC1 Heating	T (°C)	PGC1 Cooling
14	0.0060	1001	0.0053
96	0.0057	610	0.0048
500	0.0047	412	0.0047
701	0.0048	319	0.0049
799	0.0049	216	0.0049
907	0.0051	12	0.0057
1093	0.0054	-	-

Mould PGD

T (°C)	PGD1 Heating
12	0.0057
101	0.0051
316	0.0043
505	0.0042
704	0.0043
907	0.0043
1093	0.0042

Mould PGL

T (°C)	PGL1 Heating	T (°C)	PGL1 Cooling
19	0.0074	994	0.0047
91	0.0067	-	-
314	0.0054	-	-
509	0.0049	-	-
700	0.0047	-	-
903	0.0046	-	-
1094	0.0048	-	-

Mould PGM

T (°C)	PGM1 Heating	T (°C)	PGM1 Cooling
12	0.0243	996	0.0092
85	0.0194	504	0.0111
187	0.0190	-	-
319	0.0129	-	-
498	0.0107	-	-
504	0.0108	-	-
702	0.0095	-	-
794	0.0090	-	-
994	0.0086	-	-
1086	0.0088	-	-

Mould PGN

T (°C)	PGN1 Heating	T (°C)	PGN1 Cooling
16	0.0053	1093	0.0047
94	0.0053	1001	0.0046
103	0.0045	799	0.0043
215	0.0042	610	0.0041
315	0.0042	412	0.0041
503	0.0041	218	0.0043
704	0.0042	-	-
910	0.0044	-	-

Mould PHG

T (°C)	PHG2 Heating	T (°C)	PHG2 Cooling
12	0.0092	1090	0.0053
97	0.0082	996	0.0054
316	0.0063	797	0.0056
509	0.0058	704	0.0057
699	0.0055	607	0.0058
903	0.0053	415	0.0062
1087	0.0053	317	0.0063
-	-	206	0.0071
-	-	94	0.0079

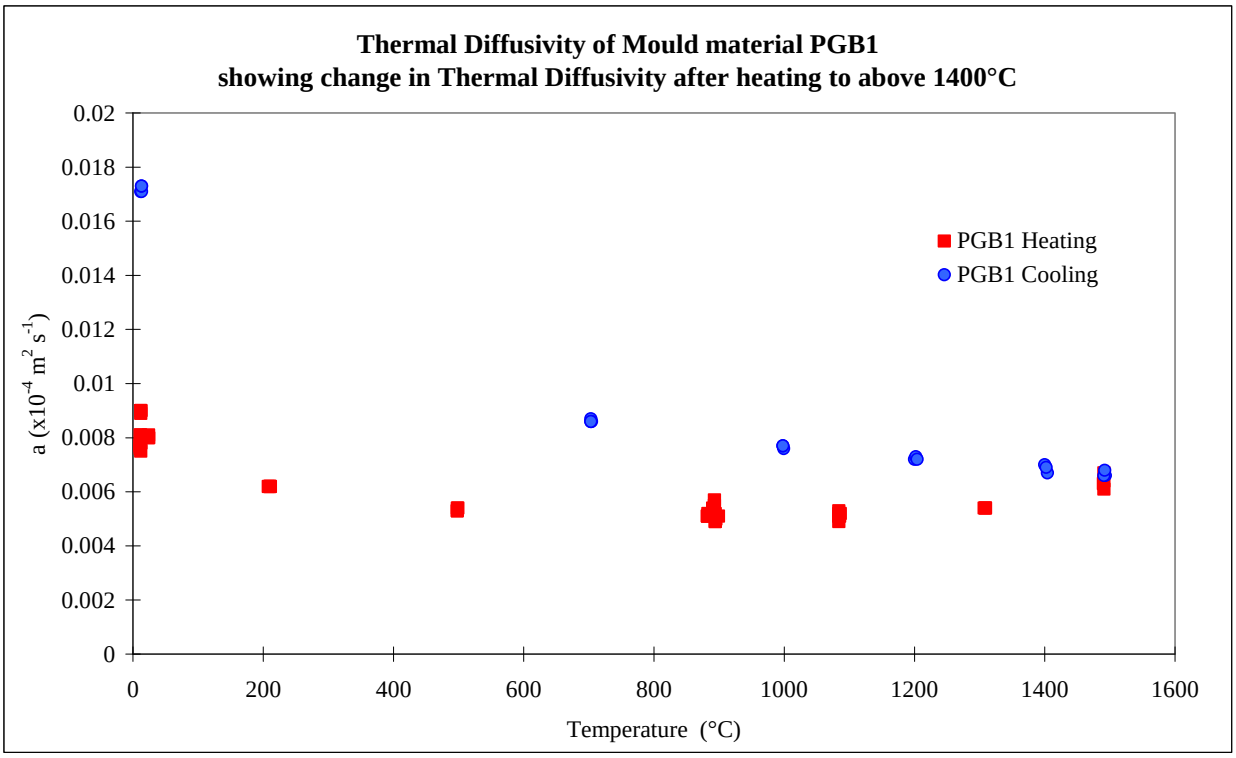
Thermal Diffusivity of Mould material PGB1
showing change in Thermal Diffusivity after heating to above 1400°C
a (x10-4 m2 s-1)
0.02
0.018
0.016
0.014
0.012
0.01
0.008
0.006
0.004
0.002
0
0
200
400
600
800
1000
1200
1400
1600
Temperature (°C)
PGB1 Heating
PGB1 Cooling

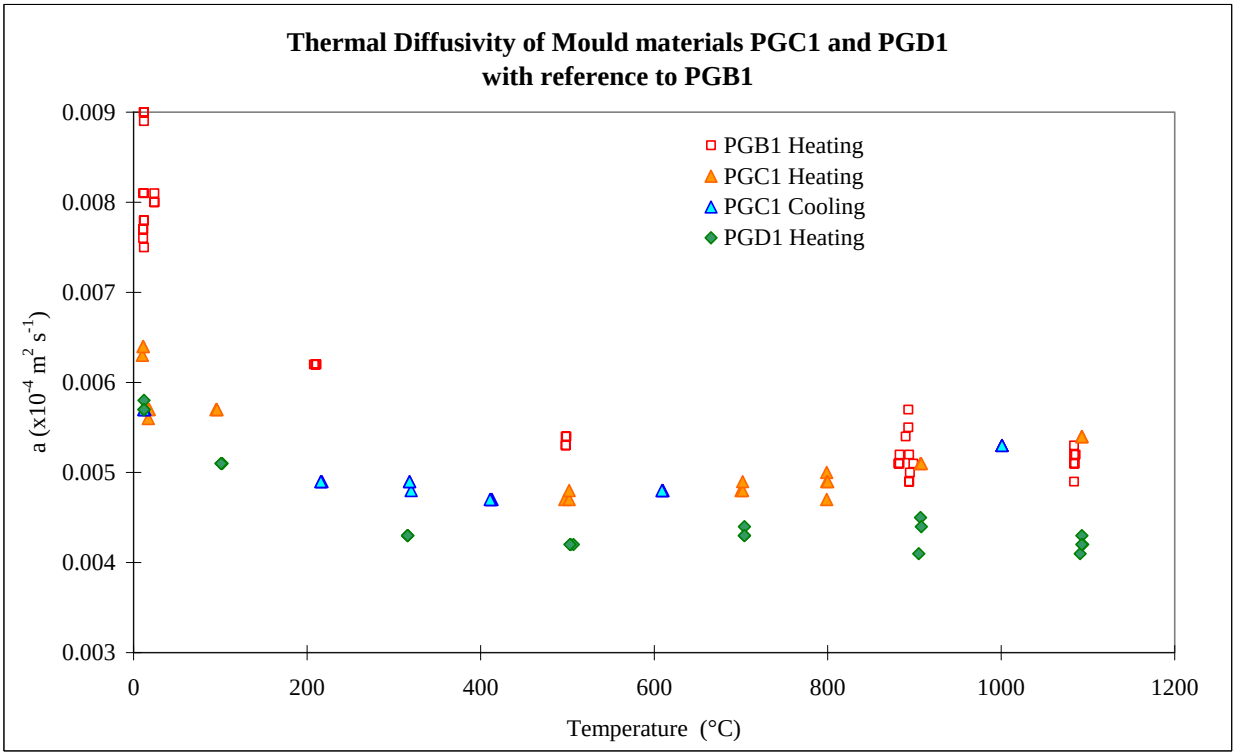
Thermal Diffusivity of Mould materials PGC1 and PGD1
with reference to PGB1
a (x10-4 m2 s-1)
0.009
0.008
0.007
0.006
0.005
0.004
0.003
0
200
400
600
800
1000
1200
Temperature (°C)
PGB1 Heating
PGC1 Heating
PGC1 Cooling
PGD1 Heating

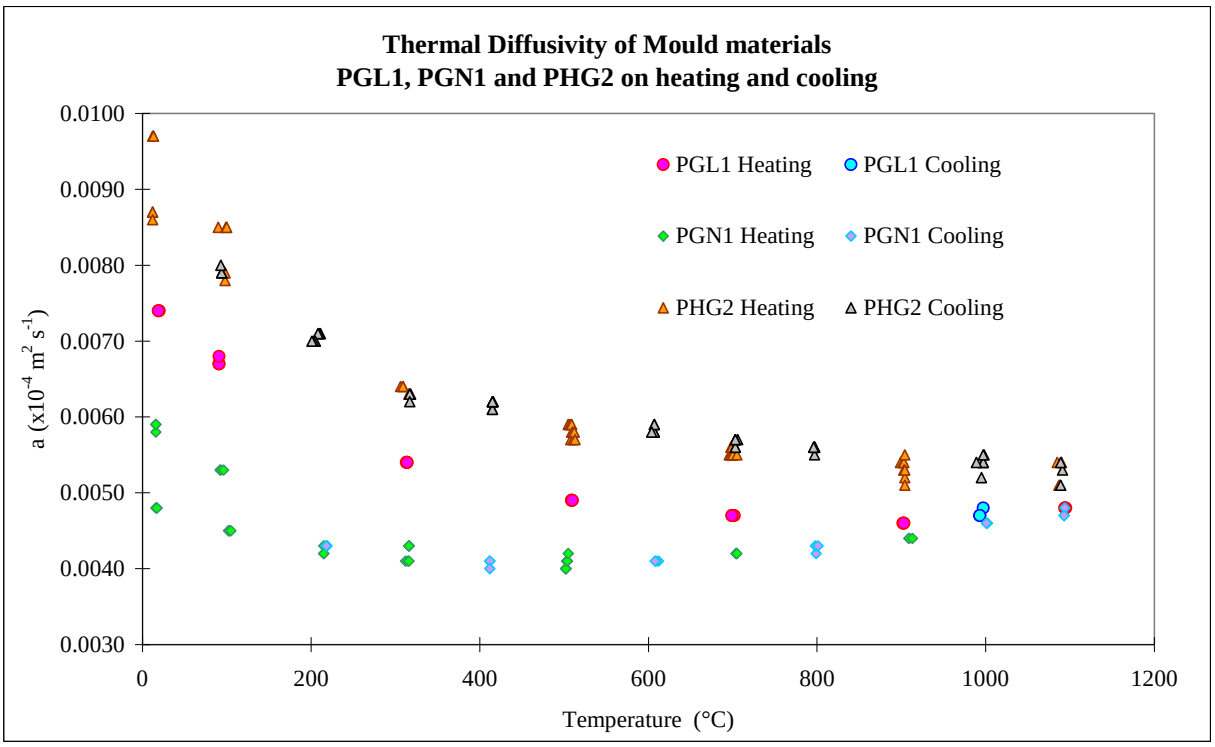
Thermal Diffusivity of Mould materials
PGL1, PGN1 and PHG2 on heating and cooling
PGL1 Heating
PGL1 Cooling
PGN1 Heating
PGN1 Cooling
PHG2 Heating
PHG2 Cooling
a (x10-4 m2 s-1)
0.0100
0.0090
0.0080
0.0070
0.0060
0.0050
0.0040
0.0030
0
200
400
600
800
1000
1200
Temperature (°C)

APPENDIX B – ProCAST ENTHALPY CALCULATIONS

The results for alloy enthalpy from ProCAST package; calculations supplied by Li-Hung Chen of Doncasters, compared with experimental results.

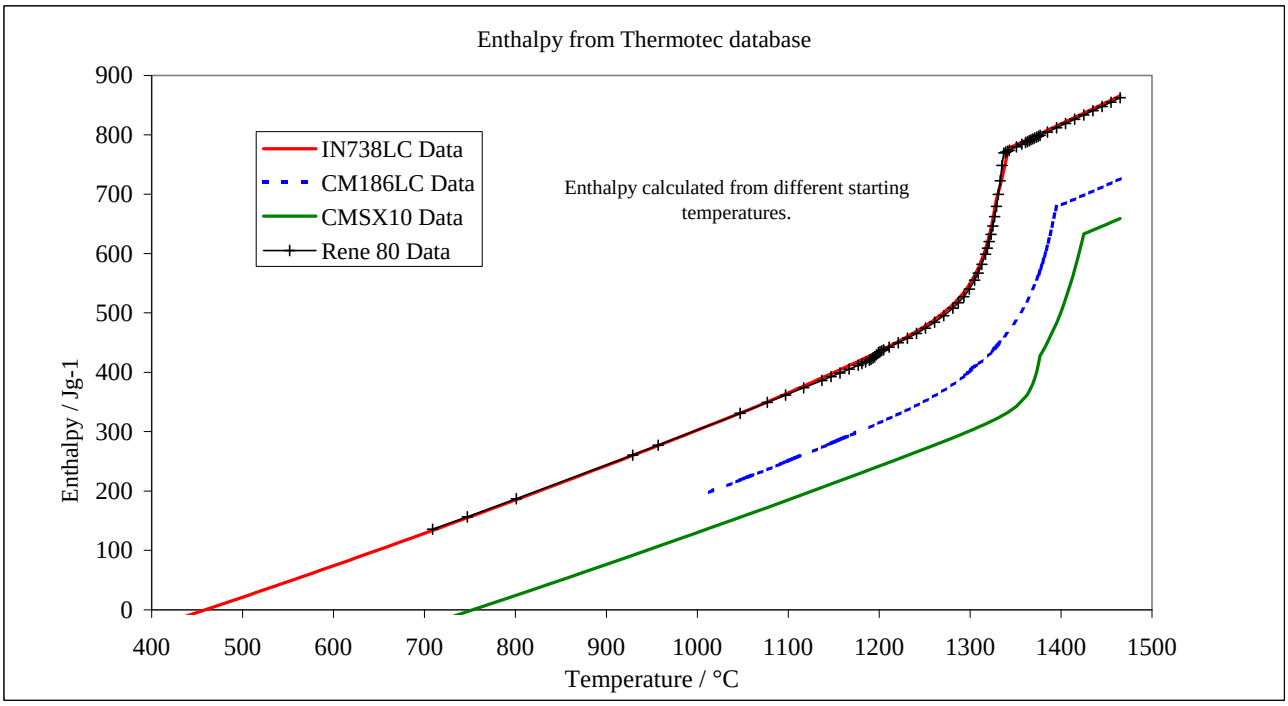

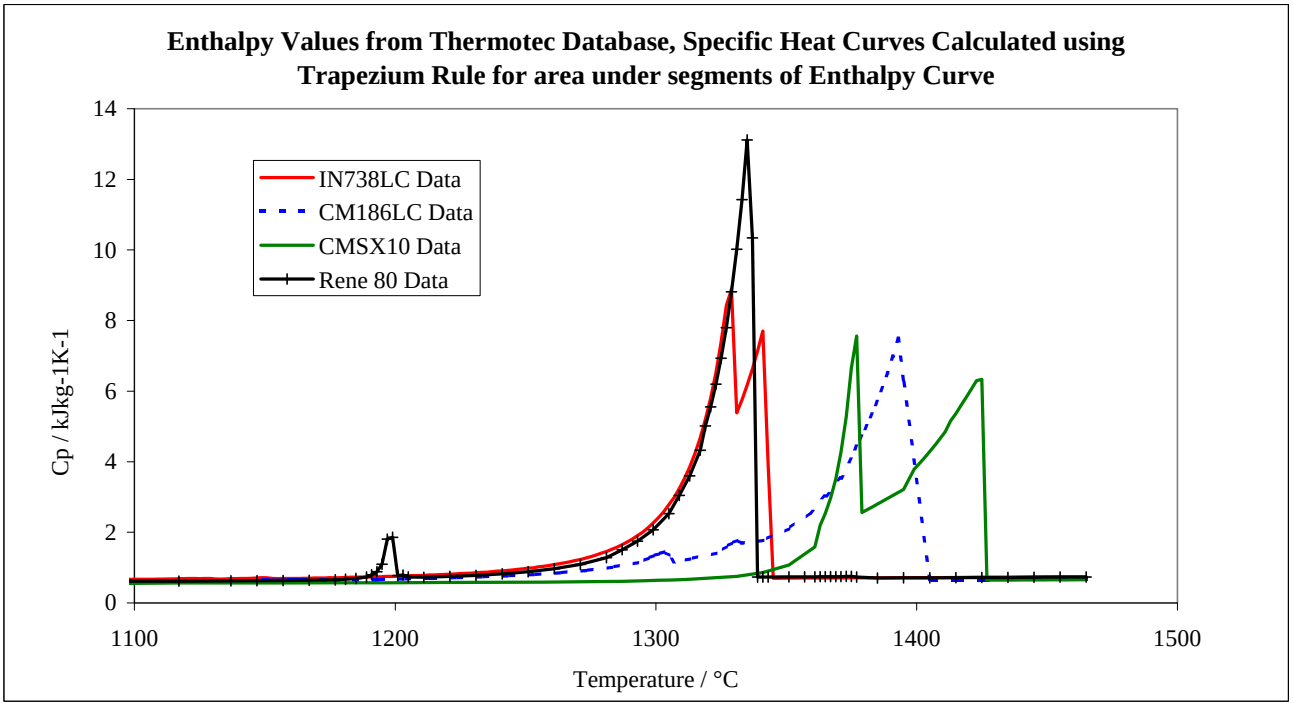

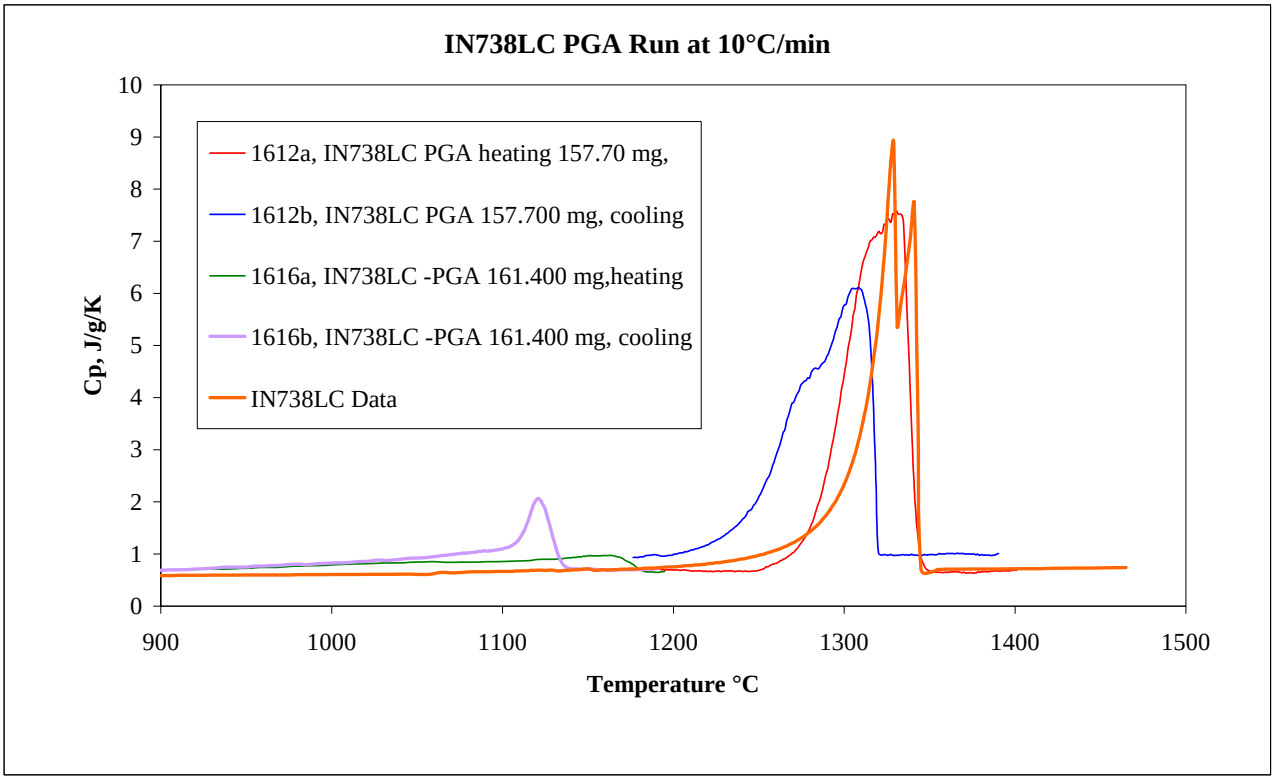
IN738LC PGA Run at 10°C/min
1612a, IN738LC PGA heating 157.70 mg,
1612b, IN738LC PGA 157.700 mg, cooling
1616a, IN738LC -PGA 161.400 mg,heating
1616b, IN738LC -PGA 161.400 mg, cooling
IN738LC Data
Cp, J/g/K
Temperature °C
0
1
2
3
4
5
6
7
8
9
10
900
1000
1100
1200
1300
1400
1500

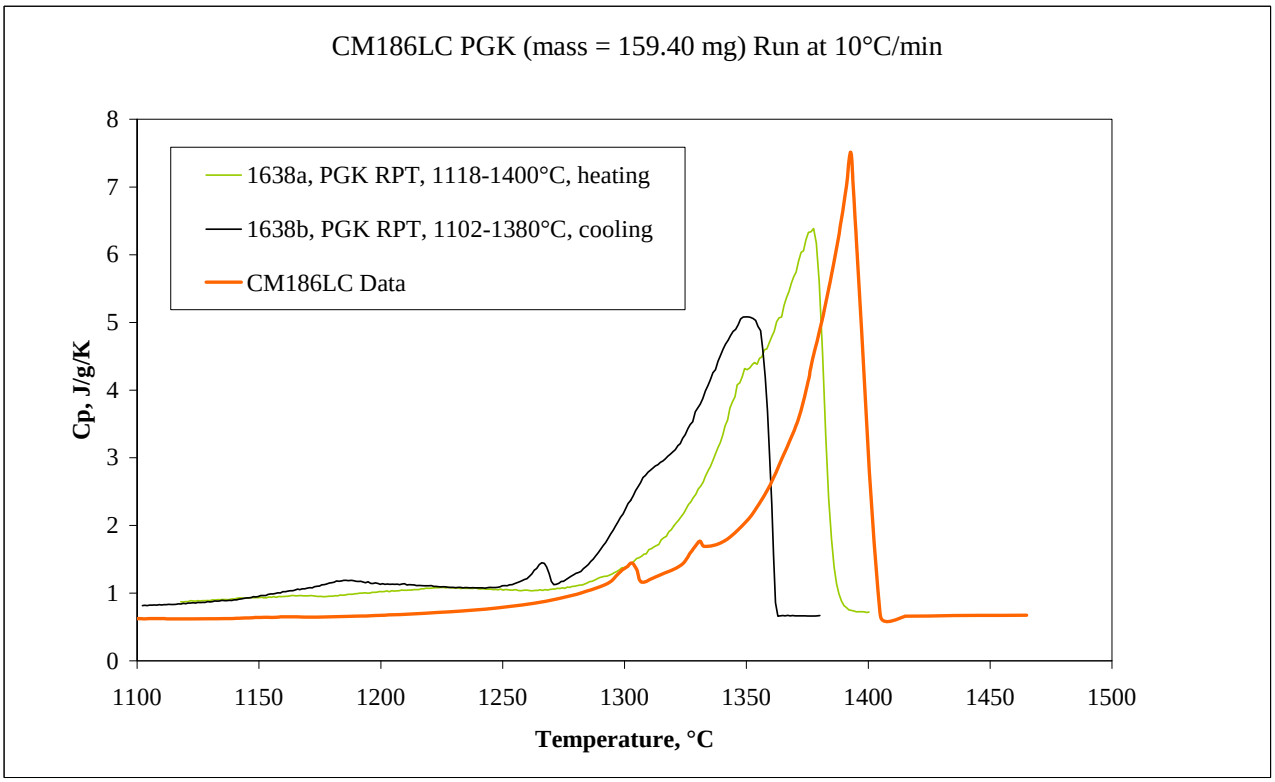
CM186LC PGK (mass = 159.40 mg) Run at 10°C/min
1638a, PGK RPT, 1118-1400°C, heating
1638b, PGK RPT, 1102-1380°C, cooling
CM186LC Data
Cp, J/g/K
Temperature, °C
0
1
2
3
4
5
6
7
8
1100
1150
1200
1250
1300
1350
1400
1450
1500

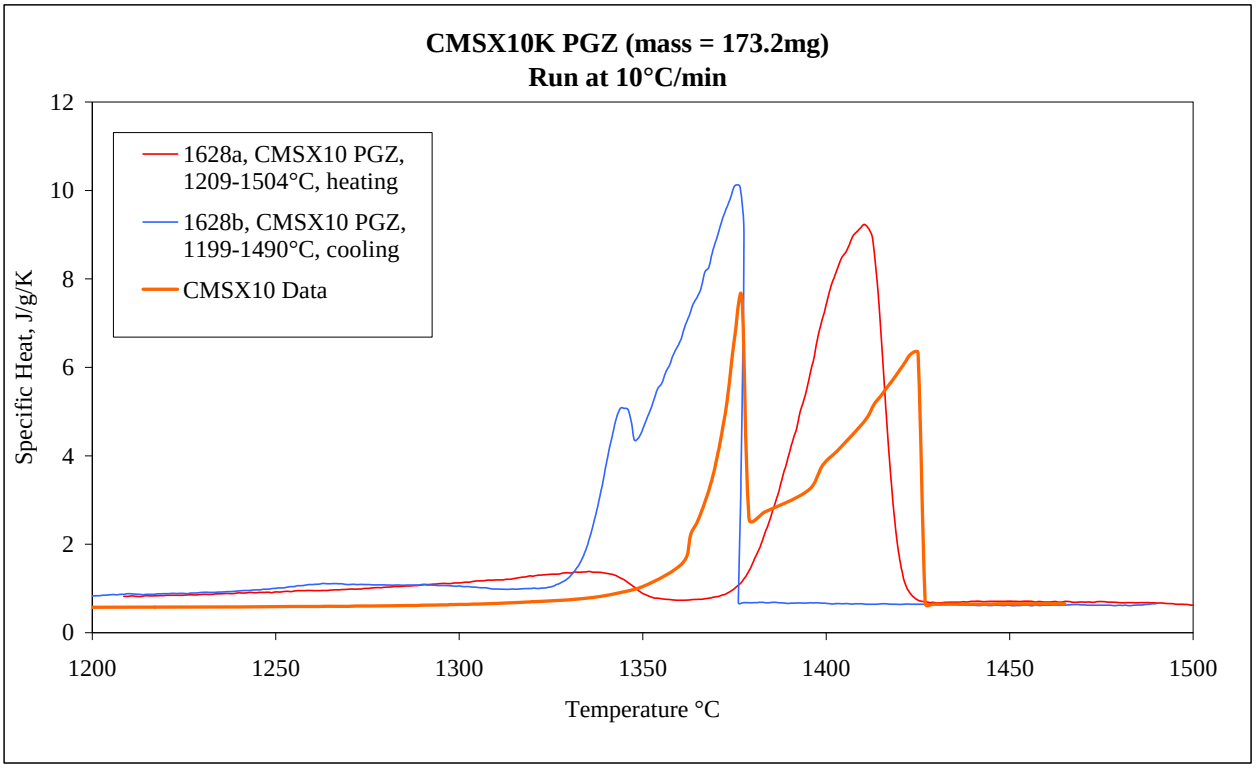
CMSX10K PGZ (mass = 173.2mg)
Run at 10°C/min
1628a, CMSX10 PGZ, 1209-1504°C, heating
1628b, CMSX10 PGZ, 1199-1490°C, cooling
CMSX10 Data
Specific Heat, J/g/K
Temperature °C
0
2
4
6
8
10
12
1200
1250
1300
1350
1400
1450
1500

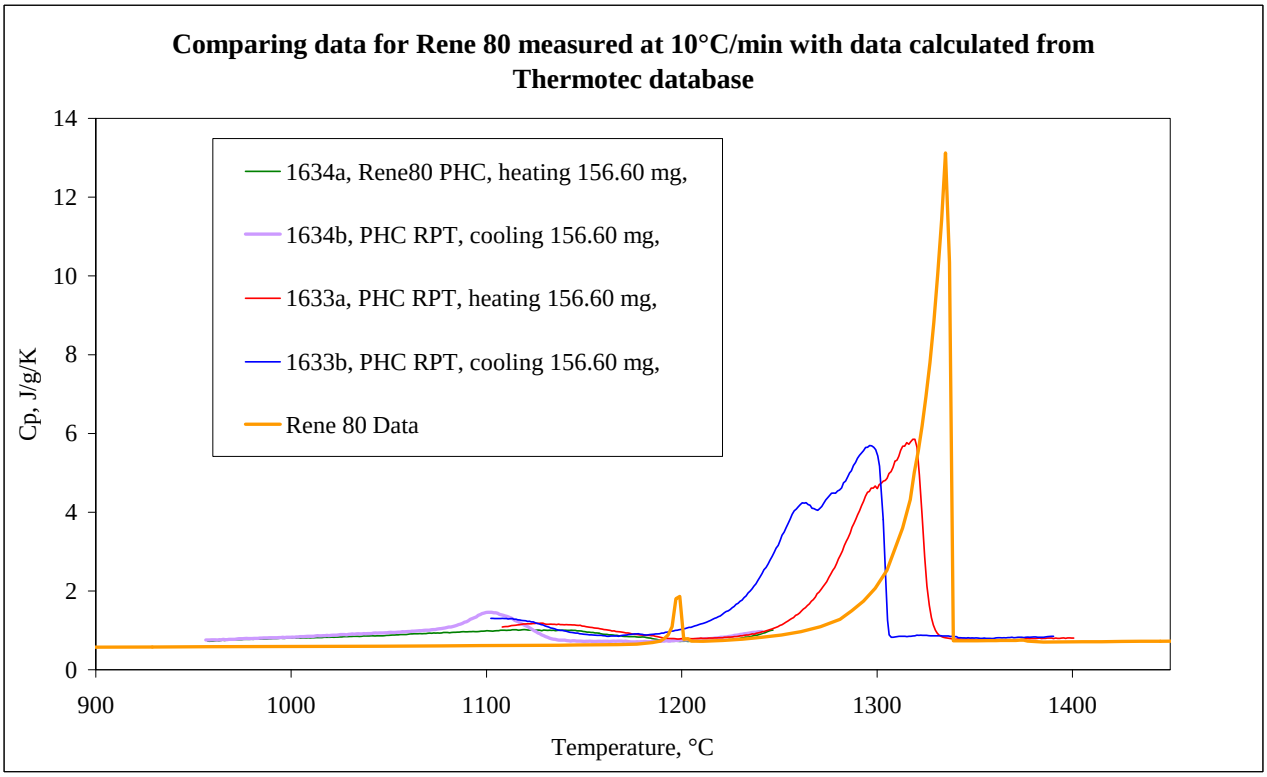
Comparing data for Rene 80 measured at 10°C/min with data calculated from Thermotec database
1634a, Rene80 PHC, heating 156.60 mg,
1634b, PHC RPT, cooling 156.60 mg,
1633a, PHC RPT, heating 156.60 mg,
1633b, PHC RPT, cooling 156.60 mg,
Rene 80 Data
Cp, J/g/K
Temperature, °C
0
2
4
6
8
10
12
14
900
1000
1100
1200
1300
1400

Second Thermotec data is correction to compare with measured data, taking into account that the measured data does not use enthalpy from T = 25°C.

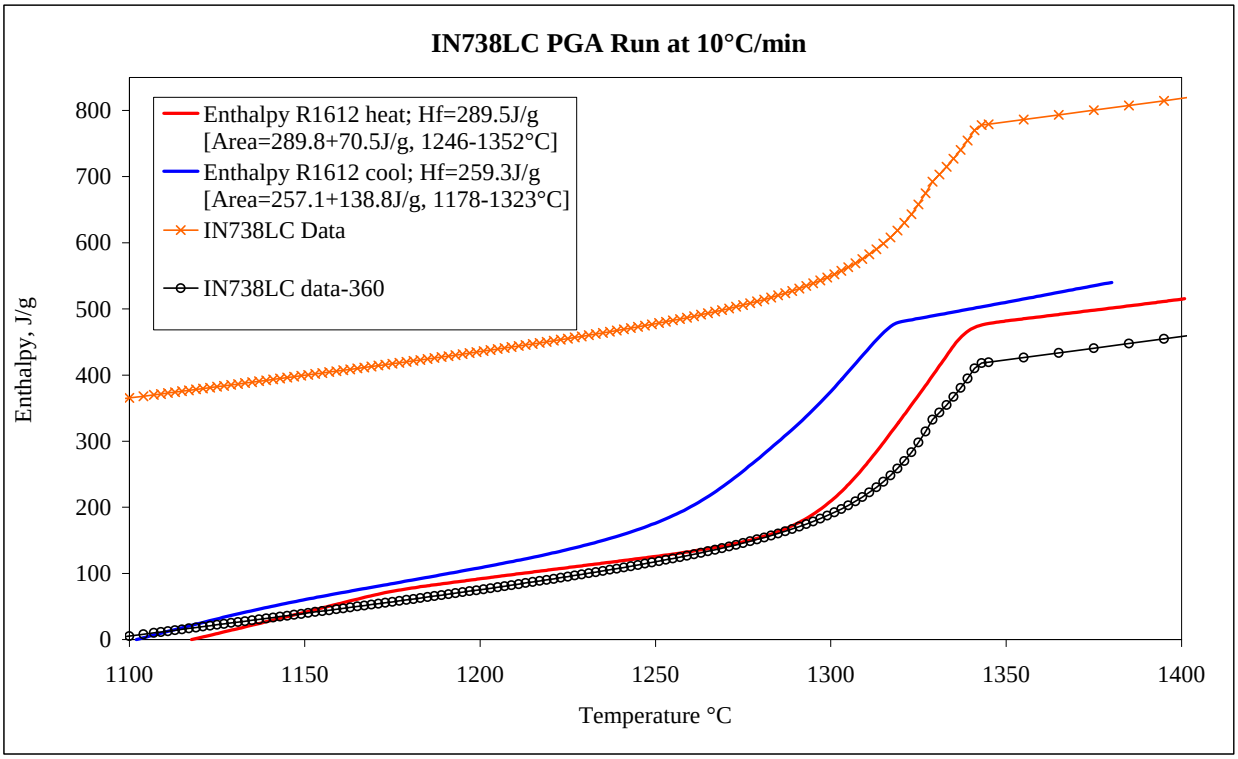

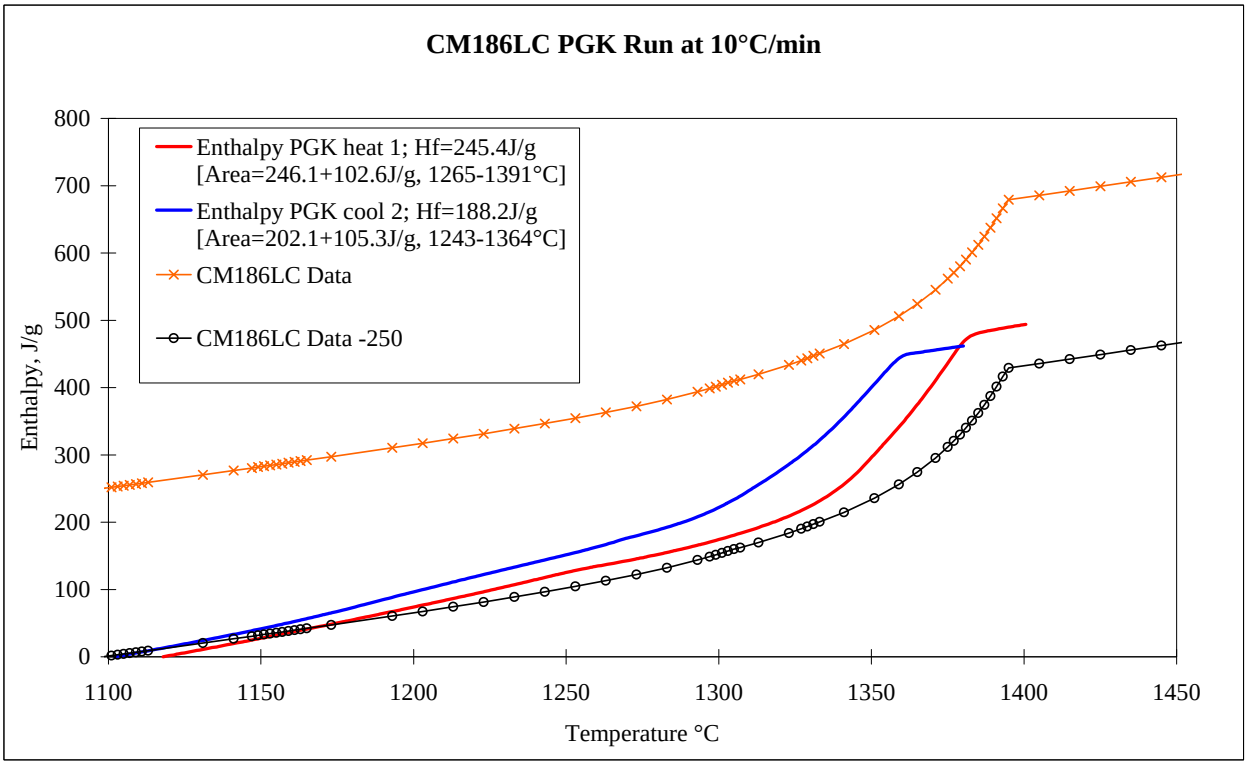

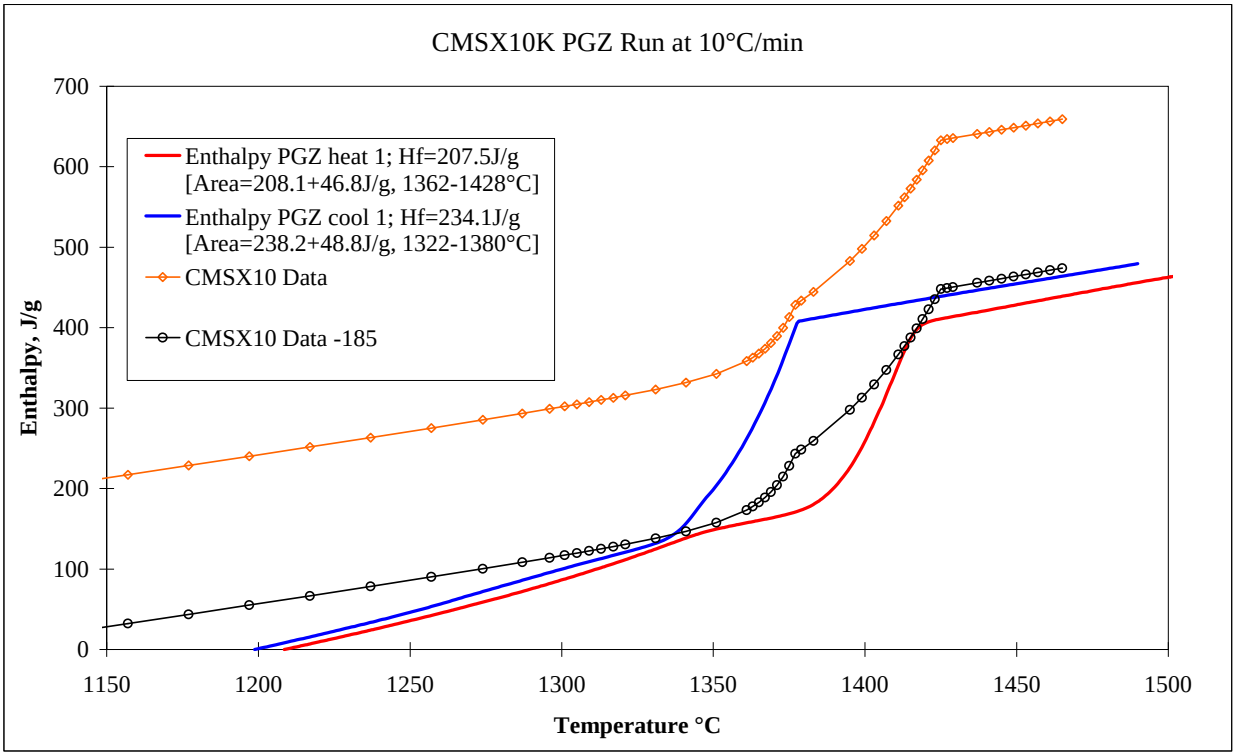
CMSX10K PGZ Run at 10°C/min
Enthalpy PGZ heat 1; Hf=207.5J/g
[Area=208.1+46.8J/g, 1362-1428°C]
Enthalpy PGZ cool 1; Hf=234.1J/g
[Area=238.2+48.8J/g, 1322-1380°C]
CMSX10 Data
CMSX10 Data -185
Enthalpy, J/g
Temperature °C
0
100
200
300
400
500
600
700
1150
1200
1250
1300
1350
1400
1450
1500

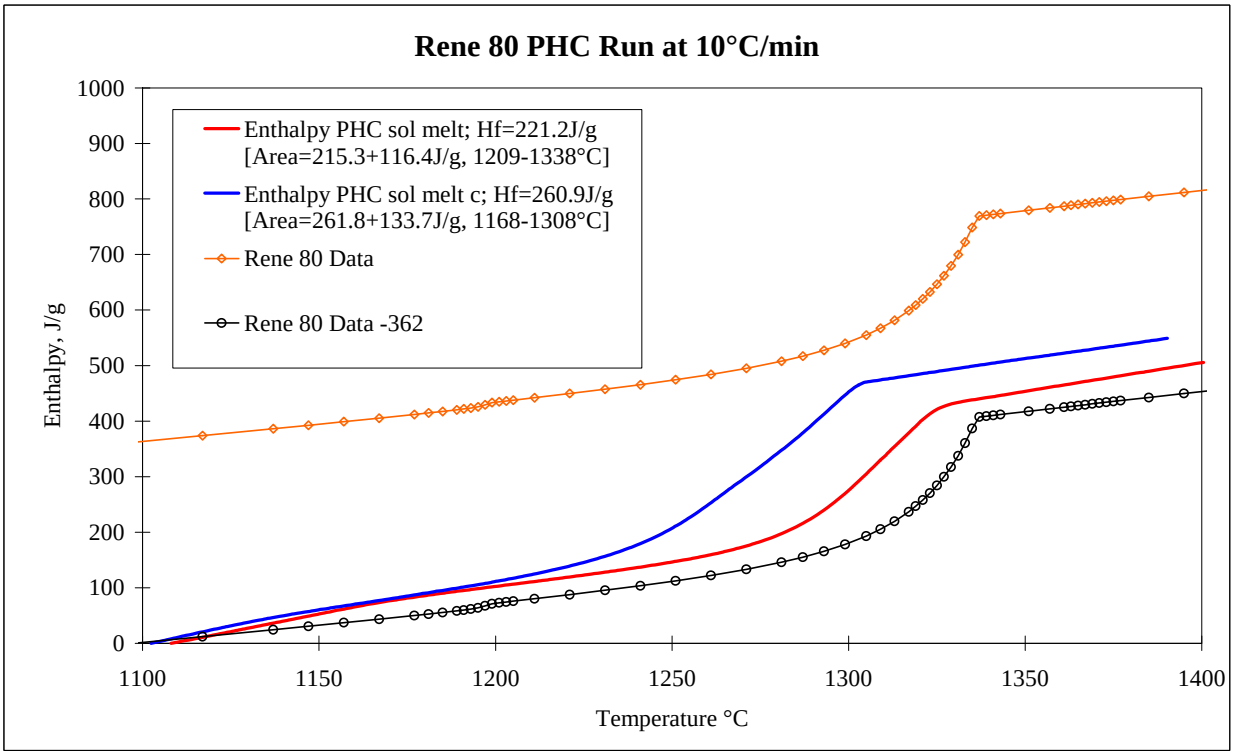
Rene 80 PHC Run at 10°C/min
Enthalpy PHC sol melt; Hf=221.2J/g
[Area=215.3+116.4J/g, 1209-1338°C]
Enthalpy PHC sol melt c; Hf=260.9J/g
[Area=261.8+133.7J/g, 1168-1308°C]
Rene 80 Data
Rene 80 Data -362
Enthalpy, J/g
Temperature °C
0
100
200
300
400
500
600
700
800
900
1000
1100
1150
1200
1250
1300
1350
1400

APPENDIX C - SENSITIVITY ANALYSIS, PRESENTATION BY DONCASTERS

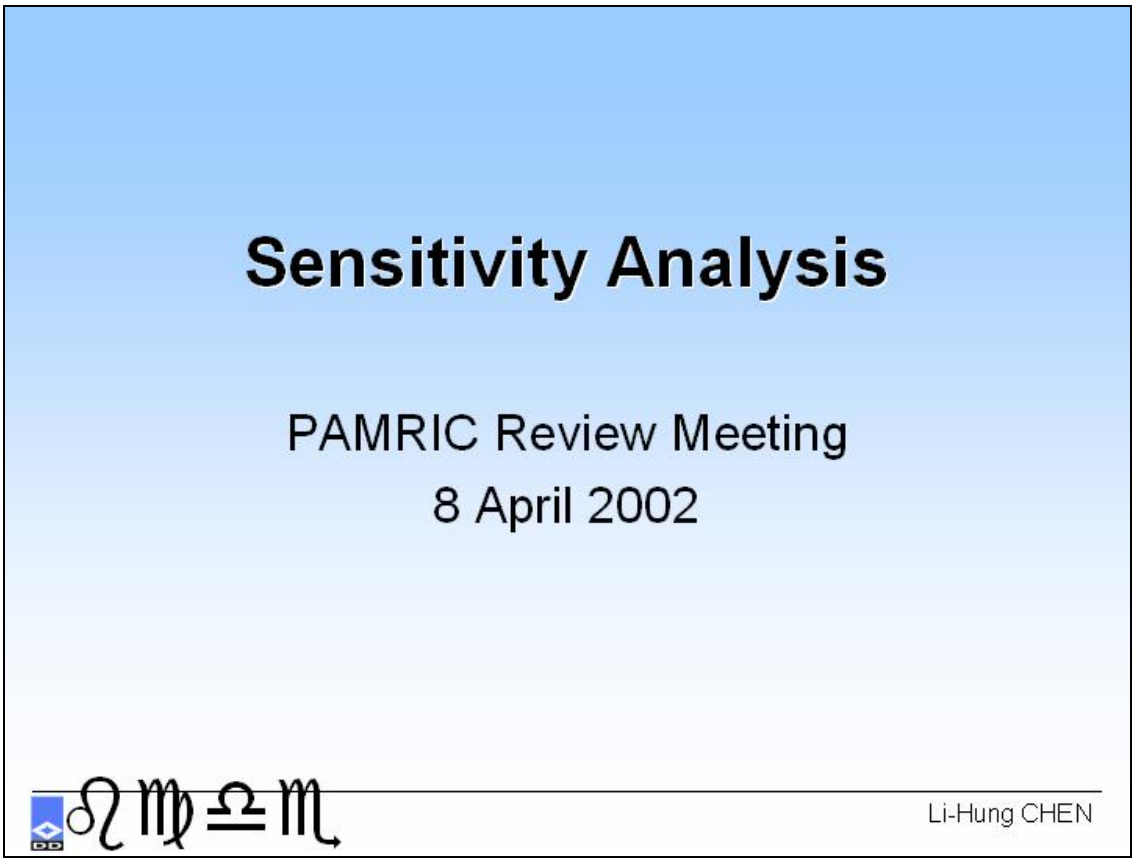

Parameters analysed

1. Effects of shell conductivity and specific heat
2. Effects of dimensional changes
3. Effects of interfacial conductivity

Dimensions of part used for analysis

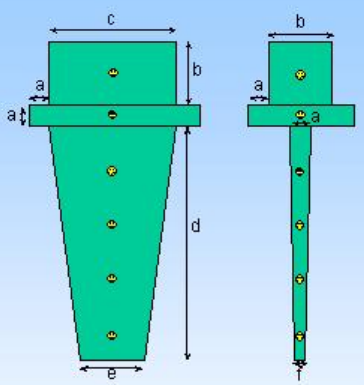

Dimensions in cm

	Small (1x)	Med (4x)	Large (14x)
a	0.50	2.00	7.00
b	1.50	6.00	21.00
c	3.00	12.00	42.00
d	5.50	22.00	77.00
e	2.00	8.00	28.00
f	0.15	0.60	2.10

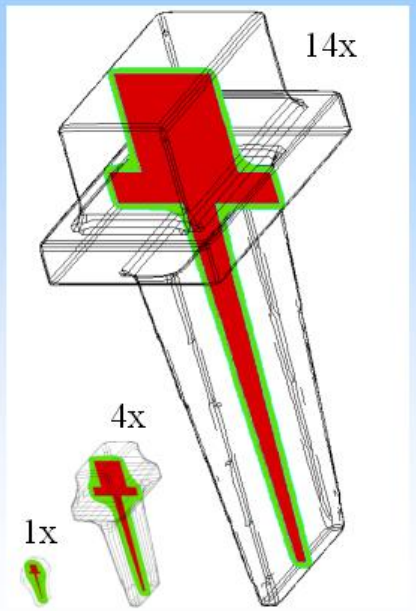

Analysis matrix

Shell conductivity and specific heat

k \ Cp	0.5 kJkg^{-1}K^{-1}	1.0 kJkg^{-1}K^{-1}	3.0 kJkg^{-1}K^{-1}
0.5 Wm^{-1}K^{-1}	--	X	--
1.0 Wm^{-1}K^{-1}	X	X	X
3.0 Wm^{-1}K^{-1}	--	X	--

- 5 simulations for each geometry

Interface conductivity

- h = 2000 Wm^{-1}K^{-1} - constant in all simulations

- Also run 1 simulation with h decreasing with T

TOTAL = 3 x (5+1) = 18 simulations

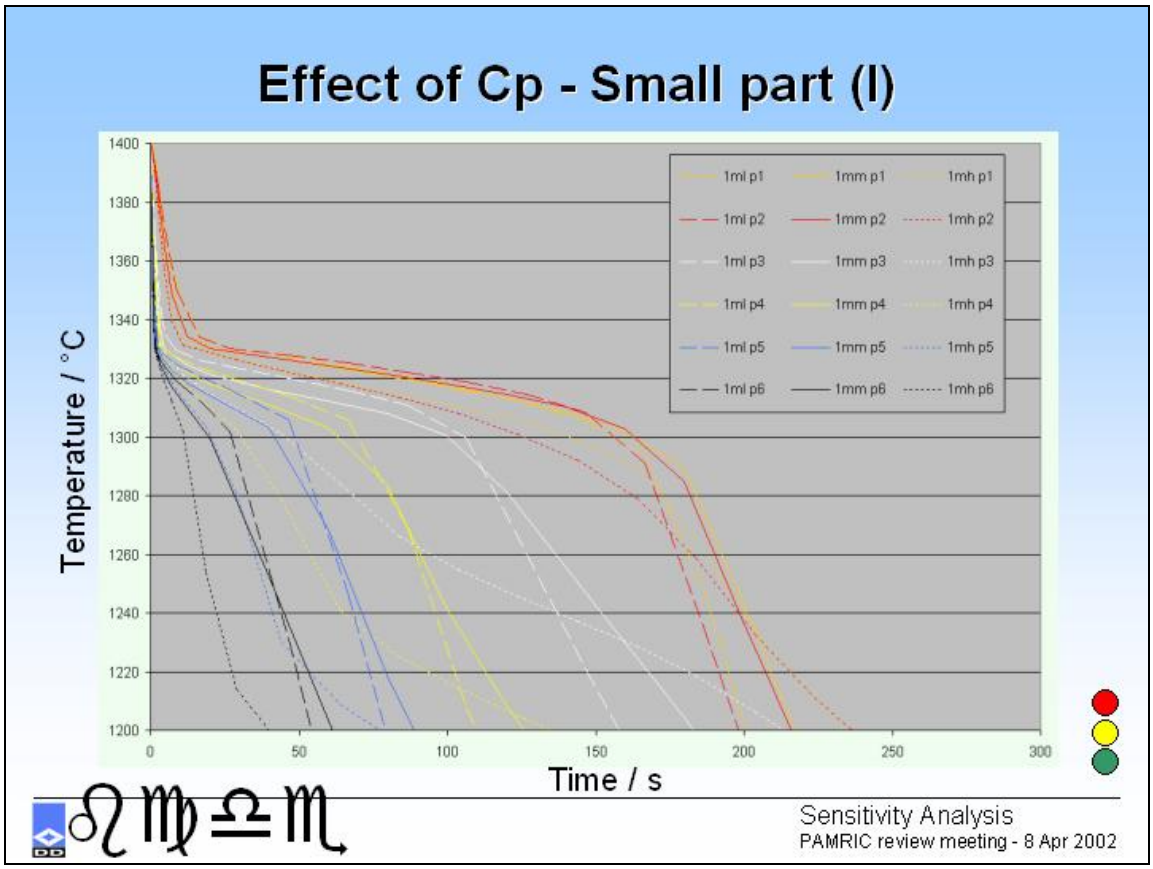
Effect of Cp - Small part (I)
Temperature / °C
Time / s
1ml p1
1mm p1
1mh p1
1ml p2
1mm p2
1mh p2
1ml p3
1mm p3
1mh p3
1ml p4
1mm p4
1mh p4
1ml p5
1mm p5
1mh p5
1ml p6
1mm p6
1mh p6
Sensitivity Analysis
PAMRIC review meeting - 8 Apr 2002

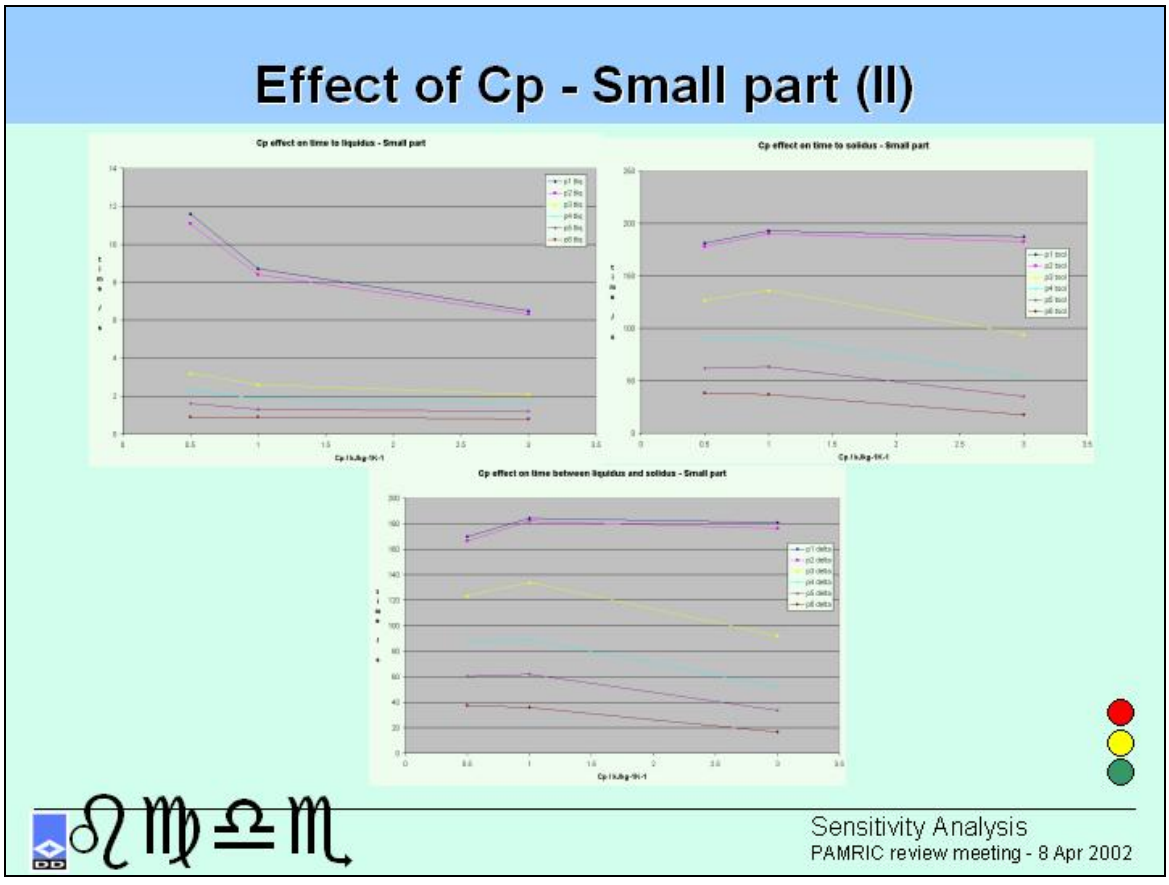
Effect of Cp - Small part (II)
Cp effect on time to liquidus - Small part
Cp effect on time to solidus - Small part
Cp effect on time between liquidus and solidus - Small part
Sensitivity Analysis
PAMRIC review meeting - 8 Apr 2002

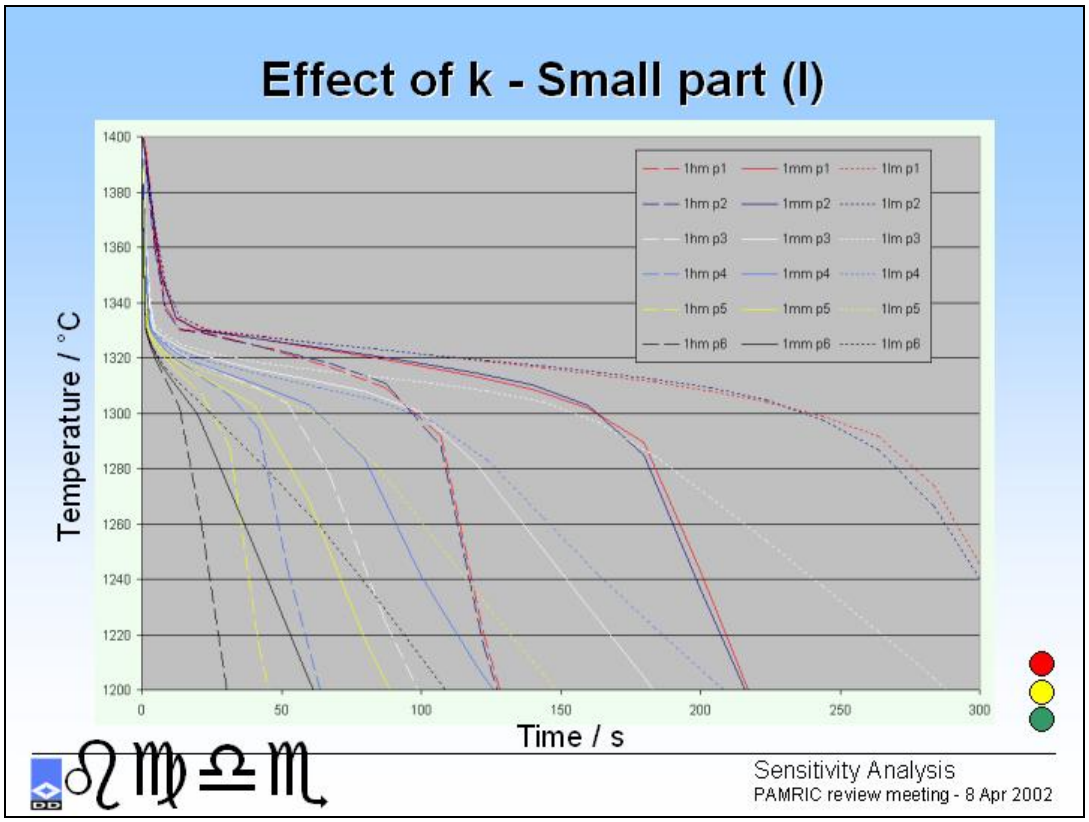
Effect of k - Small part (I)
Temperature / °C
Time / s
1hm p1
1mm p1
1lm p1
1hm p2
1mm p2
1lm p2
1hm p3
1mm p3
1lm p3
1hm p4
1mm p4
1lm p4
1hm p5
1mm p5
1lm p5
1hm p6
1mm p6
1lm p6
Sensitivity Analysis
PAMRIC review meeting - 8 Apr 2002

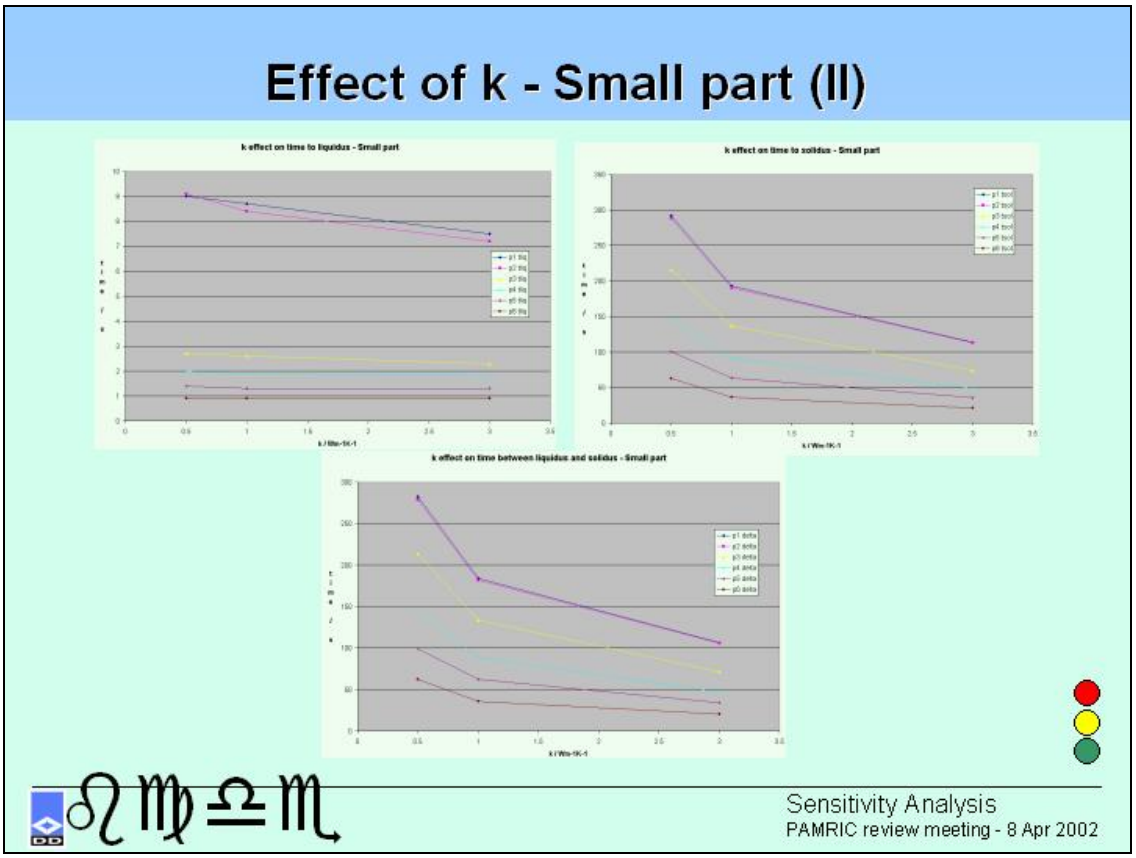
Effect of k - Small part (II)
k effect on time to liquidus - Small part
k effect on time to solidus - Small part
k effect on time between liquidus and solidus - Small part
Sensitivity Analysis
PAMRIC review meeting - 8 Apr 2002

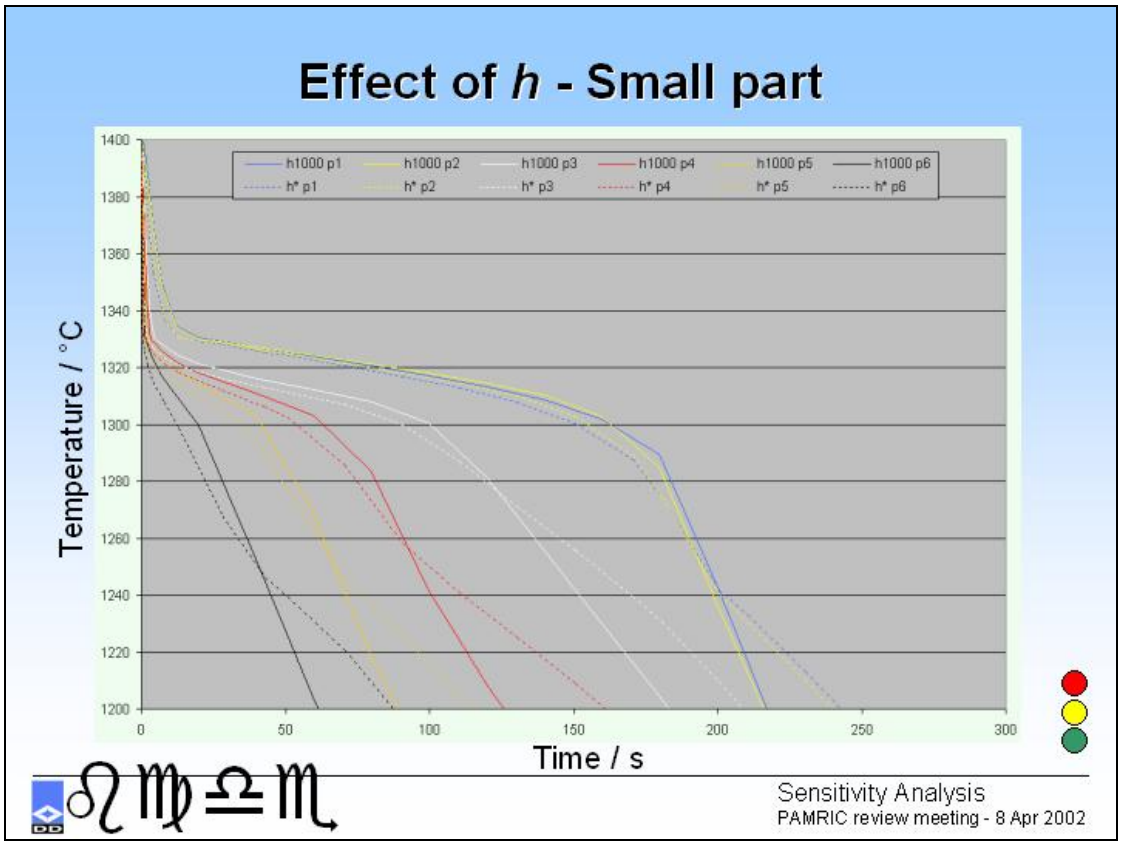
Effect of h - Small part
h1000 p1
h1000 p2
h1000 p3
h1000 p4
h1000 p5
h1000 p6
h* p1
h* p2
h* p3
h* p4
h* p5
h* p6
Temperature / °C
Time / s
Sensitivity Analysis
PAMRIC review meeting - 8 Apr 2002

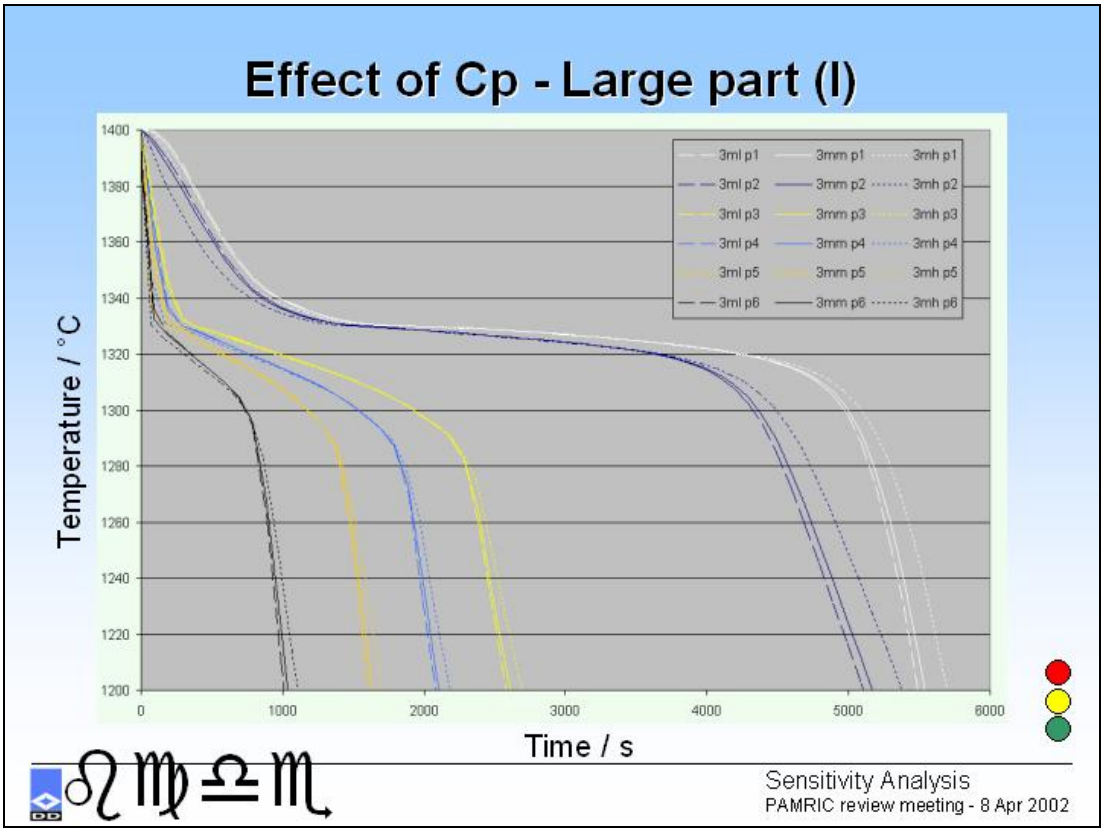
Effect of Cp - Large part (l)
3ml p1
3mm p1
3mh p1
3ml p2
3mm p2
3mh p2
3ml p3
3mm p3
3mh p3
3ml p4
3mm p4
3mh p4
3ml p5
3mm p5
3mh p5
3ml p6
3mm p6
3mh p6
Temperature / °C
Time / s
Sensitivity Analysis
PAMRIC review meeting - 8 Apr 2002

Effect of Cp - Large part (II)

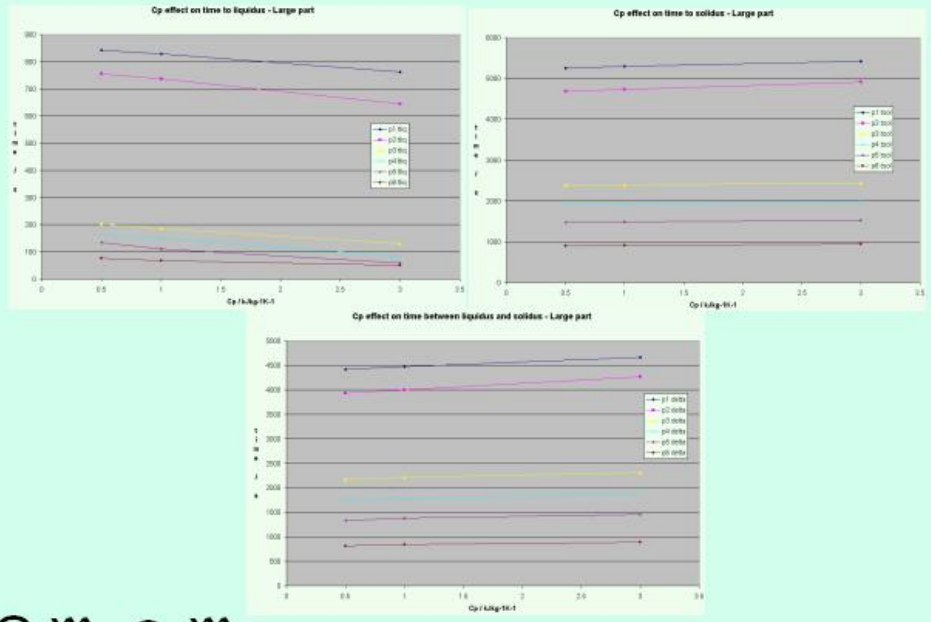

Sensitivity Analysis
PAMRIC review meeting - 8 Apr 2002

Effect of k - Large part (I)

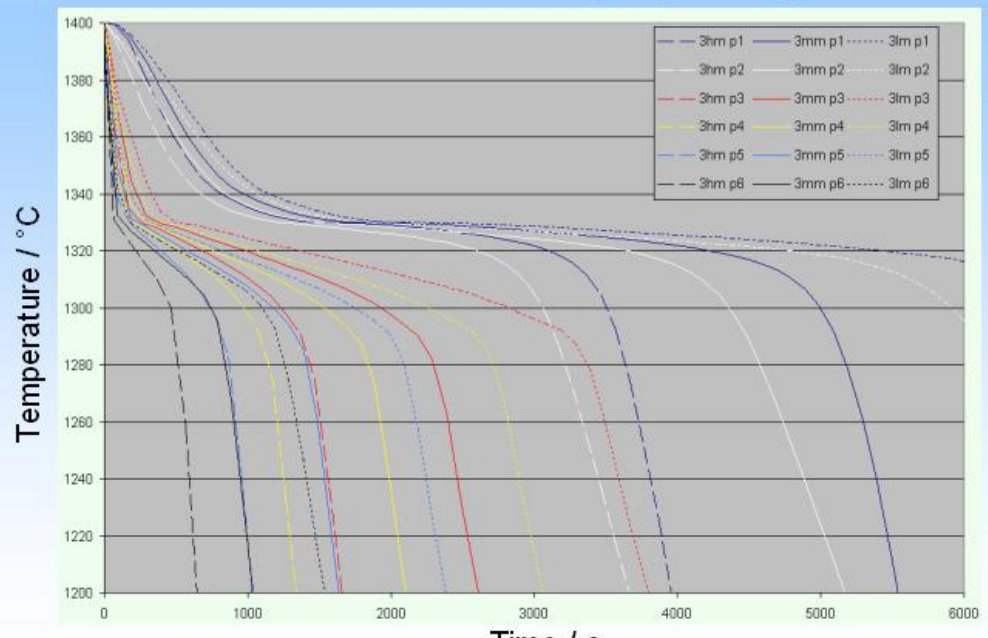

Sensitivity Analysis
PAMRIC review meeting - 8 Apr 2002

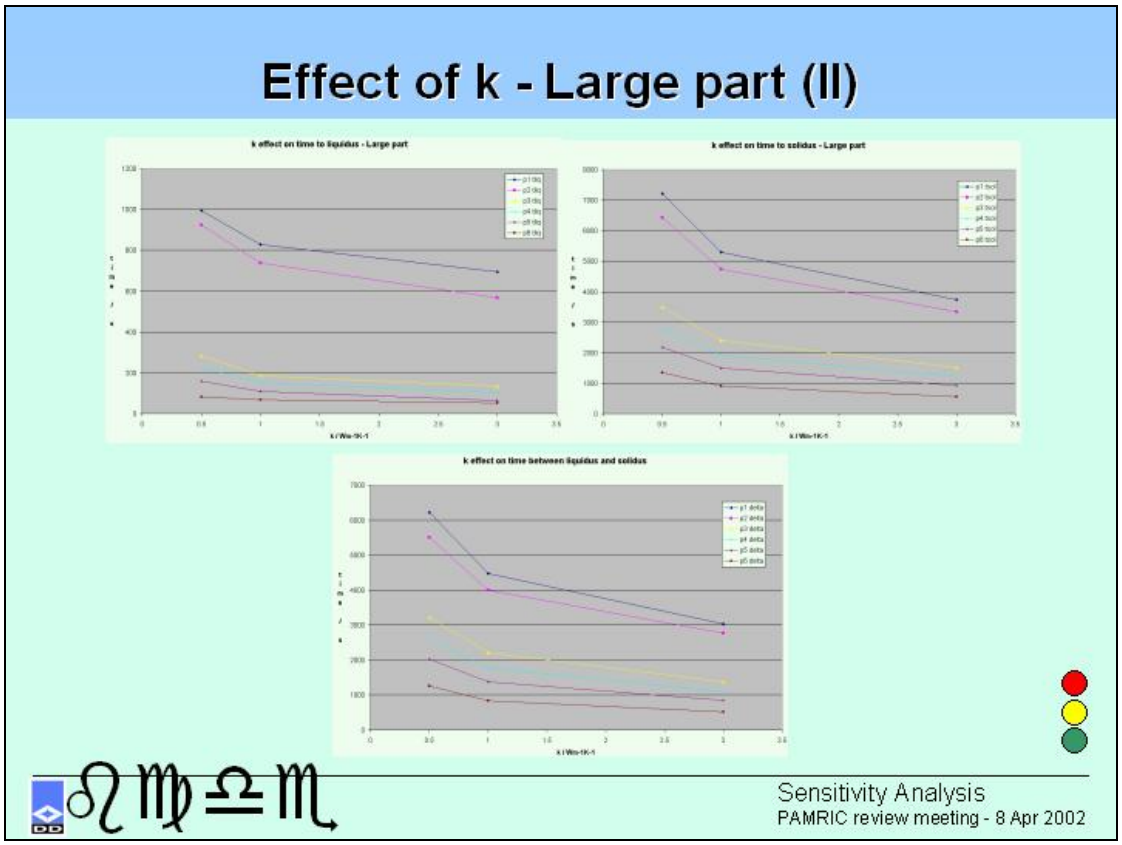
Effect of k - Large part (II)
k effect on time to liquidus - Large part
k effect on time to solidus - Large part
k effect on time between liquidus and solidus
Sensitivity Analysis
PAMRIC review meeting - 8 Apr 2002

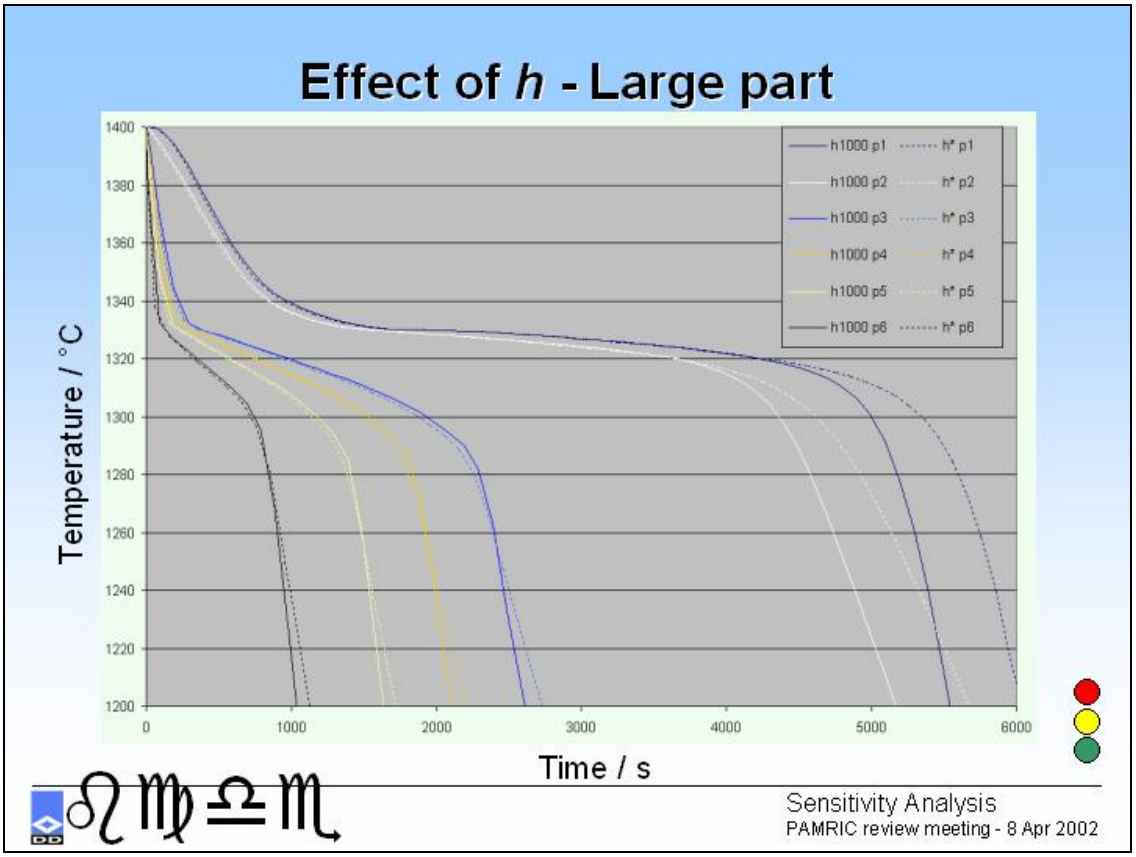
Effect of h - Large part
Temperature / °C
Time / s
h1000 p1
h* p1
h1000 p2
h* p2
h1000 p3
h* p3
h1000 p4
h* p4
h1000 p5
h* p5
h1000 p6
h* p6
Sensitivity Analysis
PAMRIC review meeting - 8 Apr 2002

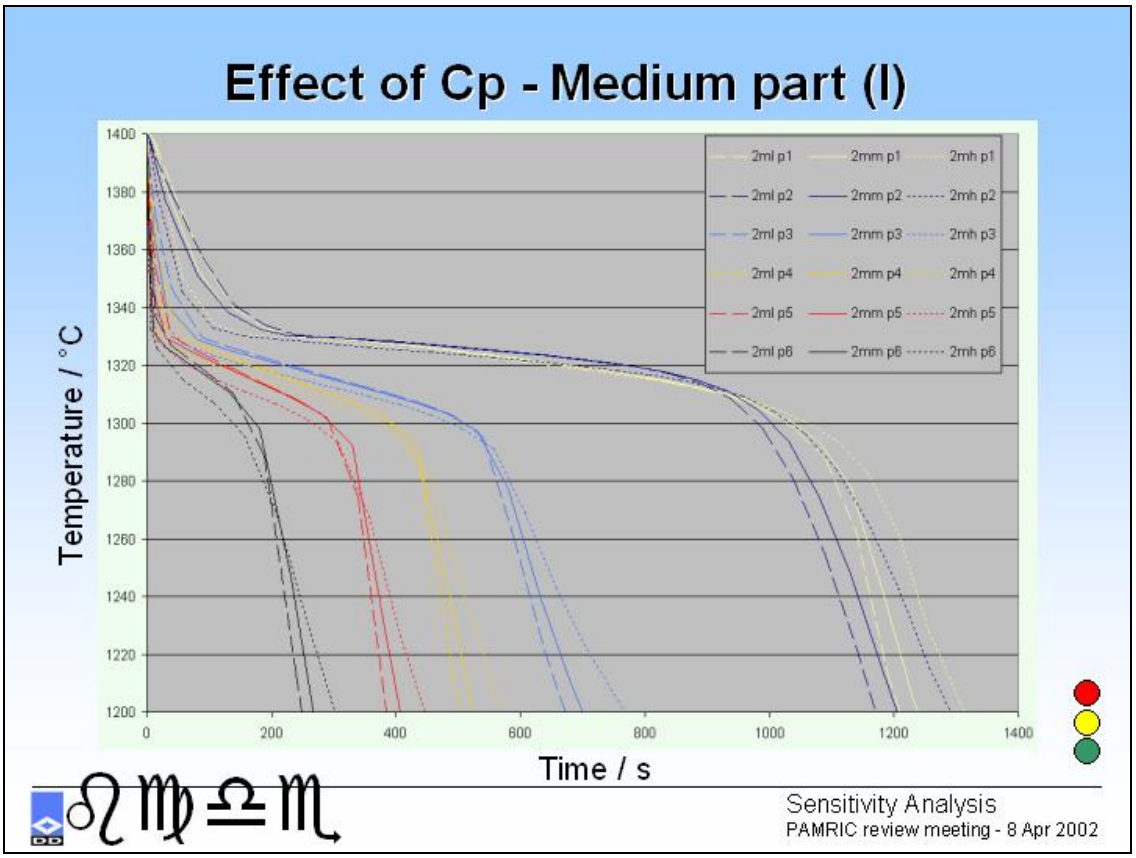
Effect of Cp - Medium part (I)
Temperature / °C
Time / s
2ml p1
2mm p1
2mh p1
2ml p2
2mm p2
2mh p2
2ml p3
2mm p3
2mh p3
2ml p4
2mm p4
2mh p4
2ml p5
2mm p5
2mh p5
2ml p6
2mm p6
2mh p6
Sensitivity Analysis
PAMRIC review meeting - 8 Apr 2002

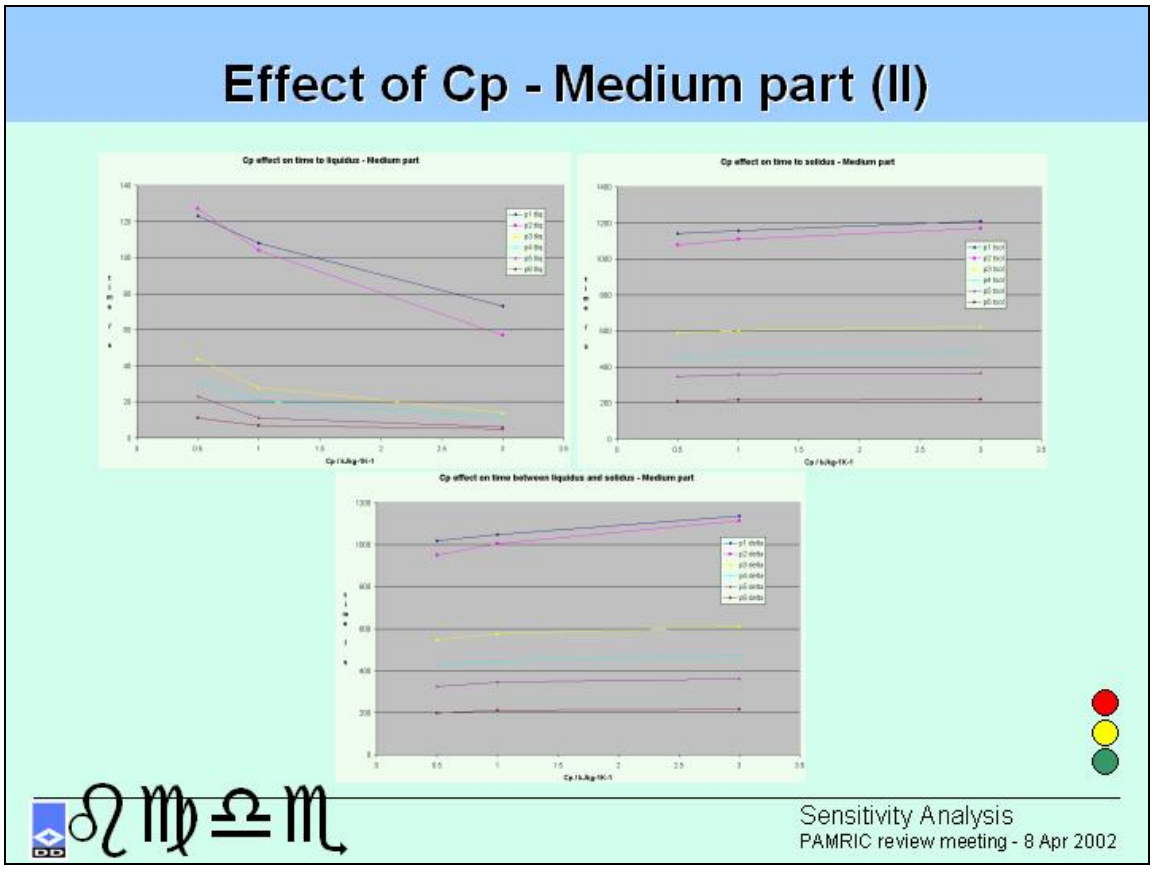
Effect of Cp - Medium part (II)
Sensitivity Analysis
PAMRIC review meeting - 8 Apr 2002

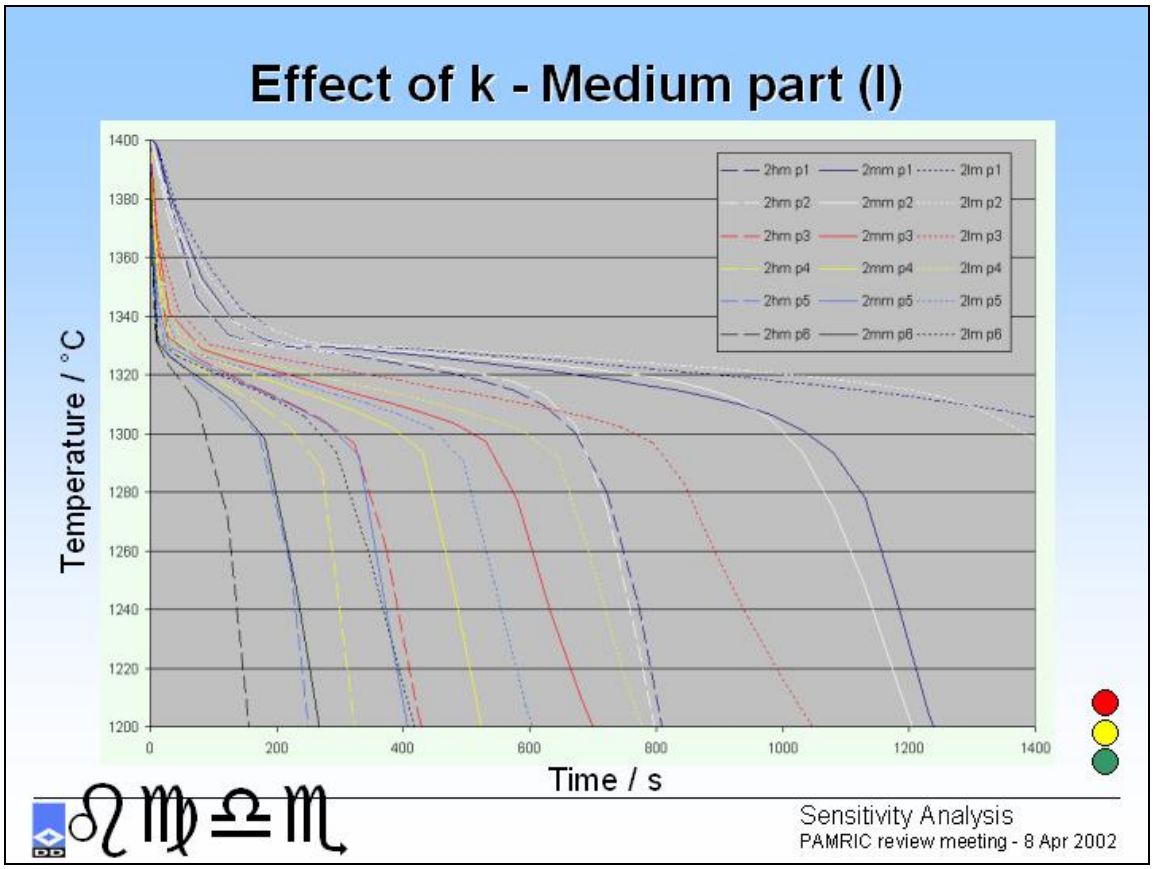
Effect of k - Medium part (I)
Temperature / °C
Time / s
2hm p1
2mm p1
2lm p1
2hm p2
2mm p2
2lm p2
2hm p3
2mm p3
2lm p3
2hm p4
2mm p4
2lm p4
2hm p5
2mm p5
2lm p5
2hm p6
2mm p6
2lm p6
Sensitivity Analysis
PAMRIC review meeting - 8 Apr 2002

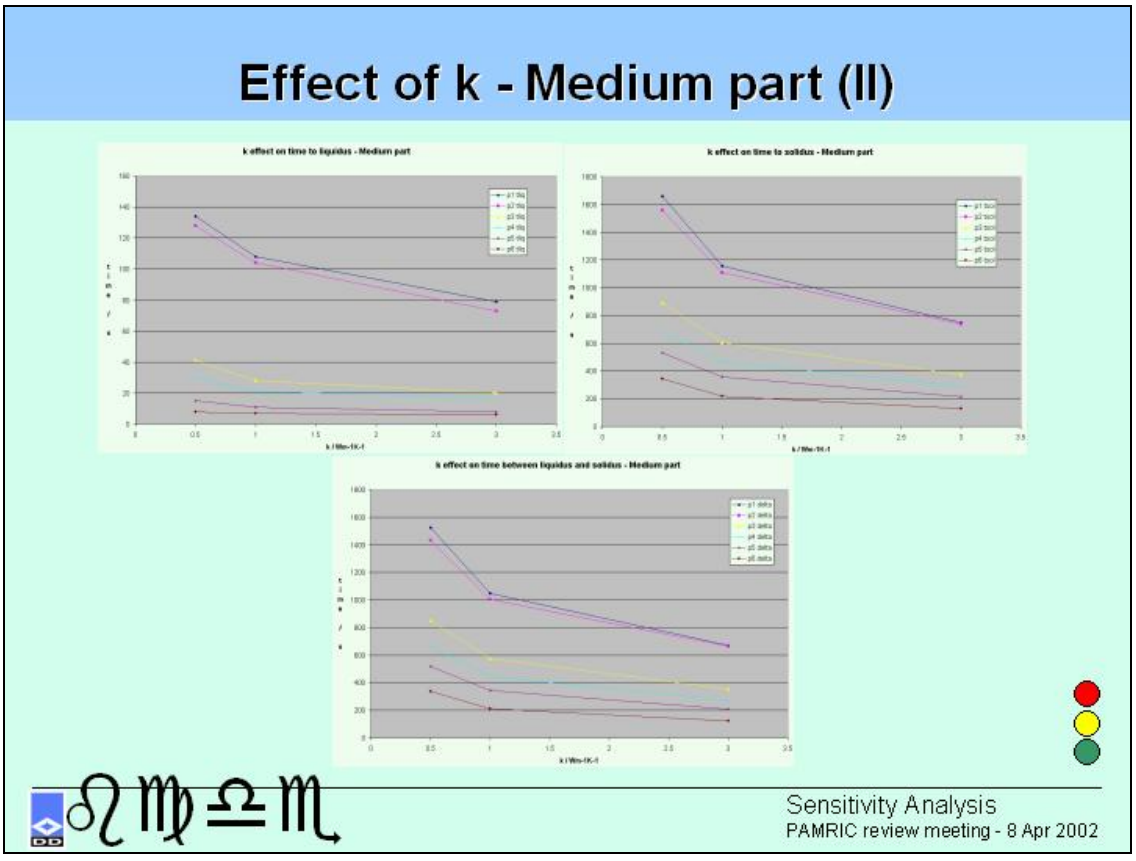
Effect of k - Medium part (II)
k effect on time to liquidus - Medium part
k effect on time to solidus - Medium part
k effect on time between liquidus and solidus - Medium part
Sensitivity Analysis
PAMRIC review meeting - 8 Apr 2002

Effect of *h* - Medium part

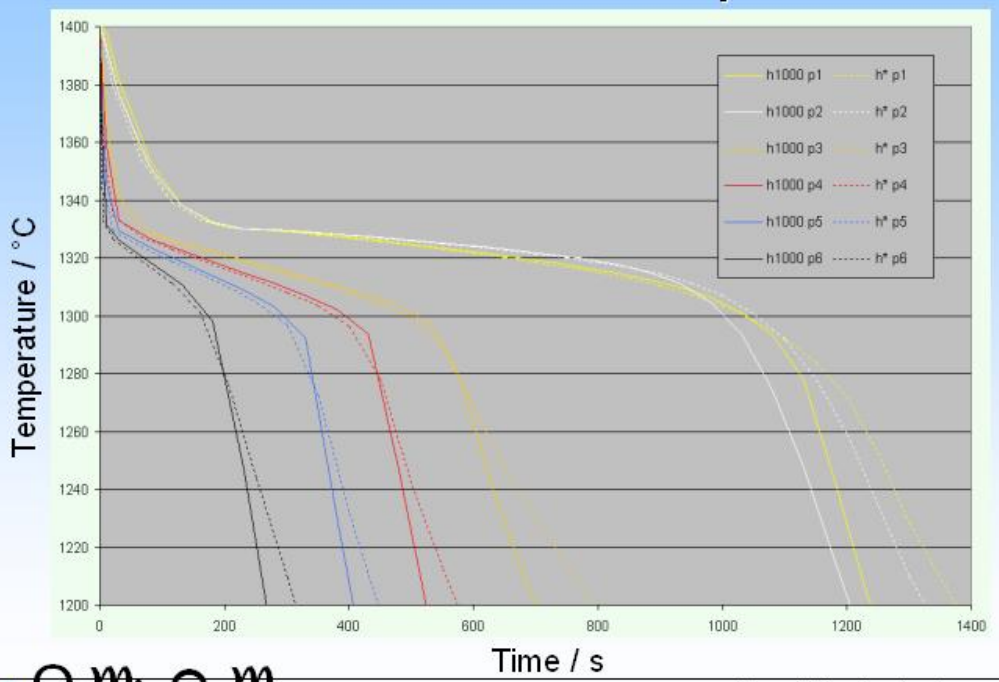

Sensitivity Analysis
PAMRIC review meeting - 8 Apr 2002

Summary (I) - Small parts

1. Main effect of *Cp* is on initial solidification time
   * crossover < Tsol *
2. *k* strongly affects the total solidification time
3. *h* has small effect

Sensitivity Analysis
PAMRIC review meeting - 8 Apr 2002

Summary (II) - Large parts

1. *Cp* has very little effect
   * high Cp slightly slower! *
2. *k* dominates cooling, non-linear
3. *h* has small effect, more important when thick

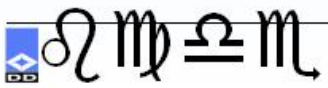

Sensitivity Analysis
PAMRIC review meeting - 8 Apr 2002

Summary (III) - Medium parts

1. Main effect of *Cp* is on initial solidification time
   * crossover at higher T, high Cp slower total *
2. *k* strongly affects the total solidification time
3. *h* has small effect, similar in magnitude to *Cp*
   More important when thick

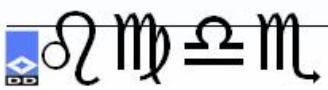

Sensitivity Analysis
PAMRIC review meeting - 8 Apr 2002

Summary (IV) - Other observations

1. *h* most important factor for thin sections
   Almost no effect from changing shell properties

2. *h* controls the extraction of heat from the inside of thick sections (as well as metal properties)

3. Accuracy of later stages of solidification - is the *h* value sensible?

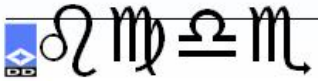

Sensitivity Analysis
PAMRIC review meeting - 8 Apr 2002